DISSERTATION

Advanced sustainability in fluid catalytic cracking: Biogenic and recycled feedstocks in the FCC process

carried out for the purpose of obtaining the degree of Doctor technicae (Dr. techn.)

submitted at TU Wien

Faculty of Mechanical and Industrial Engineering

by

Dipl.-Ing. Florian KNAUS

Mat.No.: 0928961

under the supervision of

Univ.Prof. Dipl.-Ing. Dr. Franz Winter

and

Ass.Prof. Dipl.-Ing. Dr. Alexander Reichhold

Institute for Chemical, Environmental and Bioscience Engineering, E166

Reviewed by

Ao. Univ. Prof. Dr. Simone Knaus

Institute of Applied Synthetic Chemistry,
Technische Universität Wien

Getreidemarkt 9, 1060 Wien,
Austria

Prof. Dr. Reinhard Rauch

Engler-Bunte Institute, Fuel technology,
Karlsruhe Institute of Technology

Engler-Bunte-Ring 1, 76131 Karlsruhe,
Germany

Vienna, December 2023

Signature

AFFIDAVIT

I declare in lieu of oath, that I wrote this thesis and performed the associated research myself, using only literature cited in this volume. If text passages from sources are used literally, they are marked as such. I confirm that this work is original and has not been submitted elsewhere for any examination, nor is it currently under consideration for a thesis elsewhere.

Vienna, 01.12.2023

_____

Signature

DANKSAGUNG

Zuerst möchte ich den wichtigsten Personen in meinem Leben danken, meiner Frau Stephanie und meiner Tochter Laura. Dafür, dass ihr mich immerzu motiviert, bestärkt und in mir auch immer wieder Zuversicht geweckt habt, wenn es bitter nötig war. Dafür, dass ihr mir den Rücken freigehalten habt an kurzen Tagen und in langen Nächten.
Danke dafür, dass ein Lachen von euch reicht um Farbe in jeden grauen Tag zu bringen.

Ich möchte mich auch bei meinem Betreuer und Doktorvater Professor Alexander Reichhold bedanken, der mich schon als Bachelorand in die Arbeitsgruppe aufgenommen hat. Danke, dass du immer ein fachlich und auch menschlich sehr angenehmer Leiter der Arbeitsgruppe warst. Danke für das Ermöglichen dieser Arbeiten, für die Anstellung sowohl als Tutor als auch später als Doktorand. Danke für deine soziale Art und dein Verständnis, sowohl in fachlicher als auch in sozialer Hinsicht, auf das man immer zählen kann.
Ich wünsche dir einen schönen und entspannten Ruhestand!

Außerdem möchte ich meine besondere Wertschätzung meinem Betreuer und Doktorvater Professor Franz Winter zukommen lassen, bei dem ich viele theoretische Grundlagen gelernt habe, die für die Arbeiten an dieser Dissertation unerlässlich waren.

Meinen langjährigen Freund_innen und Kolleg_innen Helene Lutz und Marco Büchele möchte ich natürlich auch meinen Dank aussprechen. Danke für die großartige Zusammenarbeit, das Zusammenstehen auch in turbulenten Zeiten während einer Pandemie. Danke für lange Tage an der Anlage und manchmal auch lange Abende im Büro. Danke, dass ich mich immer auf euch verlassen konnte und dass ihr immer mit Rat und Tat zur Seite gestanden seid.
Danke Helene und Marco, ohne euch wäre diese Arbeit nicht möglich gewesen.

Mein Dank gilt auch meinen Eltern Brigitte und Peter und meinem Bruder Daniel, die mich immer in jeglicher Hinsicht unterstützt haben und ohne die das Studium für mich nicht möglich gewesen wäre. Ihr habt mir vorgezeigt was man durch Arbeit, Konsequenz und Resilienz erreichen kann. Sie waren und sind mir bis heute Vorbilder.

Außerdem möchte ich mich bei Alexandre Pazos Costa und Chandrasekhar Ramakrishnan bedanken. Ohne den kollegialen und fachlichen Rat einerseits und natürlich der Finanzierung andererseits wäre diese Forschungsarbeit nicht möglich gewesen.
Danke für die Chance, die ihr mir ermöglich habt!

ABSTRACT

Finding ways to integrate abundant resources such as plastic waste into the value chain is a key requirement for a more sustainable society. Another key goal is to lower the carbon intensity of industrial processes as far as possible. The aim of this thesis is to show more or less feasible ways to achieve both with an existing, established, well known and already upscaled process.
Fluid catalytic cracking is one of the most important conversion processes used in modern oil refineries. This versatile process is used to convert high-boiling, high-molecular weight hydrocarbon fractions of crude oil into high-octane gasoline, basic materials for petrochemical industry (such as olefins and aromatics) and other products, such as lubricants. Using FCC units to co-process vacuum gas oil (the standard feedstock for FCC units), pyrolysis oil (obtained by pyrolization of plastic waste feedstocks, two synonyms are pyoil or syncrude) and biogenic oils (such as. used cooking oils) can contribute to reach future defined defossilization and circular economy targets.

The first batch of experiments conducted during this thesis aims to indicate a pathway towards the integration of pyrolysis oil into the FCC process, and to partially de-fossilize the process by adding biogenic oils to the feedstock.
The second batch of experiments aims to omit the usage of fossil, non-circular feeds altogether by substituting the fossil-based vacuum gas oil for biogenic feedstocks such as canola oil or used cooking oil.
The third batch of experiments aims to optimize the product yields of selected feedstock admixtures by increasing the severity of the cracking process.
The last experiment was conducted to indicate the feasibility of a highly circular FCC process by feeding 100 %wt circular feedstock to the pilot plant.

In the first experiments it was shown that pyoil derived from municipal plastic waste is a suitable feedstock for co-processing in an FCC pilot plant. The feedstock can be used in the pilot plant in very high admixture rates, topping out in a successful experiment with pure pyoil as FCC feedstock. However, due to certain challenges in FCC operation and shifts in the product spectrum very high admixture rates may not be feasible in industrial sized FCC units due to economic reasons.
Nevertheless, the utilization of pyoil in FCC units can be a way to lower the required amount of pristine petroleum for petrochemical products, bringing materials back into the value chain which are otherwise lost. It can also attribute a certain value to deteriorated mixed municipal plastic waste in order to enhance collection and recycling in heavily plastic-polluted areas of certain countries.

Decarbonizing the FCC process is another challenge, as carbon intense recycling is not contributing to a more sustainable petrochemical industry. Adding biogenic feeds to the process could lower the carbon intensity whilst still retaining most of the process's economic profitability. The addition of canola oil and pyoil improved the yield of olefins in the hydrocarbon gases at cost of the gasoline yield and the production of higher amounts of carbon oxides and water. However, in order to improve the sustainability of the refinery overall and the FCC process in particular co-processing multiple feedstocks will be necessary and drawbacks need to be overcome.

A way to decarbonize the FCC to a maximum is the substitution of fossil based VGO through biogenic oils. Lipids have shown in the past their ability to sustain FCC operation as a base feedstock. The addition of pyoil makes a bio-based process a biobased and partially circular process. Also, it increases gasoline, olefin, and coke yields whilst co-feeding reduced the alkanes, light cycle oil and residue yields. Co-processing of the base feed canola oil with pyoil is currently not feasible on industrial scale due to a lack of available feedstock. However, the future will tell which paths are taken to produce sustainable low carbon circular fuels, olefins and other petrochemical compounds, lubricants and dry gas.

The usage of used cooking oil as a substitute for pristine canola oil was investigated, in order to avoid the usage of food-grade oils and instead use waste biogenic oils. The result of the substitution is slightly changed yields of gasoline, LCO and coke.

Maximizing the ratio of directly usable olefins is a major incentive for usage of pyoil in the FCC process. The RED II directive clearly states that waste-to-fuel is not counted as recycling, putting pressure on chemical recycling processes to produce petrochemicals instead of gasoline or diesel. Increasing the severity of the fluid catalytic cracking process by increasing the temperature generally increases the yields in hydrocarbon gases in the FCC process.
Although increased temperature has positive effects on the product yields of the base feeds, the co-feeding of pyoil reverses these positive effects.
The addition of pyoil seems to move the temperature of the maximum gasoline production towards higher values. Increasing the temperature had the effect of a maximized naphtha and LCO fraction. On the plus side, naphtha is a relatively common feedstock for steam cracking in order to produce ethene and a low amount of heavier olefins.

The last goal to achieve during this thesis was a 100 %wt pyoil feeding experiment. Due to restrictions regarding feedstock availability only one sample was obtainable, biasing the obtained data due to a missing water fraction.
However, the experiment showed remarkable good results with an incredibly high olefin, especially propene, yield whilst maintaining a high gasoline yield.

KURZFASSUNG

Die Möglichkeit reichlich vorhandene Ressourcen wie Kunststoffabfälle in die Wertschöpfungskette zu integrieren, ist eine wichtige Voraussetzung für eine nachhaltigere Gesellschaft. Ein weiteres wichtiges Ziel ist es, die Kohlenstoffintensität industrieller Prozesse so weit wie möglich zu senken. Das Ziel dieser Arbeit ist es, mehr oder weniger gangbare Wege aufzuzeigen, um beides mit einem bestehenden, etablierten und bereits in industriellem Maßstab eingesetzten Prozess zu erreichen.
Das katalytische Cracken in der Wirbelschicht (auch im deutschen Sprachraum besser bekannt unter Fluid Catalytic Cracking oder FCC) ist eines der wichtigsten Umwandlungsverfahren in Raffinerien. Das vielseitige Verfahren wird zur Umwandlung von sehr hochsiedenden, hochmolekularen Kohlenwasserstofffraktionen aus Rohöl in hochoktaniges Benzin, Grundstoffe für die petrochemische Industrie (wie Olefine und Aromaten) und andere Produkte wie Schmierstoffe eingesetzt. Der Einsatz von FCC-Anlagen zur Verarbeitung von Gemischen aus Vakuumgasöl (dem Standardeinsatzmaterial für FCC-Anlagen), Pyrolyseöl (das durch Pyrolyse von Kunststoffabfällen gewonnen wird) und biogenen Ölen (wie z. B. Altspeisefetten) kann dazu beitragen, die für die Zukunft festgelegten Ziele für die Dekarbonisierung und die Kreislaufwirtschaft zu erreichen.

Die erste Versuchsreihe, die im Rahmen dieser Arbeit durchgeführt wurde, soll einen Weg zur Integration von Pyrolyseöl in den FCC-Prozess aufzeigen und den Einsatz von fossilen Rohstoffen durch die Zugabe von biogenen Ölen zum Einsatzmaterial reduzieren.
Die zweite Versuchsreihe zielt darauf ab, die Verwendung fossilen, nicht recycelten Einsatzstoffen zu vermeiden, indem aus Erdöl hergestelltes Vakuumgasöl durch biogene Einsatzstoffe wie Rapsöl oder Altspeiseöl ersetzt wird.
Die dritte Versuchsreihe zielt darauf ab, die Ausbeute an wertvolleren Produkten bei der Verwendung von biogenen und recycelten Einsatzstoffen zu optimieren, indem die Cracktiefe des Crackprozesses durch eine erhöhte Cracktemperatur erhöht wird.
Das letzte Experiment bestätigte die Durchführbarkeit eines hochgradig kreislauffähigen FCC-Prozesses durch den Betrieb der FCC Pilotanlage ausschließlich mit Pyrolyseöl.

In der ersten Versuchsreihe wurde gezeigt, dass aus kommunalen Kunststoffabfällen gewonnenes Pyrolyseöl eine geeignete Beimischungskomponente zum Einsatzstoff einer FCC-Pilotanlage ist. Dies gilt selbst für sehr hohe Beimischungsraten. Aufgrund der Anforderungen an Anlagenteile, die dem Reaktor nachgeschaltet sind und Verschiebungen im Produktspektrum sind sehr hohe Beimischungsraten in industriellen FCC-Anlagen aus wirtschaftlichen Gründen jedoch möglicherweise nicht realisierbar.
Nichtsdestotrotz kann die Verwendung von Pyrolyseöl in FCC-Anlagen eine Möglichkeit sein, die benötigte Menge an Rohöl für petrochemische Produkte zu verringern und Materialien in die Wertschöpfungskette zurückzubringen, die sonst verloren gehen würden. Außerdem kann es dazu beitragen, dass Kunststoffabfällen ein gewisser Wert beigemessen wird, um die Sammlung und das Recycling in stark kunststoffverschmutzten Gebieten bestimmter Länder zu verbessern.

Die Dekarbonisierung des FCC-Prozesses ist eine weitere Herausforderung, da emissionsreiches Recycling nicht zu einer nachhaltigeren petrochemischen Industrie beiträgt. Die Zugabe von biogenen Rohstoffen zum Prozess könnte die Emission von Treibhausgasen fossilen Ursprungs senken, und gleichzeitig die wirtschaftliche Rentabilität des Prozesses weitgehend erhalten. Die Zugabe von Rapsöl und Pyrolyseöl verbesserte den Anteil der Olefine in den gasförmigen Produkten auf Kosten der Benzinausbeute und der Produktion höherer Mengen an Kohlenoxiden und Wasser im Produkt. Um die Nachhaltigkeit der Raffinerie im Allgemeinen und des FCC-Prozesses im Besonderen zu verbessern, ist jedoch die gleichzeitige Verarbeitung mehrerer Einsatzstoffe biogenen und recycelten Ursprungs erforderlich. Die sich daraus ergebenden Nachteile stellen durchaus überwindbare Hürden dar.

Eine Möglichkeit zur Maximierung der Dekarbonisierung des FCC Prozesses ist der Ersatz von fossilem VGO durch biogene Öle. Diese haben in der Vergangenheit gezeigt, dass sie den FCC-Betrieb als Basisrohstoff aufrechterhalten können. Durch die anschließende Zugabe von Pyrolyseöl wird ein bio-basierter Prozess zu einem bio-basierten und teilweise kreislauffähigen Prozess. Außerdem erhöht sich dadurch die Ausbeute an Benzin, Olefinen und Koks, während sich die Ausbeute an Alkanen, LCO und der schweren Rückstandsfraktion verringert.
Die gemeinsame Verarbeitung von Rapsöl mit Pyoil ist derzeit aufgrund des Mangels an verfügbaren Rohstoffen im industriellen Maßstab nicht möglich. Die Zukunft wird jedoch zeigen, welche Wege eingeschlagen werden, um nachhaltige, kohlenstoffarme, kreislauffähige Kraftstoffe, Olefine und andere petrochemische Verbindungen, Schmierstoffe und Heizgase herzustellen.
Die Verwendung von Altspeiseöl als Ersatz für Rapsöl in Lebensmittelqualität wurde untersucht, um die Verwendung von lebensmitteltauglichen Ölen zu vermeiden. Das Ergebnis der Substitution sind leicht veränderte Ausbeuten an Benzin, LCO und Koks.

Der Anteil direkt nutzbarer Olefine ist ein wichtiger Anreiz für die Verwendung von Pyrolyseöl im FCC-Prozess. Die RED-II-Richtlinie legt eindeutig fest, dass die Umwandlung von Abfallstoffen in Kraftstoffe nicht als Recycling gilt, wodurch Druck auf chemische Recyclingprozesse ausgeübt wird, petrochemische Grundstoffe anstelle von Benzin oder Diesel zu produzieren. Die Erhöhung der Cracktiefe des FCC Prozesses durch die Erhöhung der Cracktemperatur erhöht im Allgemeinen auch die Ausbeute an gasförmigen Produkten im FCC-Prozess.
Obwohl sich eine erhöhte Temperatur positiv auf die Produktausbeute der Basis Einsatzstoffe VGO und UCO auswirkt, werden diese positiven Effekte durch die Zugabe von Pyrolyseöl wieder aufgehoben.
Eine Erklärung dafür kann sein, dass die Zugabe von Pyrolyseöl die Temperatur der maximalen Benzinproduktion in Richtung höherer Werte verschiebt. Die Erhöhung der Temperatur hatte eine Maximierung der Naphtha- und LCO-Fraktion zur Folge. Hierbei positiv anzumerken ist, dass Naphtha ein häufig anzutreffender Ausgangsstoff für den Raffinerieprozess des Steamcrackens ist, bei dem Ethen und eine geringe Menge an schwereren Olefinen erzeugt werden, was den Kreislaufcharakter der gesamten Wertschöpfungskette zuträglich wäre.

Das letzte Ziel, das im Rahmen dieser Arbeit erreicht werden sollte, war ein Versuchsaufbau mit 100 %wt Pyrolyseöl als Einsatzstoff in der FCC Anlage. Aufgrund von Beschränkungen bei der Verfügbarkeit von Pyrolyseöl, konnte durch die kurze mögliche Betriebszeit nur eine Probe entnommen werden, was zu einer Verzerrung der erhaltenen Daten aufgrund eines fehlenden Wasseranteils führte.
Der Versuch zeigte jedoch bemerkenswert gute Ergebnisse mit einer sehr hohen Ausbeute an Olefinen, insbesondere Propen, bei gleichzeitig hoher Benzinausbeute.

TABLE OF CONTENTS

FUNDING ACKNOWLEDGEMENT

This project was funded by ILF Consulting Engineers Austria GmbH

LIST OF ABBREVIATIONS

Table 1: List of abbreviations

%wt	Mass fraction
ABS	Acrylonitrile butadiene styrene
AV	Acid value
BP	British petroleum company
BTX	Benzene, Toluene and Xylene
C/O ratio	Catalyst to oil ratio
CCR	Conradson carbon residue
CPD	Catalytic pressure-less depolymerization
DIN	Deutsches Institut für Normung (German Institute for Standardisation)
EN	Europäische Norm (European Standards)
FCC	Fluid catalytic cracking
FFA	Free fatty acids
GC	Gas chromatography
GDP	Gross domestic product
HDPE	High-density polyethylene
ISO	International Organization for Standardization
LCO	Light cycle oil
LDPE	Low-density polyethylene
LPG	Liquefied petroleum gas
MON	Motor Octane Number
NIR	Near-infrared
PC	Pyrolysis condensate, often referred to as “syncrude” or “pyoil”
PET	Polyethylene terephthalate
PFD	Process flow diagram
PIONA	n-paraffins, iso-paraffins, olefins, naphthenes and aromatics
PONA	paraffins, olefins, naphthenes and aromatics
PP	Polypropylene
PS	Polystyrene
PV	Peroxide value
PVC	Polyvinylchloride
Pyoil	Pyrolysis oil, often referred to as “syncrude” or “pyrolysis condensate”
RED II	Renewable Energy Directive 2
RON	Research Octane number
SimDist	Simulated distillation
UCO	Used cooking oil
UOP	Universal oil products
VGO	Vacuum gas oil
ZSM	Zeolite Socony Mobil

FORMULA SYMBOLS

Table 2: Formula symbols

R	Alkyl side chain of a molecule	-
H	Hydrogen atom	-
C	Carbon atom	-
H^+	Proton	-
H^-	Hydride ion	-
μ	kinematic viscosity	m²/s
A	area	m²
A_P	projection area of the particle	m²
Ar	Archimedes number	-
C/O	Catalyst to oil ratio	-
c_W	Drag coefficient	-
Δp	pressure drop	mbar
$\Delta p_{regenerator}$	pressure drop regenerator	mbar
d_k	diameter catalyst particle	m
d_{sv}	Sauter diameter	µm
ε	porosity	-
F_A	buoyancy force	N
F_G	gravitational force	N
F_W	drag force	N
g	Standard acceleration due to gravity	m/s²
H	height of particle bed	m
H_L	height of catalyst bed at minimum fluidization gas velocity	m
$\dot{m}_{catalyst}$	catalyst circulation rate	kg/h
$\dot{m}_{feed}$	mass flow rate feedstock	kg/h
$\dot{m}_{gas}$	mass flow rate gaseous products	kg/h
$\dot{m}_{gasoline}$	mass flow rate gasoline	kg/h
π	Pi	-
Re	Reynolds number	-
ρ_G	gas density	kg/m³
ρ_P	particle density	kg/m³
T	Temperature	K
t	time	s
$\bar{T}_{Riser}$	Mean riser temperature	K
TFY	total fuel yield	-
$T_{Riser,in}$	Inlet riser Temperature	K
$T_{Riser,out}$	Outlet riser Temperature	K
u	velocity	m/s
u_L	linear gas velocity	m/s
u_{mf}	minimum fluidization velocity	m/s
u_t	Terminal velocity	m/s
$\dot{V}$	Volume flow	m³/s

LIST OF TABLES

LIST OF FIGURES

1 INTRODUCTION

When we think about our future on planet earth most of us paint a grim picture. Climate change, raging pollution and unprecedented biodiversity loss are only a few symptoms of the earth's condition.

However, upon further reflection there might be hope for us. Societies worldwide are changing towards more careful resource utilization, including vastly increasing recycling capacities, defossilization of energy sources and chemical resources and protection of natural resources. In developed countries these changes sooner or later result in adaptions in strategies and legislation. Some examples of these developments are the European Union's "Circular Economy Action Plan", "the European Green Deal" and the set of "Renewable Energy Directives" as well as the US' "Inflation Reduction Act" and the Chinese "14th Five Year Plan of the People's Republic of China" , addressing domestic climate issues as well as international agreements and commitments to long-lasting ecologic and economic progress towards a more sustainable future. [1]–[4]

By 2050 the world is expected to be consuming as if we had three times the resources given on our planet [1]. It is expected that by 2050 our annual waste production increases by 70 % from 2018s levels [5]. Until 2060 the global consumption of materials such as fossil fuels, biomass, metals and minerals is expected to double. [6]
In order to avoid this scenario, lawmakers are developing and implementing laws, action plans, directives, strategies and policies, intended to achieve climate neutrality by 2050, decoupling economic growth from resource, especially energy, use and doubling the circular material usage rate within a decade.[3], [7]–[9]
To cope with the changing demands and circumstances of the European economy the European commission initiated a set of policy initiatives in 2019 (approved in 2020) to make the European Union climate neutral by 2050. One part of the policy set, also called the "European Green Deal", is the "Circular Economy Action Plan". [1], [9]
With the Circular Economy Action Plan the EU intends to lead the global efforts to implement circular approaches to most waste streams, first and foremost the issue of plastic waste.
By implementing circular economy principles in the European industry, it is projected that the EU's GDP will experience a 0.5 % growth by 2050, leading to the creation of around 700,000 new jobs.[10]
The Circular Economy Action Plan rests on 5 pillars, the first of which aims to increase the recycling rate of plastic waste. Decoupling economic growth from resource use is one of the main aspects of the EU's ambitious strategy to achieve climate neutrality by 2050.[1]

These strategies and legislations are part of a global attempt to implement the demands and measures of international agreements and commitments, such as the Paris climate agreement[1].
The Paris climate agreement aims to limit global warming to well below 2 °C above pre-industrial levels, and to pursue efforts to limit the temperature increase to 1.5 degrees Celsius. This is to be achieved by reducing greenhouse gas emissions from human activities, such as burning fossil fuels and deforestation [11].
The pledges made by the participating countries were reviewed and enhanced at the 26th Conference of the Parties (COP26) in Glasgow in 2022[2]. Another focus of COP26 was on the role of the private sector and finance in driving the transition to a low-carbon economy and fostering sustainable development. This includes efforts to mobilize private sector investment in

[1] The Paris Agreement is an international treaty adopted in 2016 by the United Nations Framework Convention on Climate Change (UNFCCC) at the 21st Conference of the Parties (COP 21) in Paris, France.

[2] COP26, also known as the 26th United Nations Climate Change conference, is a global summit being held in Glasgow in 2021 to discuss and negotiate measures to address the ongoing issue of climate change.

clean energy, energy efficiency, and sustainable infrastructure, as well as efforts to enhance transparency and accountability in the financial sector in relation to climate risks.

2 THE HISTORY OF CATALYTIC CRACKING

In the beginning of the 19th century, naphtha was available to the public at relatively high cost and purity in pharmacies, but not as it is today at gas stations nearly everywhere. Petroleum had its early use as lighting oil, replacing expensive animal and vegetable oil. For this purpose only fractions with boiling curves between approximately 100 and 300 °C where used, low and high boiling fractions (called “naphtha” and “tar” fraction) where generally declared waste and where thrown away [12]. The niche existence of naphtha changed with the victorious march of the internal combustion engine, namely the otto engine. The abundant fraction fast became a high value fuel for mass produced vehicles such as Ford’s famous Model-T. The rise of the car led to the creation of a whole value chain for crude oil products, including gasoline, lubricants and bitumen for asphalt-paved roads.

Around the time of 1910 it became clear to refiners that the so-called straight run naphtha, or as this product now was called “gasoline”, production capacities couldn’t satisfy the ever-growing demand. Thermal cracking of long hydrocarbon molecules has been known back then, but these methods rarely produced gasoline suitable for internal combustion engines and the earliest thermal cracking plants had problems with the relatively high temperatures and pressures needed.
It was until 1915, when A. M. McAfee discovered at Gulf Refining Company (Texas, USA) that heavy petroleum fractions crack efficiently in presence of $AlCl_3$, which acts as a catalyst. Due to high costs associated to the manufacturing of the catalysts and despite its higher gasoline yield than thermal cracking the first catalytic cracking process was economically not successful [13].

This changed in the 1920s, when E. J. Houdry (utilizing previous work by E. A. Prudhomme) discovered that the aluminosilicates contained in a mineral contained in clay, namely “Fuller’s Earth”, could convert heavy hydrocarbons to a gasoline-like product. Houdry worked on applying his findings in the petroleum industry, developing a fixed bed catalytic cracking reactor. Houdry also worked on the catalyst reactivation by thermally oxidizing coke depositions on the deactivated catalyst particles.
In 1937 the first fully commercial catalytic crackers went into operation, processing up to 15.000 barrels of gas oil, a heavy fraction of petroleum, per day with a gasoline yield of approximately 45 %wt (compared with 25 %wt gasoline yield of the then state-of-the-art thermal crackers). To cope with the increasing demand of catalyst for cracking the first large-scale plant of synthetic aluminosilicate catalysts went into operation in 1940. [14] [15]
A high level schematic of the Houdry process is depicted in the following figure 1.

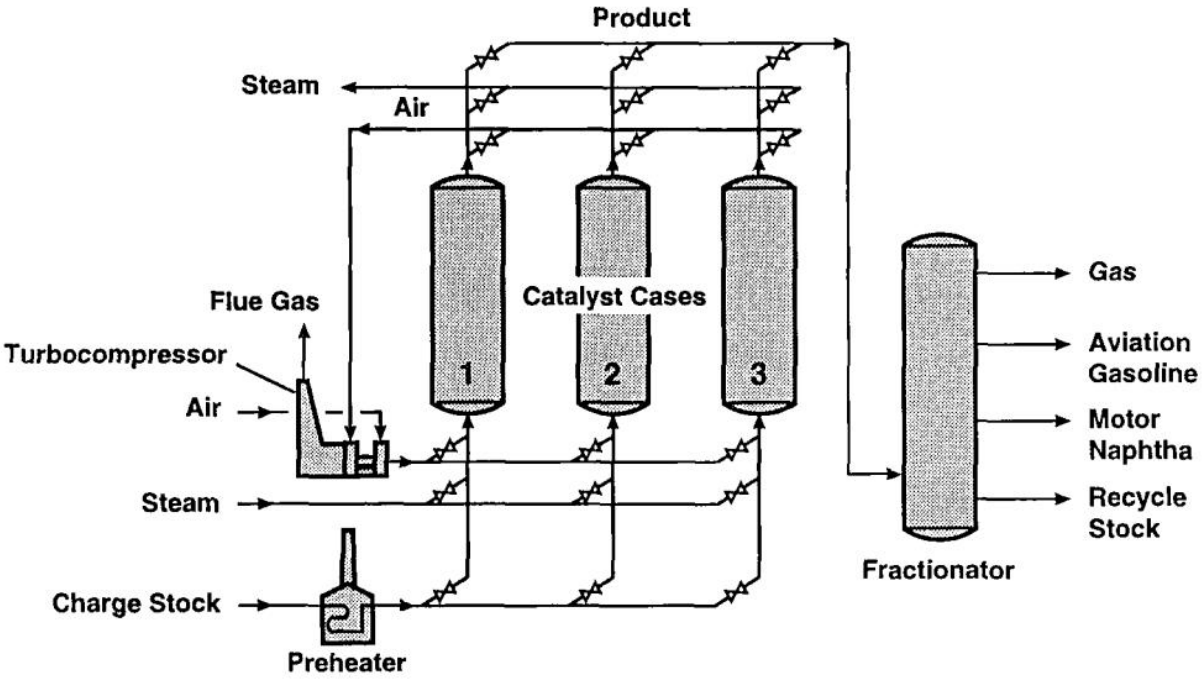

Figure 1: Schematic of the Houdry process [16]

Houdry's catalytic cracking process worked with at least two parallel operating catalytic solid-bed reaction vessels, one in operation and one in regeneration mode. This semi-continuous operation mode had one major drawback, which was the changing activity of the catalyst during operation. At the beginning of the cracking cycle the activity of the reactivated catalyst was very high, resulting in light (so-called "over-cracked") products. Due to the formation of heavy hydrocarbon structures (heavy polyaromatic coke) on the catalyst particles the active areas of the catalyst were blocked and the activity of the catalyst decreased progressively.
The so-called "Houdry unit" in the Marcus Hook refinery is depicted I the following figure 2.

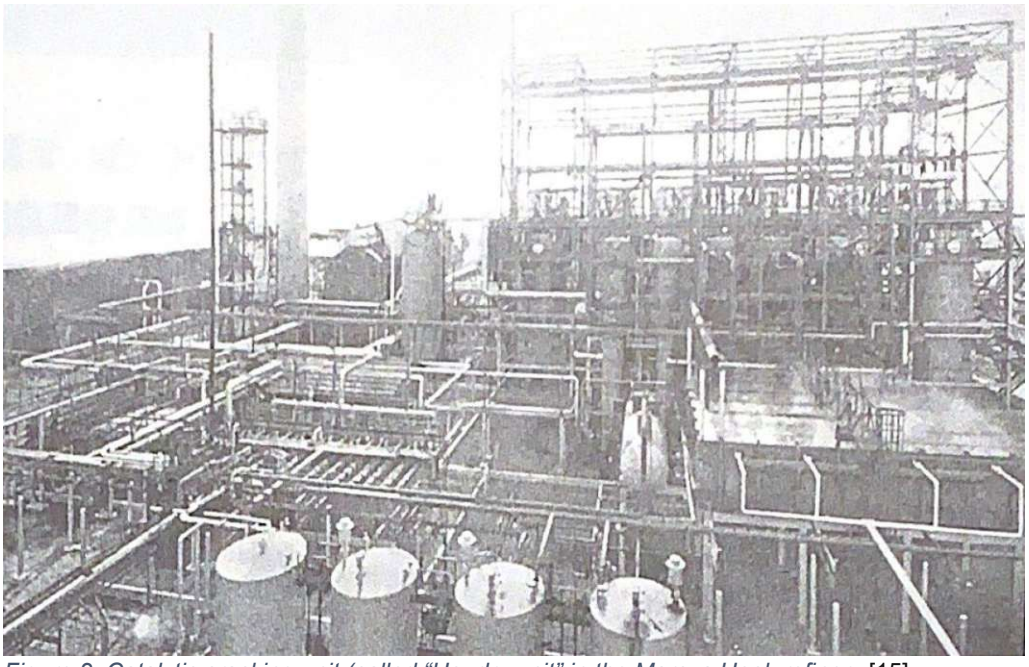

Figure 2: Catalytic cracking unit (called "Houdry unit" in the Marcus Hook refinery [15]

After proving the catalytic cracking concept from Houdry on an industrial scale in the Houdry unit in the Marcus Hook refinery, the next major iteration of catalytic cracking reactor was planned. To overcome the drawbacks, it was planned to move the catalyst continuously between the two reaction zones, namely the “cracking” zone where the feed was cracked to lighter products and the “regeneration” zone where the deactivated catalyst is reactivated via thermal oxidation of the formed coke. In the beginning of the 1940s almost simultaneous two concepts reached technical maturity, first a concept based on moving catalyst beds and second a concept based on fluidized beds.

2.1 Fluid catalytic cracking

Due to excessive licencing cost of the Houdry/ Sun Company process a consortium called “Catalyst Research Associates (CRA)” by Standard Oil Jersey, the M. W. Kellogg Company (London), I. G. Farben and Standard Oil Indiana set the goal to develop a catalytic cracking process outside of Houdry’s and Sun Company’s patents. By 1938 the research division of Standard Oil Jersey (a former division of Standard Oil, today part of ExxonMobil) put the first pilot plant in service. The pilot unit was continuously catalytic cracking vaporized oil and was utilizing powdered catalyst in a heated tubular reactor. Shortly after these developments Anglo-Iranian Oil Company (today known as BP), the Texas Oil Company (today known as Texaco), Universal Oil Products (UOP) and Royal Dutch Shell joined the consortium to develop the first industrial scale fluid catalytic cracking unit [17].
This first commercial FCC unit was called “Model I”, situated in Baton Rouge with a feed rate of more than 17.000 barrel per day. A schematic of “Model I” is depicted in the following Figure 3.

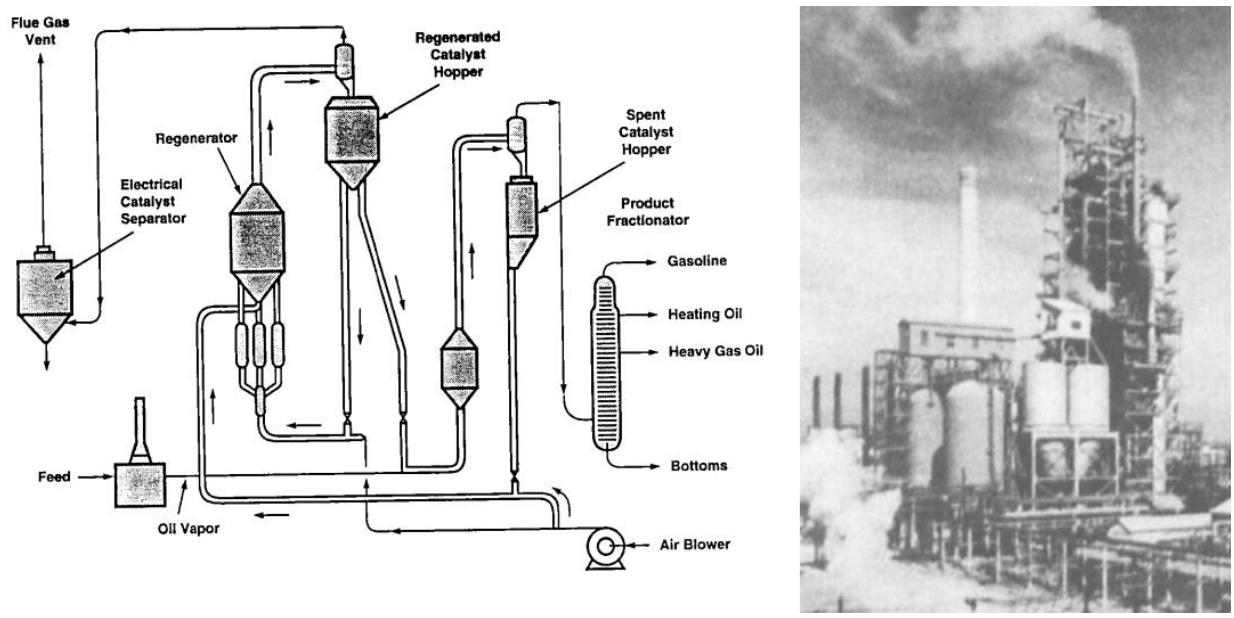

Figure 3: Model I (Powdered Catalyst Louisiana I (PCLA I)) Baton Rouge [16]

Due to modifications and enhancements the FCC process became more versatile, more compact and more robust, allowing operation at full capacity for years before revamps and maintenance works were necessary [16].

Today FCC units are in operation in many petroleum refineries worldwide. Depending on the geographical area, petroleum properties and gasoline demand they are producing large shares of the local gasoline blend. For example China is producing approximately 75 %wt of the gasoline via FCC units [18]).

3 THE FCC PROCESS

3.1 Introduction

As seen in the following figure 4, FCC units can be split into three main areas, distinguished by their functionality:

- Reactor (including the so called “Riser”, indicated in red color)
- Regenerator (indicated in green color)
- Fractionation (indicated in blue color)

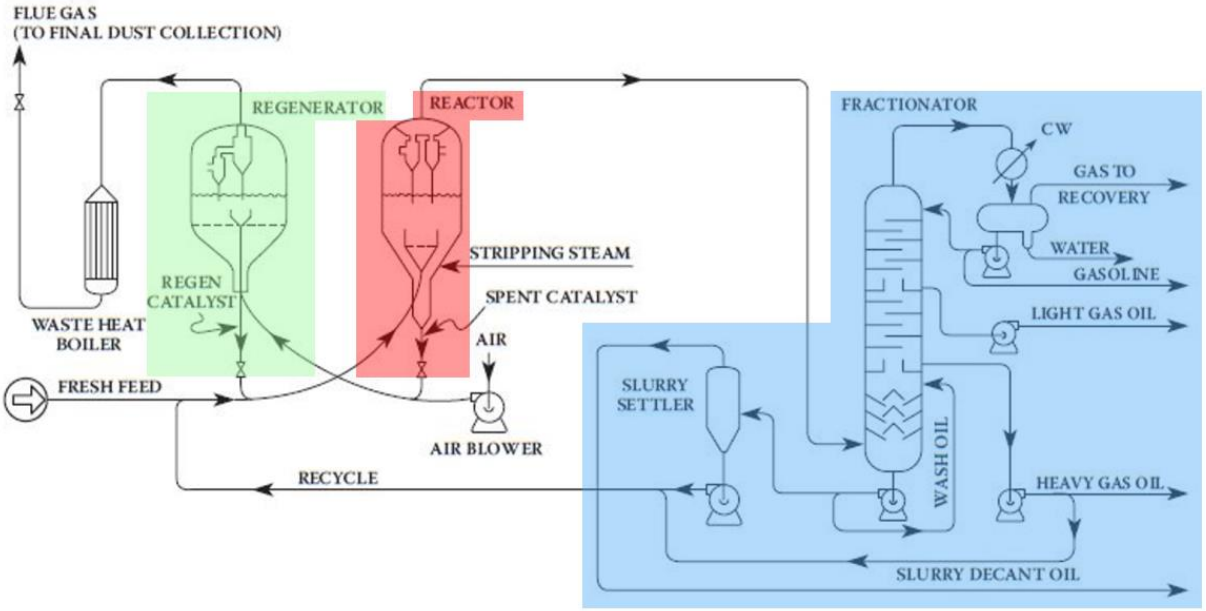

Figure 4: The FCC process, adapted from [19]

3.1.1 Reactor (Riser)

In the riser, which is designed as an entrained flow reactor, the endothermal cracking reactions take place. In today’s FCC units, bottom-up riser arrangements are most common, meaning that catalyst and feedstock are introduced in the bottom section and the cracking products as well as the spent catalyst are withdrawn on top of the reactor, thus explaining why the reactor is called a “Riser”. During the residence time of a few seconds all cracking and recombination reactions take place.
The process begins at the bottom, where the preheated feed is introduced into the reactor pipe and encounters the hot catalyst. The feed evaporates instantly, thereby increasing its volume massively and carries the catalyst particles with it through the riser. After the catalyst and feed mixture have passed the riser it enters the freeboard section, where catalyst and products are separated. The used catalyst falls into a return pipe and is headed towards the regenerator. The product gases are further dedusted by cyclones or similar units and are then routed to the fractionation unit.

3.1.2 Regenerator

During catalytic cracking coke deposits form and accumulate on the catalyst particles. These coke deposits block the evaporated feedstock from entering the active sites on the catalyst, thereby deactivating it. To reactivate the catalyst, it is transferred to the regenerator section.

Here the catalyst is fluidized by steam and air to burn the coke depositions and reactivate the catalyst. This process is done in a fluidized bed to utilize the good material and heat transport properties of such aerated beds. As a side effect the produced thermal energy is used to increase the temperature of the catalyst to the high temperatures needed in order to start and sustain the cracking processes in the riser. Additionally, the excessive heat produced in the regenerator is often used to preheat the feedstock or to produce steam.
The regenerated, and thereby reactivated, catalyst is fed back into the bottom of the riser.

3.1.3 Fractionation

As it is common for many refinery processes the FCC process produces a broad product spectrum instead of single products. This spectrum consists of various products in various configurations. To separate these a rectification column is used, fractionating the spectrum into the fractions described in section 3.3.

3.2 Advantages of fluidized bed systems compared to solid bed systems

Fluidized bed systems offer certain advantages over solid bed or moving bed approaches.
To name a few, fluidized beds offer:

High heat and mass transfer in fluidized beds

Due to good aeration and penetration of the catalyst bed by air and steam, a very uniform burning of the coke deposition on the catalyst particles is possible. This results in stable process conditions and product yields.

High catalyst activities due to short contact times and turbulent contact in the reactor section

The freshly regenerated catalyst has a high activity. When the catalyst comes into contact with the feedstock, coke depositions form on the catalyst particles and reduce the activity thereof. By operating the reaction section in a dilute phase fluidized bed, contact time between feed and catalyst is very short. Additionally, the contact itself between feed and catalyst is very turbulent, resulting in a fast border layer renewal rate. This aids the cracking process by removing products exiting the catalyst particle and supplying uncracked feedstock to the catalyst very fast.

Reaction and regeneration section operate in a relative equilibrium

This results in very stable process conditions and product yields by decoupling the production rates of light or heavy products from residence times. For example, solid bed reactors start with fully regenerated catalyst, resulting in high reaction rates and tending to lighter products. Over time the catalyst gets deactivated, which results in slower cracking reactions and in heavier product spectrum. In a fluid catalytic cracking reactor each catalyst particle is regenerated after one pass of the riser section, resulting in minimal fluctuations of the activity from the bottom to the top and overall operation at a nearly equilibrium state.

3.3 Products of the FCC process

Product	*Consists of*	*Boiling range (approximation)*
Fuel gas (dry gas)	C1 – C2 hydrocarbons	n.a.

Fuel gas, also often called “dry gas”, describes a gaseous hydrocarbon product faction which consists mainly of C1 and C2 hydrocarbons (methane, ethane and ethene), hydrogen and hydrogen sulfide (H_2S). This low-value fraction is often used as fuel gas in the refinery after a cleansing step to remove often present contaminants such as H_2S. A high hydrogen content can be separated from the dry gas (e.g. by membranes or pressure shift adsorption units) and used in hydrotreatment units.
Dry gas can contain non-condensable gases such as N_2, CO, CO_2 and O_2.

LPG (Liquified petrol gas)	C3 – C4 hydrocarbons	< 20 °C

This gaseous fraction contains mostly C3 and C4 hydrocarbon gases. Unsaturated hydrocarbon gases are called olefins and are a main building block for the petrochemical industry, especially the polymer industry. Propene (unsaturated C3 hydrocarbon gas) and butenes (unsaturated C4 hydrocarbon gases) are base chemicals for polypropene (older name polypropylene) production or alkylation and fuel production. These gases represent a very valuable product fraction of FCC units.

Gasoline	C5 – C12 hydrocarbons	20 – 215 °C

Gasoline is the main product of the FCC process, accounting for approximately 55 %wt of the overall product yield of the process (strongly depending on the process conditions and type of feedstock) [20]. Although the octane number (often referred as MON and RON) of FCC gasoline is relatively high compared to straight-run gasoline, modern engines require even higher octane ratings. For this reason FCC gasoline is today a major blending component for commercially available gasoline besides reformate, pygas (pyrolysis gasoline), alkylate etc. An important benchmark of gasoline is its sulfur content. FCC gasoline is, depending on the type of used VGO, the main source of sulfur in the commercially available gasoline, which requires desulfurization steps of either the FCC feedstock or the product (often via hydrotreatment)

Light cycle oil (LCO)	C12 – C20 hydrocarbons	215 – 320 °C

Light cycle oil has a diesel-like boiling range and due to its low cetane number (approximately 15 – 25) it can be used as a low quality blending agent to diesel fuel. It has a high aromatics content and is often recycled into the reactor of the FCC unit or upgraded via hydrotreatment.

Residual oil/ Slurry	> C20 hydrocarbons	> 320 °C

Residual oil and slurry are very low-value products of the FCC process and are very often recycled into the FCC plant, partially to pre-heat the fresh feedstock.
Residual oil can be upgraded in a hydrocracker if its economically feasible.
Depending on the type of VGO, slurry contains sulfur, high amounts of ash from carried-over catalyst particles and consists almost entirely of aromatics.

Coke	n.a.	solid

Coke is an unwanted by-product of the FCC process and at the same time essential for operation of the process unit. Coke consists of various very heavy, often aromatic hydrocarbons formed on catalyst particles by secondary cracking and condensation reactions. Coke provides the necessary process heat, needed to start and conduct the endothermic catalytic cracking reactions in the riser section. Apart from that, the regeneration unit is very often highly integrated in process heat recovery and heat integration efforts in refineries.
During the cracking process coke depositions form on and in the catalyst particle and thereby partially deactivate it. Burning of the coke so not only provides the required heat for the FCC unit, but it also reactivates the catalyst.

3.4 Catalysts

3.4.1 General

In the beginning of FCC, synthetic clay catalysts were used, consisting of amorphous silicon dioxide and aluminum dioxide. The catalysts act as solid acids, providing acidic caverns inside their crystal structure where the catalyzed cracking reactions occur. These synthetic clay silica-alumina catalysts have a lower acid site density (resulting in a lower acidity) and a lower surface area than the also silica-alumina-based modern zeolites. Amorphous silica-alumina catalysts are mesoporous with a broad pore-diameter distribution. Due to their larger pore size and volume, these catalysts offer adequate diffusion to large hydrocarbons [21].

3.4.2 Modern zeolite catalysts

Today's catalysts are fine powders with average particle sizes of approximately 75 µm. They consist of the following compounds.

- Zeolite
- Matrix
- Filler
- Binder

Zeolites

Influence selectivity, activity and product quality

In the 1960s zeolite-based catalysts revolutionized catalytic cracking by increasing the activity by an order of magnitude and improving the selectivity significantly compared with the former clay catalysts. The key to this development, and thereby the breakthrough of FCC in refining, is zeolite Y which provides more profitable liquid product yields and additional refining capacity.

Zeolite Y is a molecular sieve with a well-defined mesh structure. Compared to the mesoporous pores of the formerly used artificial clay catalysts with pore sizes between approximately 3 to 20 nm, the zeolites have pore sizes smaller than 1 nm (8 Å), thereby limiting the size of the hydrocarbon molecules able to enter. The network of pores inside the zeolite structure amounts to an approximate size of 600 m²/g [22], [23].

As previously stated, the catalytic activity is based on the zeolites acidity. The acidity has its origin in the synthesizing process of the zeolite. Soda Y zeolite is synthesized from a sodium

hydroxide containing solution. However, soda Y (also called NaY) zeolite is not hydrothermally stable and ammonium ions are often used to replace the sodium ions. During drying of the zeolite, the ammonium is vaporized, revealing both Brønsted and Lewis acid sites. The acid sites are depicted in the following figure. Often the Brønsted acid sites are exchanged to some degree by rare earth metals to modify some of the catalysts' properties.

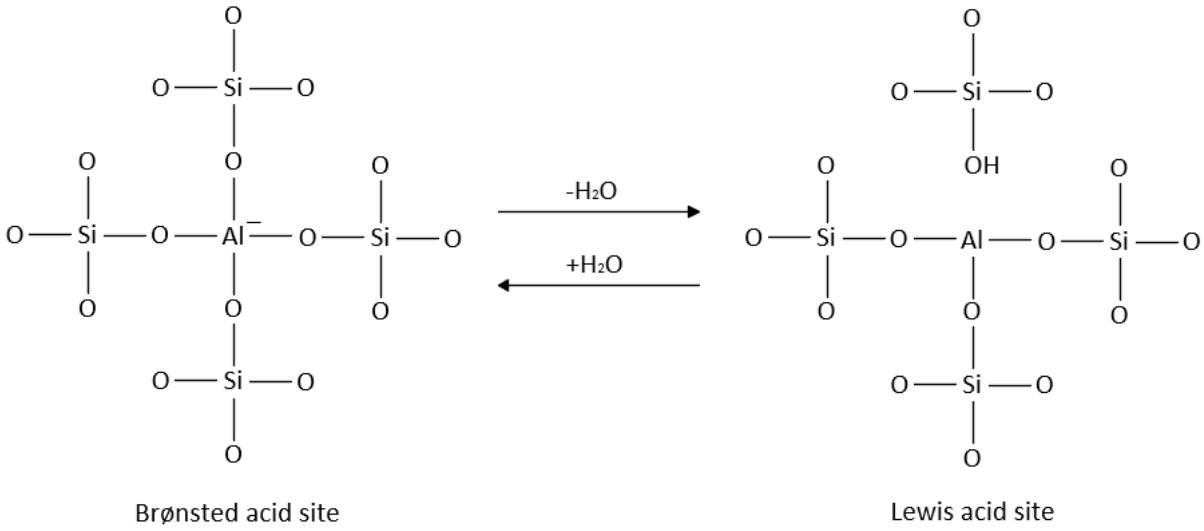

Figure 5: Active sites on a zeolite

Pic Catalyst sites

There are various types of zeolites of which only the types X, Y and ZSM-5 have applications in FCC. Due to its lower thermal and hydrothermal stability type X has virtually disappeared from catalyst manufacturers product portfolios and todays FCC catalysts rely on type Y and ZMS-5 zeolites [23].

Matrix

Can improve cracking of heavy hydrocarbons and offers resistance to contaminants

The zeolite crystals in a catalyst particle are integrated in an agglomerate with other materials with various tasks. One of these materials is called matrix. When the matrix contributes to the catalytic activity of the catalyst it is called an active matrix. Active matrices are often amorphous and contribute significantly to the performance of a catalyst. As previously mentioned, zeolites have a very narrow and well-defined pore size, which restricts the size of the molecules able to enter the active zones inside the crystal to substances with a boiling point below 482 °C. By providing the primary cracking sites, active matrices pre-crack hydrocarbons on their way through the matrix to the zeolite and thereby maximize the effectiveness of the catalyst [23].

Filler

Provides physical strength and modifies the catalysts activity

Fillers are incorporated into the catalyst particle to modify physical properties of the catalyst particle, e.g. attrition resistance, particle size distribution and density. Another purpose of the filler is to lower the activity of the particle in order to optimize the product yield distribution. [23]

Binder

Glues zeolites, matrix and fillers together

Binders are used to combine the zeolite crystals with the matrix and the filler. Binders can be catalytic active. [23]

3.5 FCC Parameters

As previously mentioned the catalysts activity, selectivity and product spectrum depends heavily on the catalysts components. However, there are other factors influencing the mentioned parameters, such as deactivation via deposited coke or the addition rate of fresh catalyst to the process or the feedstocks quality regarding deactivating contaminants.
A minimization of remaining coke deposits on the catalyst particles leaving the regenerator section of the unit is desired. The removal of the coke maximizes the catalysts activity and selectivity and therefore improves product yields.
Another variable is the addition rate of the fresh catalyst, although in some units only the catalyst losses are compensated with fresh catalyst and no “spent” catalyst is extracted from the process. Catalyst losses occur due to the imperfect separation techniques to separate catalyst from the product streams. As a rule of thumb, particles smaller than 20 µm cannot be separated from the stream by primary and secondary cyclones and, thus, are carried over to downstream processes and out of the FCC unit. Tertiary catalyst recovery devices are not very common. Nevertheless, to maintain the desired parameters fresh catalyst with slightly different properties can be added, for example with a higher activity. This can be done to equalize slight changes in feedstock quality or concentration of catalyst-deactivating contaminants present in the feedstock like heavy metals. [23]

The complex FCC process can be influenced via various parameters to maintain the desired product spectrum in terms of quality and quantity while operating the FCC plant in its optimal point of operation.

Reaction temperature

The cracking temperature is one of the most important parameters in the FCC process. It is optimized to various other parameters such as feedstock quality and feeding rate, feedstock preheat temperature, regeneration temperature of the catalyst and catalyst to oil ratio. As a rule of thumb, an increase in the reaction temperature leads to a higher severity, which leads to an increased conversion. As a result, the proportion of higher-boiling fractions decreases, while the fraction of gaseous products increases. The reason for this is the endothermic nature of the β-scission, meaning that the probability of occurrence of this reaction is increasing with rising cracking temperatures.

For each combination of feedstock, catalyst, etc. there is a maximum in the naphtha production rate. Whether the naphtha fraction formed increases or decreases with a variation of the cracking temperature depends essentially on whether the naphtha maximum has already been exceeded or not.
Increasing the reaction temperature increases the olefin and aromatics fraction in the naphtha, which results in an increased octane number of the resulting gasoline. This can be attributed to an increased dehydrogenation rate of cycloalkanes.

In contrast to the naphtha yield, the coke production rate passes a minimum when the temperature is increased. This can be explained by a reduced desorption of precursors from the catalyst surface, resulting in longer residence times and an increased probability to produce polycyclic aromatic hydrocarbons (PAHs), a precursor of coke. When the temperature exceeds a certain limit the coke yield increases again due to a higher reaction rate.
The impact of higher reaction temperature is usually also a decreased LCO yield due to the higher severity and the shift to generally lighter products. [19], [24], [25]

Preheating of the Feedstock

Preheating of feedstocks is often used to maximize heat integration in refineries in general. The FCC feedstock is preheated by a network of heat exchangers operated with different hot streams and/or by using an external heating source (e.g. by fuel gases from the refinery). The maximum preheating temperature is limited to approximately 400 °C to avoid thermal cracking reactions, which typically start at (approximately) this temperature. The preheating of the feedstock introduces additional energy into the cracking process, potentially influencing some of the other parameters of the FCC unit. The preheating temperature has a decisive influence on the evaporation of the feed and must therefore be adapted to its boiling point. If the feed temperature is too low, there is a risk that the feedstock does not evaporate when comes into contact with the catalyst, resulting in a conversion directly into coke. If the feed temperatures are too high, undesirable coke deposits can form in the preheating furnace or the heat exchangers.

Recirculation of products

One parameter which directly influences the product spectrum of the process is the recirculation rate of the plant. Recirculation of low-value products such as light and heavy cycle oil or residual fractions can be used to optimize the product spectrum and maximize the capitalization of the feedstock. The recycled feedstocks are very aromatic, therefore other parameters of the plant might need to be optimized.
With the zeolite catalysts used today, the maximum conversion is reached at process conditions under which secondary reactions are not present to a high extent. For this reason, modern, non-residual FCC plants are normally operated at relatively low recirculation rate.

Feeding rate

Increasing the feed mass flow reduces the contact time with the catalyst, since the velocity of the hydrocarbon vapors in the reactor increases. The selected feed mass flow rate is therefore decisive for the residence time of the hydrocarbons in the riser. Likewise, the catalyst to oil ratio is influenced by a change in the feed mass flow rate. This can suppress thermal cracking reactions that take place in the downstream plant components. For economic reasons, industrial FCC plants are always operated with the maximum feed mass flow rate.

Catalyst activity

Due to deactivation and fouling of the catalyst a certain exchange rate of the catalyst is needed to retain the overall activity of the catalyst bed.
As previously mentioned, the catalyst activity can be maintained via addition of fresh catalyst or catalyst with different properties to the circulating catalyst bed.

Catalyst to oil (C/O) ratio and catalyst circulation rate

The C/O ratio describes the ratio of the mass flows of catalyst and feed used. Typical C/O ratios range from 4-12. In industrial FCC plants, it is mainly influenced by coke production, which is an essential part of the heat balance of the cracking process. The occurring effects of a changed C/O ratio cannot be considered in isolation, but always need to be seen in the context of the additional variations induced by the other process variables .

Regeneration Temperature

The regeneration temperature depends on the produced coke, the allowable delta coke (meaning the coke which remains on the external and internal surface of the catalyst particle) and therefore the aeration rate of the regenerator. Additionally it can be influenced by catalyst coolers and multi-stage regeneration approaches.

Feedstock type and quality

The type and quality of the feedstock has an inherent influence on the technical and economic aspects of FCC operation. The versatility of the FCC process makes it the swiss-army-knife of the refinery. The non-extensive list of possible feedstocks includes heavy- and light vacuum gas oil, heavy gasoil, de-asphalted oil and heavy fractions or residues such as visbreaker distillate and heavy coking oils. Current research focuses on gaining valuable products from even heavier, more complex and recycled feedstocks. The processing of lipid-based bio oils or pyrolysis oils, made from highly problematic municipal plastic waste or from lignocellulosic biomass is thus the next logical step in the evolution of the process.

3.6 Feedstocks of the FCC process

The feedstock has an impact on a process' sustainability and eco-friendliness. The types of feedstock utilized for this work are depicted in the following figure 6.

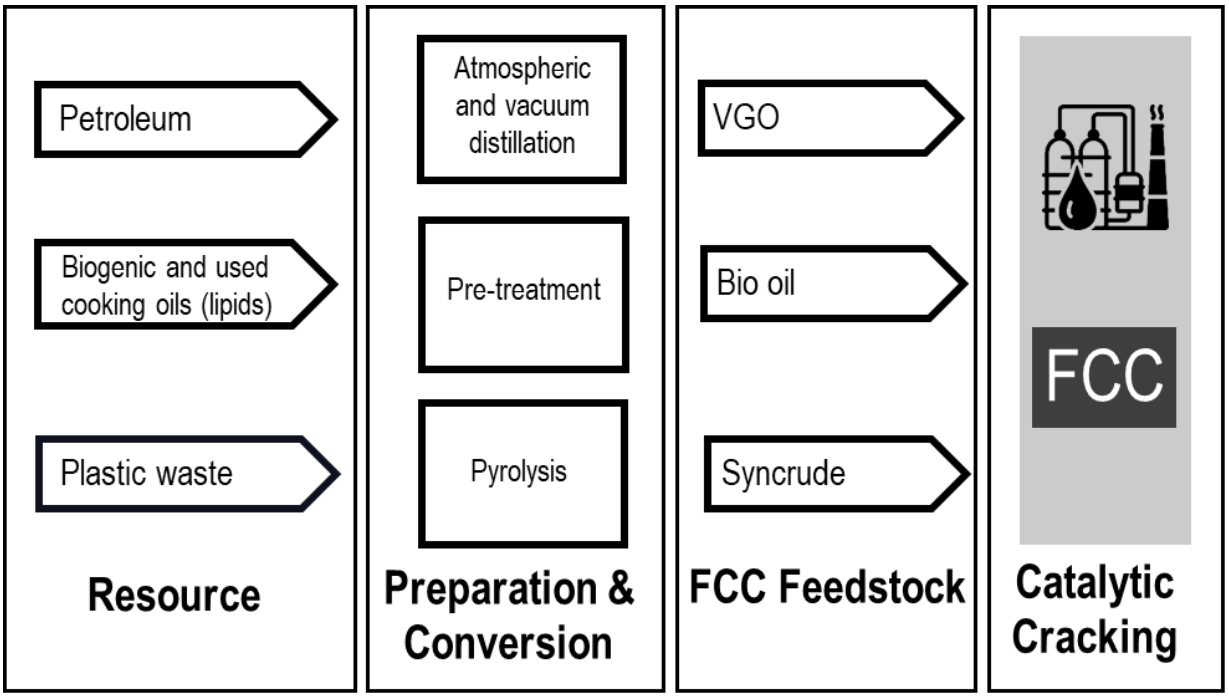

Figure 6: Alternative feedstocks for FCC

3.6.1 Petroleum-based feedstock

The regular feedstock for the FCC process is a heavy petroleum fraction, typically vacuum gas oil (VGO). Vacuum gas oil is the top fraction of the vacuum distillation unit upstream of the FCC process with a boiling range between 350 and 560 °C. VGO is a mixture of many organic substances. VGO predominantly consists of paraffines, cycloalkanes (also often referred to as "naphthenes") and aromatics. Depending on the versatility of the FCC unit also fractions of other refinery processes can be utilized, depending of the boiling range and the degree of contamination of the additional feedstock.
To remove contaminants a hydrogenation step is often conducted either on the feedstock or on the products of the FCC process. Hydrotreatment of the feedstock comes with the advantage of removing possible catalyst poisons (such as heavy metals and sulfur) upfront and thereby

increasing the catalyst lifespan. Additionally it reduces the amount of contaminants entering the regenerator section, reducing the needed flue gas treatment.

3.6.2 Biogenic Feeds

Biogenic feeds can be divided into lipid-based feeds and pyrolized lignocellulosic feeds. For more information and research regarding lignocellulosic biogenic feedstocks the work of H. Lutz [26] and M. Buechele [27] can be recommended.
Lipid based biogenic feedstocks are well known within the FCC world. Lipids have a clear structure and a well-defined behavior inside FCC units [28]–[30]. Their physical properties match those of fossil feedstocks for the FCC unit relatively well and co-processing is technically feasible. They are virtually free of contaminants such as sulfur or heavy metals, although they introduce a certain amount of oxygen into the FCC process, thereby posing technoeconomic challenges for refiners.

Vegetable oils

Vegetable oils consist of triglycerides, which are esters of the trivalent alcohol glycerol and three fatty acids. Small amounts of mono- or diglycerides, free fatty acids and other substances can be present.

Fatty acids can be characterized by the number of double bonds present on the aliphatic chain. In general, it can be stated that double bonds on the fatty acid increase its reactivity and lower the melting point of the triglyceride. The below depicted stearic acid is a saturated fatty acid, whereas the shown oleic acid is a monounsaturated fatty acid and linoleic acid is a polyunsaturated fatty acid.

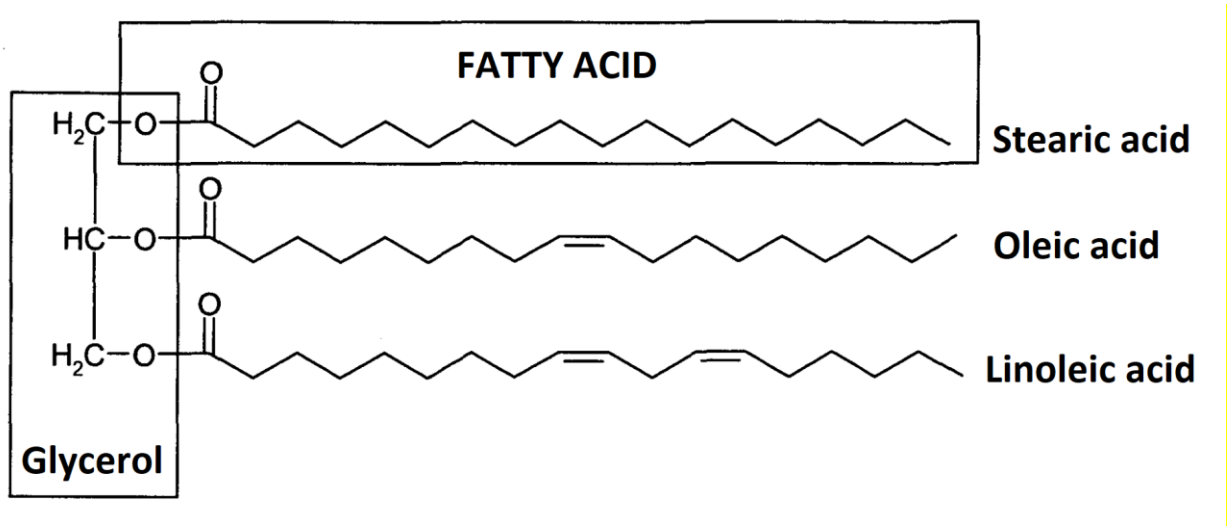

Figure 7: Triglycerol molecule, adapted from [30]

Triglycerides differ in their fatty acid composition, which is the main factor determining their physical properties. In the depicted triglyceride in Figure 7 three different and very common fatty acids can be seen. Analogous to other hydrocarbons the fatty acids can be present in various length and degree of saturation.
A first characterization can be done based on the number of carbon atoms of the aliphatic chain of each fatty acid. Based on their number the acids are:

- Short-chain fatty acids (SCFA)
  SCFA are defined by an aliphatic tail of a length of 2 to 6 carbon atoms. They are produced by gut bacteria through metabolic pathways during fermentation of polysaccharides and have anti-inflammatory, antitumorigenic and antimicrobial effects [31], [32].

- Medium-chain fatty acids (MCFA)
  MCFA are either saturated or unsaturated fatty acids with a length from 6 to 12 carbon atoms on the aliphatic tail [32]. Similar to SCFAs they have an important role in metabolism and fermentation, especially in the production of ketones [33]. In comparison to long-chained fatty acids they have a lower melting point and provide slightly lower energy [34].

- Long-chain fatty acids (LCFA)
  LCFA have more than 14 carbon atoms and can be either unsaturated or saturated. Naturally unsaturated fatty acids have the double bonds in a cis configuration, whereas technically processed fatty acids often have double bonds in trans configuration, resulting in so-called trans-fats [32], [35].

Used cooking oils

To avoid a food versus energy debate (often referred as “tank vs plate”), used cooking oils (UCO) come into the focus when it comes to bio oil integration into refinery processes. In this perspective, bio FCC competes against the established fuel production pathways from UCO, namely biodiesel and hydrotreated vegetable oil.

Throughout their lifespan and application as cooking oils, bio-oils endure continual exposure to harsh conditions. The exposure to high temperatures, the presence of oxygen, light (especially UV light), as well as the presence of prooxidants and biological activity from bacteria or enzymes cause alterations to the triglycerides, collectively referred to as rancidity [36].

In more detail, fat and oil deterioration can be caused by the following mechanisms:

Hydrolytic cleavage

The initial stage of lipid deterioration is characterized by hydrolytic cleavage, whereby moisture and either the fat-cleaving enzyme family of lipases, increased levels of free fatty acids, acidic or alkaline conditions cause the breakdown of triglycerides into glycerol and free fatty acids (FFAs) in a process called lipolysis. Incomplete cleavage of the fatty acids from the glycerol residue can result in the formation of mono- or diglycerides, which have detrimental effects on the overall quality of the lipids. Lipase can be deactivated to a great degree by temperatures of approximately 72 °C and be totally deactivated at 80 to 82 °C [36].

Autoxidation

The presence of unsaturated (especially di-unsaturated and poly-unsaturated) fatty acids, free fatty acids, oxygen, increased temperatures, light and the presence of prooxidants speed up autoxidation over the lifetime of the lipids. Autoxidation is a gradual process that does not occur suddenly. Prooxidants such as iron or copper ions accelerate the start of the process. The same applies for the presence of free fatty acids, direct sunlight or light from fluorescent tubes or other UV light emitting sources [36], [37].
However, once the chain reaction is triggered, deterioration occurs at a fast rate via a radical reaction mechanism where a fatty acid radical is formed. The so-called initiator radical (R·) reacts with oxygen to a peroxyl radical (ROO·). Through propagation steps the reactions lead to hydroperoxides. The unstable hydroperoxides break down further to fission products such as

aldehydes and ketones among others. Aldehydes and other volatile products are characterized by strong and unpleasant odors and flavors and are main contributors to the sensory perception “rancid”. Additionally, some of the products (especially the peroxides) can be toxic. [37].

Microbial deterioration

To protect oils and fats from deterioration via autoxidation cool, dry and dark places offer the needed storage conditions. These conditions can be a habitus for microorganisms to spread. A characteristic of these organisms is their ability to produce extracellular lipases with a relatively high temperature resistance. Lipases in fats and oils split triglycerides in a process called lipolysis, producing the products described above for hydrolytic deterioration of lipids. [38], [39]

3.6.3 Municipal plastic waste as a feedstock for refineries

A challenge for the usage of municipal plastic waste in refineries is the composition of the feedstock. The type and degree of contamination of feedstocks coming from a post-consumer background is hard to predict. Pretreatment by means of sorting the feedstock to remove unwanted fractions is often required to provide a constant quality of base material for further processing.
This becomes especially important when it comes to residual waste from mechanical or solvent-based recycling plants. These feedstocks are often highly contaminated with organic and inorganic materials, bearing challenges on the one hand to the pyrolysis process itself and on the other hand to downstream process steps for the resulting pyoil such as hydrotreatment, FCC units or thermal/steam crackers. Additionally, the variations in the grade of contamination add another dimension of complexity to the topic of bringing such waste streams back into the value chain.

As mentioned before, an approach to the high degree of contamination can be excessive cleaning of the plastic waste feedstocks e.g. via NIR-sorting, decanting, washing or even hot caustic washing. Since these processes put enormous financial pressure on the overall value chain, rigorous cleaning of the waste may not be feasible.

Pyrolysis oil derived from plastic waste (so-called syncrude or pyoil) can be integrated into petroleum refineries. The integration of these pyrolysis oils into feed streams of refineries can omit the high financial barriers to circulation of plastic waste streams. Depending on the further pathway of the pyoil, a certain degree of circularity can be obtained. Highly contaminated plastic waste, which is otherwise designated to incineration, landfilling or bleeding into oceans through rivers can be upcycled in refinery processes to high quality products.

One possible pathway could be the production of previously mentioned pyoil followed by co-processing in an FCC unit to produce olefins, naphtha and heavier fractions. The olefins could be directly used to produce polyolefins, the most produced type of polymers. Due to the fact that in the RED II issued by the European Commission the production of fuels out of recycled feedstocks cannot be counted as recycling per se, further processing of the naphtha fraction is currently investigated by a high number of refiners, petrochemical producers and catalyst manufacturers. One idea is to send the naphtha fraction to a steam cracker to produce mainly ethene and propene. From these the path continues to polyethene (also called polyethylene) and polypropene (also called polypropylene) and a various number of other polyolefinic polymers and copolymers.

Mechanical recycling of plastic waste

Recycling of plastic is at the same time one of our biggest challenges as well as one of the biggest opportunities for the next decades to come. Recycling of abundant plastic waste via mechanical processes bears chances for more sustainable feedstock for plastic goods in the

future. Mechanical recycling techniques require a certain feedstock quality in terms of purity, type of contamination and degradation. In the feedstock preparation section of mechanical recycling plants a big amount of feedstock is sorted out because it is either a contaminant, not the required type of plastic or it was ejected by the sorter unintentionally as “bycatch”. Pyrolysis could allow these residues from mechanical recycling to be used as feedstocks for chemical plastic recycling in the future.

Chemical recycling of plastic waste

Another future source of feedstock for chemical plastic recycling via pyrolysis can be heavily degraded mixed plastic waste from landfills, illegal landfills and plastic waste collected from rivers and the oceans. These “second choice” feedstocks can find their way back into the value chain by chemical recycling by breaking down the polymers (and indeed all other organic molecules and macromolecules such as fats, cellulose or lignin among others) to smaller molecules via pyrolysis.

At the moment there are numerous approaches to chemically breaking down organic matter (such as polymers or biomass) to intermediate products (such as liquids or gases) suitable for processing in upgrading steps. Amongst others there is:

- Chemolysis
  Hydrolysis or solvolysis of (mainly) polycondensated and polyadded polymers. This chemical recycling method is currently used in industrial-sized process units for polyethene terephthalate (PET) [40], [41].

- Bio enzymatic plastic recycling
  Specialized enzymes called depolymerase are used to break down the polymer chains to shorter molecules. At the moment this technology is not applied in industrial-sized application due to too low enzymatic activity (and therefore low decomposition times) and the need for highly specialized enzymes for each polymer type [42], [43].

- Catalytic pressure-less depolymerization (CPD)
  CPD works with a broad spectrum of feedstocks such as plastics, biomass and other organic waste. The feedstock is mixed with an alkali-doped silica-alumina catalyst and $Ca(OH)_2$ for pH moderation and decomposes in a reactor at approximately 270 to 320 °C. The process is prone to water contents higher than 5 %wt in the feedstock [44].

- Gasification
  Gasification is a very versatile process, offering numerous recycling pathways to a vast amount of organic feedstocks. The process itself is relatively simple. In most cases organic matter is gasified to syngas ($CO + H_2$) via under-stoichiometric combustion ($\lambda < 1$). The syngas can then be converted to hydrocarbons such as synthetic natural gas or Fischer-Tropsch fuels and -waxes among others [45]–[47].

- Pyrolysis
  one of the currently most mature technologies on chemical recycling of plastic waste is pyrolysis.
  Due to the importance of pyrolysis and pyrolysis oil for the conducted experimental work, pyrolysis is explained in more detail in the following chapter 4.

4 PYROLYSIS

While pyrolysis itself is known for centuries the recent societal awareness regarding emission of climate-active gases, sustainable energy and chemicals demand and the strive towards a circular economy placed emphasis of liquid pyrolysis products that can be used as precursor for liquid fuels, chemicals polymers.

Pyrolysis is a thermal degradation process of solids (or liquids) where large and complex molecules degrade into smaller molecules at temperatures between 300 to 650 °C. To prevent the formation of oxides the absence (or near absence) of oxygen is essential. Under these conditions random chain scission (promoting the formation of liquid products) and β-scission (promoting the formation of gaseous products) occurs, resulting in a random generation of free radicals. By means of secondary reactions this leads to the production of alkanes, alkenes, dienes, aromatics etc. Depending on the feedstock and the desired product range several factors of the process can be adapted.[48]

4.1 Pyrolysis Parameters

4.1.1 Temperature

Due to the nature of the occurring thermal cracking reactions temperature is one of the most significant parameters. The process temperature governs the kinetics of the thermolysis of the long-chained macromolecules for the primary (decomposition and dehydrogenation) and secondary (isomerization and polymerization) cracking reactions. This strongly affects the distribution of the product yields and their quality. As described by Zhang et al [49] the increased temperature elevates the intensity of molecular vibration, inducing the cleavage of macromolecules to shorter molecules. This goes hand in hand with the release of free radicals, aiding the degradation of the polymer chains and facilitating the transition from solid to melt by means of depolymerization, β-scission, random chain scission and side group elimination reactions.[49]
Generally, it can be said that increased pyrolysis temperatures favor the formation of liquid product up to a point of approximately 450 to 560 °C, depending on further process parameters and feedstocks.[50], [51]
Beyond this temperature level the non-condensable gas yield increases. This can be explained by secondary cracking reactions of the primary fragments of the macromolecule chains, occurring due to the severe cracking conditions.

4.1.2 Heating rate and residence time

As previously mentioned, pyrolysis reactions can be categorized mainly as primary or secondary reactions. An important factor influencing the dominance of either of these reaction types on the product yields is the heating rate and the residence time. It can be stated that low to medium residence times, combined with low to moderate heating rates and moderate temperatures promote the dominance of primary reactions and thereby increasing the yield of liquid products. Under these conditions volatiles resulting from the primary cracking reactions stay in the heating zone of the reactor.
Depending on the specific process deviations of this rule may apply, for instance batch or continuous operation mode or presence of catalysts.

As a first rough classification of a given pyrolysis process the ratio between heating time and the pyrolysis reaction time can be used. Under such a premise a pyrolysis process can either be considered slow or fast, resulting in a classification as torrefaction, slow, fast or flash pyrolysis. [52]

Torrefaction is a mild pyrolysis process, utilizing temperatures between 230 and 300 °C. This thermal treatment improves the energy density, reduces the oxygen-to-carbon ratio, dries and partly devolatilizes the biomass feedstock. For example, roasting of coffee beans is done in a torrefaction process. [52]

Slow pyrolysis' heating rates and residence times can vary. Common to this form of pyrolysis is the focus on mainly solid product yields. An example of slow pyrolysis is carbonization, where heating rate is very low, residence time very long and temperature is relatively low (approximately 400 °C) to maximize charcoal formation.[52]
With higher heating rates, higher temperatures and shorter residence times the yields shift towards liquid and gaseous product yields. However, these lighter product yields are significant lower compared to fast pyrolysis. [52]

Fast pyrolysis is characterized by high heating rates, which can reach 1000 to 10.000 °C/s. At these heating rates the feedstock inside the reactor reaches the required pyrolysis temperature before decomposition at lower temperatures becomes predominant. Depending on the desired product range the target temperature can be below 650 °C for liquid product (typically in the range between 425 to 600 °C) or below approximately 1000 °C for gaseous products. Additionally fast pyrolysis can be characterized by a short residence time (in the order of under 3 s) and a rapid quenching of the product gas/vapor stream. [52]

Flash pyrolysis is an even faster process than fast pyrolysis. The feedstock is heated to 450 to 600 °C with a very short residence time of 30 to 150 ms. Due to the fast operation mode the liquid product yield can be maximized to approximately 70 to 75 %wt of the total product and char formation can be reduced. [53]
Especially the vapor residence time, meaning the time the volatile cracking products of the primary cracking reactions stay in the heating zone of the reactor, has a high impact on the product yields of flash pyrolysis. Here, shortening the vapor residence time by very fast quenching of the volatiles promotes the production of liquid products. [48]

4.1.3 Pressure

Raising or lowering the operating pressure influences the product spectrum of the pyrolysis process.
The principle of Le Chatelier states, that at an increased pressure reactions with less volatile products, such as liquids or solids, are favored over reactions with more volatile products such as gases. Lopez et al. [54] found, that pyrolysis of waste tires under vacuum conditions resulted in higher yields of gaseous products.
However, the influence of pressure on the product yields may not be as clear as the principle of Le Chatelier suggests. Murata et al. [55] and Cheng et al. [56] found, that increased pressure raises the amount of gaseous products for pyrolysis of some plastic feedstocks.
Miranda et al. [57] and Parku et al. [58] reported that reduced pyrolysis pressures can be linked to a significant increase of waxy pyrolysis oils, which are composed of long-chained alkanes and alkenes with high boiling points and C-chain lengths >C20. Such waxy oils often require further cracking and could be a suitable feedstock for processing or co-processing in FCC units.[59]
Due to the associated costs of compression and decompression, pyrolysis is predominantly done at atmospheric pressure. [48]

4.1.4 Catalyst

Optimizing energy consumption is essential for new technologies to gain leverage in the market, reduce the energy demand of the process and replace formerly common technologies. Introducing catalysts into the process is often the way to go. [60]

The most common catalysts used for pyrolysis applications are either solid acid or solid base catalysts, including silica-alumina (SA-1), zeolites (natural zeolite, zeolite-Y, ZSM-5, HZSM-5, spent fluid catalytic cracking catalysts etc.), metal oxide catalysts (such as magnesium oxide, nickel-alumina) minerals (kaolin, clay) and fly ash.
In general, Peng et al. states that polyolefins are easier to crack with acidic catalysts such as zeolites, clays or fly ash. A possible reason for this may be that solid acid catalysts could be more efficient in depolymerizing polymers into monomers and chemicals such as styrene and toluene. [61], [62]

4.1.5 Reaction atmosphere

The reaction atmosphere is usually inert, consisting of N_2, because it is safe to handle and bears lower costs compared to alternatives (e.g. Ar or He). Such inert carrier gases do not take part in the pyrolysis itself but in transportation of products (volatiles) and in controlling secondary reactions.[48]
However, reactive atmospheres are also very common to influence the pyrolysis process. H_2 has shown certain capabilities in reducing the char formation due to suppressing polymerization reactions via reactive radical quenching. [63]

4.1.6 Feedstock and feedstock properties

One of the major influences on the product yields regarding either physical state or chemical composition are type, quality and physical properties of the feedstock.
Different types of feedstocks can be described via proximate analysis, taking into account the various compositions of the feedstock by reporting the moisture content, the fixed carbon, volatile matter and the ash content of the feedstock.[60]

The ratio of volatile matter of the overall feedstock influences the production of liquid products directly, meaning that a relatively high amount of volatile matter increases the liquid product yield. In contrast to this is the ash content. A high amount of ash in the feedstock (such as inorganics like glass, sand, pigments, fillers such as chalk or talcum) reduces the yield in liquid products.[60]

Pyrolysis of plastic feedstocks produces high yields of liquid products and one of the reasons for this can be the low permeability of gases through plastics. Unlike biomass, plastics have no pores in which pyrolysis products can be trapped. This would increase the residence time, increasing the potential for secondary cracking reactions and thereby increasing the potential for char production.[52]

5 CRACKING OF HYDROCARBONS IN GENERAL

Analogous to pyrolysis, where organic molecules are broken down to shorter fragments by means of thermal energy and optionally a catalyst, the average carbon chain length for hydrocarbons derived from petroleum can be reduced by multiple methods. When these techniques are applied on petroleum and its derivates this is called cracking. There are two major techniques for petroleum cracking: thermal and catalytic cracking.

5.1 Thermal cracking

Thermal cracking is the splitting of higher-boiling fractions into lower-boiling products by (controlled) thermal decomposition. In the past, thermal cracking was used to increase the petrol yield but it was replaced by catalytic methods due to certain advantages regarding yield, energy input and product quality.
Although thermal cracking was surpassed by catalytic cracking methods for fuel production it still plays a major role in olefin production in form of modern steam cracking units. Steam crackers are basically furnaces, in which ethane, LPG or naphtha is mixed with steam and pushed through the hot coils of the reactor at approximately 850 °C. The high temperature is combined with a very short residence time followed by (often several) quenching steps to minimize secondary cracking reactions. [64]
Steam cracking is today the major source for light alkenes, such as ethene and propene. Steam is used as a diluent to lower the hydrocarbon partial pressure and thereby suppress the formation of coke by inducing a gasification reaction instead.[65]
However, due to the lower propene yield (compared to the ethene yield) of the process, the high demand of propene as a petrochemical feedstock and the ever-rising capabilities of modern FCC catalysts to provide high yields of olefins (mainly propene and butenes) FCC has surpassed steam cracking as the major propene source in the United States. [20], [64]

Thermal cracking is based on the fact that the bonding energy between two carbons is between 330 and 360 kJ/mol compared to the one between a carbon and a hydrogen atom which is between 380 and 400 kJ/mol. The cleavage of a C - C bond is therefore energetically favored, and occurs statistically more often than the cleavage of a C - H bond. The cleavage tends to take place at the end of the chain, resulting in increased production in the C1-C3 region (see Figure 18). The products are gases, petrol, coke and heavy residual oils. The product composition of the process can be controlled by varying the residence time in the reactor.

Since thermal (steam) cracking is a major source for olefins, one of the main groups of base petrochemicals for polymer production, the main reactions occurring during the process are described in the following paragraphs.

In the initiation step the organic molecule undergoes homolysis because of excessive molecular vibration due to the input of thermal energy into the molecule as seen in equation (1).

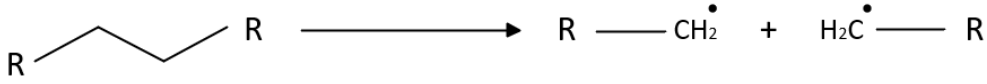

(1)

The resulting uncharged molecules with an unpaired electron each are called free radicals. Those free radicals are highly reactive and therefore short-lived. The reactivity of the formed radicals strongly depends on the position where the homolytic cleavage in the base hydrocarbon occurred.
Depending on the number of organic residues covalently bonded to the radical-forming C-atom the radicals can be organized according to their respective reactivity. This can be explained by inductive effects of the neighboring carbon groups.

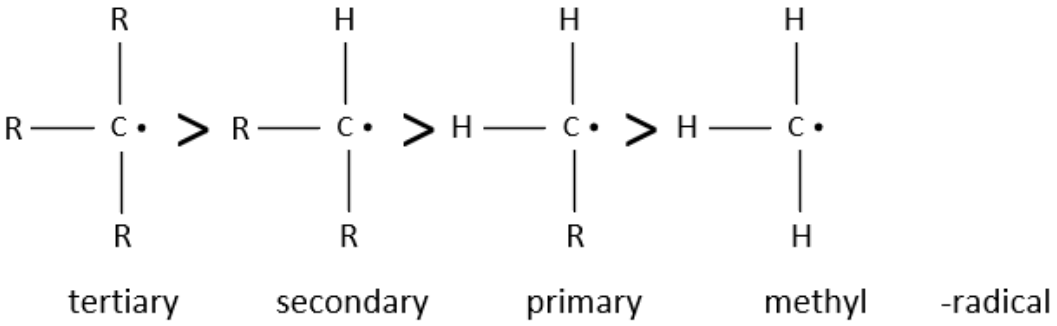

(2)

Tertiary radicals are the most stable of the shown radicals due to the three stabilizing organic residues attached to the radical carbon atom.

As previously mentioned, these radicals are short-lived, performing further reactions to stabilize themselves by means of hydrogen abstraction, α- or β-scission or polymerization.
Hydrogen abstraction means that the radical abstracts a hydrogen atom from another hydrocarbon molecule to form a short-chained alkane and another radical.
A reaction via α-scission leads to the formation of a very unstable methyl radical, which tends to hydrogen abstraction from another molecule, and therefore methane formation. As a result the H-donating molecule becomes a secondary or tertiary free radical. α-scission is thermodynamically disadvantaged compared to β-scission and therefore not the preferred reaction path. Nevertheless, α-scission occurs in thermal (steam) crackers.[66]
The scission positions are depicted in the following figure.

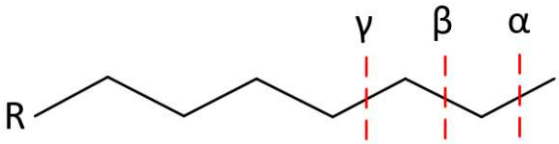

Figure 8: Position of α-, β- and γ-scission in a paraffinic molecule

The thermodynamically preferred path is cleavage via β-scission, leading to the creation of an ethene (ethylene) molecule and a new primary radical.

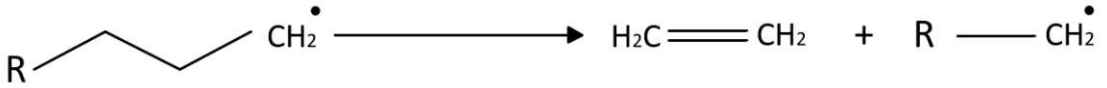

(3)

The newly formed radical can then proceed with the cracking reactions, propagating the thermal cracking reaction.
The reactions are stopped either by polymerization, forming coke, or via annihilation of two radicals.

Radical cracking reactions of hydrocarbons preferably produce C1 and C2 hydrocarbons with a high amount of olefins. Due to less favorable reactions paths isomerization only occurs to a low extent, resulting in low fuel quality of the liquid cracking product and thereby paving the way for catalytic cracking approaches regarding fuel production.

5.2 Catalytic cracking

One of the main differences between catalytic and thermal cracking is that in catalytic cracking, carbocations (namely carbenium ions) are formed instead of radicals.

The formation of the carbenium ions takes place at the acid centers of the zeolite catalyst, whereby a distinction is made between Brønsted and Lewis centers. A Brønsted acid is defined by its ability to donate protons (proton donor). A Lewis acid can be characterized by its ability to accept electron pairs (electron acceptor).

At the beginning of the cracking reaction, a carbenium ion is formed whose positive charge is stabilized by the molecular residue via inductive effects. There are two ways in which a carbenium ion can be formed. The first way is the abstraction of a hydride ion (H^-) at the Lewis acid center on the catalyst surface. This is the preferred formation mechanism for alkanes and is shown in the following equation.

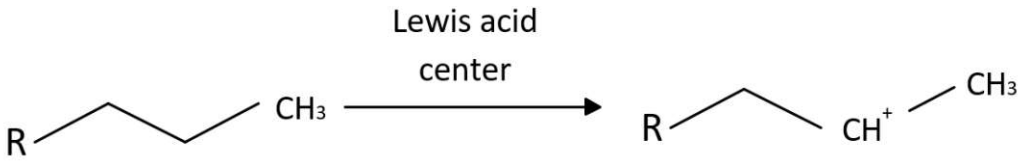

(4)

The second possible reaction path is the formation of the carbenium ion at the Brønsted acid center by the addition of a proton to an olefin, see Figure 20. This olefin must have been formed by a previous thermal dissociation process (thermal cracking) or needs to be present in the feedstock natively.

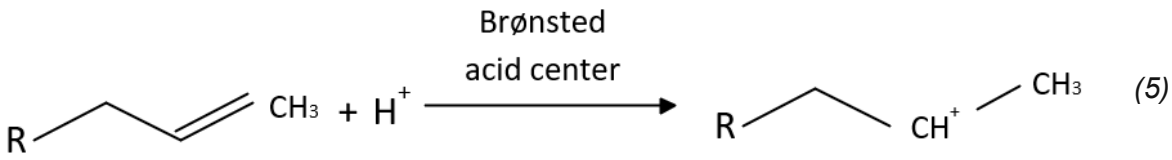

(5)

In principle, the formation of different carbocations is possible, which also differ in terms of their stability. Analogous to radicals, carbenium ions can be stabilized by a mesomeric or by an inductive effect.

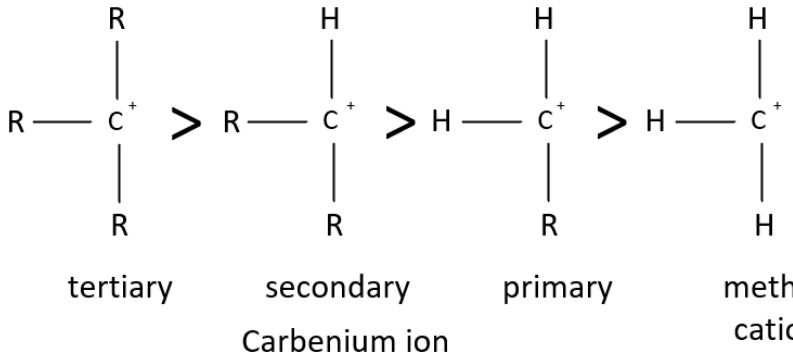

(6)

From the left (tertiary carbenium ion) to the right (methyl cation), the reactivity increases. This is due to the fact that inductive effects stabilize the positive partial charge of the central carbon atom if mesomerism (by e.g. a neighboring vinyl or aryl group) is not possible. The number and

type of substituents is decisive for the I-effect, thus a substituent with +I-effect contributes to stability, while an electron-withdrawing substituent (-I-effect) would have a destabilizing effect.

After ion formation, one of the following reactions can take place:

- β-scission of C - C bonds
- Isomerization
- Hydrogen transfer

The chain reactions of the carbenium ions end when it either loses a proton to the catalyst and becomes an olefin or the carbenium ion receives a hydride ion from a donor (e.g. coke) and becomes an alkane.

The β-scission represents the most prominent reaction and the actual cracking mechanism of the hydrocarbon chains. This can be explained by the lower energy level required for splitting of the β- bond compared to the α-bond. [66] The rather high ratio of olefins in the product gas of the FCC plant can be explained by β-cleavage.

The following equation describes the cleavage of the ionized hydrocarbons at the β-position into an olefin and a primary carbenium ion.

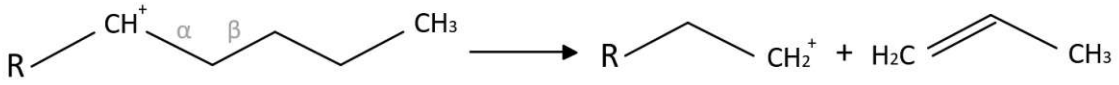

(7)

The mono-molecular β-scission is endothermic, and therefore favored by high temperatures, and non-equilibrium-limited. [66]

The olefins formed can in turn react further in the Brønsted acid center of the catalyst to form carbenium ions. These rearrange themselves through isomerization to form secondary and tertiary carbenium ions. This occurs due to the increased relative stability of the same and is shown in the following figure.

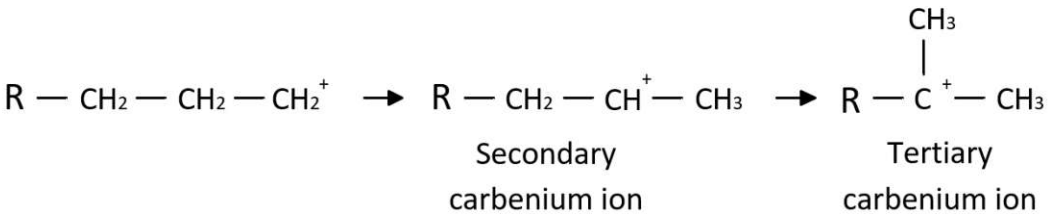

(8)

Hydrogen transfer is a bimolecular reaction in which one reactant is an olefin. For two olefins to react, they must both be adsorbed at acidic centers and be very close to each other. The hydrogen transfer causes one olefin to become an alkane and the other to become a cyclic olefin. The cyclic olefin reacts further with another olefin and another alkane and a cyclo-diene is formed. In the next step, this rearrangement is carried out again and the cyclo-diene becomes an aromatic.
Hydrogen transfer is also possible with cycloalkanes, whereas the cycloalkane acts as a hydrogen donor. The product of this is again an alkane and an aromatic. Aromatics are very stable and cannot be split in a catalytic crack process, which means that the cracking process ends here.

The exact causes of coke formation are not yet fully known. In some of the cracking reactions described above, hydrogen, in the form of a hydride ion, is split off from the hydrocarbon molecule of the feed. The remaining molecule can condense and form polycyclic systems, which further dehydrogenate and form aromatics. These polycyclic aromatic hydrocarbons (PAHs) accumulate at the active centers of the catalyst particle as coke and lead to loss of activity. For this reason, in the FCC process, the actual cracking step is always followed by a regeneration step, in which the activity of the catalyst is restored by oxidation of the coke layer attached to the catalyst particle.
A certain amount of coke is necessary to maintain the overall autothermal FCC process, as it provides the needed thermal energy in the regenerator.
Similar to hydrogen transfer, coke formation uses a bimolecular mechanism. In theory, the amount of coke produced should increase when the reaction rate of hydrogen transfer is increased. It is also known that unsaturated hydrocarbons and multiple ring aromatics serve as coke precursors.

5.2.1 Cracking of biogenic oils

The chemical composition of bio-oils is partially similar to the paraffinic components of heavy oil, which make up the main part of vacuum gas oil. However, there are two major differences:

- Bio-oils are esters, i.e. compounds of a carboxylic acid with an alcohol and have a higher oxygen content compared to petroleum intermediate products
- Only alkanes and aromatics occur in petroleum, but not alkenes - in contrast to the unsaturated fatty acids of bio-oils.

From these two essential differences, the cleavage mechanisms for bio-oils can now also be derived, especially since oxygen increases the charge shifts in the chemical bonds of the chain and, thus, also the cleavability of the hydrocarbon chains.

Basically, it was shown that the basic splitting reactions for the bio-oils (decarboxylation and deoxygenation) take place independently of the type of catalyst used. The catalysts influence much more the further splitting of the molecules, i.e. the secondary cracking, and thus the product yields. Ramakrishnan et. al [30] found, that the product yield (gas and liquid hydrocarbons) is highest when using HZSM-5 or calcium oxide at high cracking temperatures (550°C). These basics where also reproduced during the experimental work in order to maximize the gas yield and thereby maximize the recycled feedstock in compliance with the RED II directive issued by the European commission.

It can be stated that the cracking of bio-oils to lighter fractions, especially in the boiling range of petrol, as well as to gaseous reaction products is possible. As in the processing of petroleum, the use of zeolites, above all HZSM-5, achieves a significantly higher overall conversion due to the high selective catalytic effect, combined with a significantly increased yield of unsaturated and aromatic compounds in the desired products.

During catalytic cracking of lipids two reaction paths are possible which compete with each other.

The first one is towards decarboxylation, which is shown in the following Figure 9 in the left direction. In this process, carbon dioxide is split off from the carboxyl group of the acid or ester, leaving behind the hydrocarbon part of the fatty acid, which from this moment on is further cracked like a paraffinic alkane to gaseous products. As a by-product of this reaction path, only carbon dioxide is thus produced; in addition, there is an increased yield of product gas.

The decarboxylation path competes with the deoxygenation path, where a condensation reaction of two acids or esters with the formation of a ketone and the splitting off of water as a by-product

occurs. These ketones further condense to higher ketones and aldehydes, whereby water is split off with each step again. The latter are then cracked or polymerized to complex aromatic ring systems, so that a gaseous product is formed from the cracked components and coke from the polyaromatics.

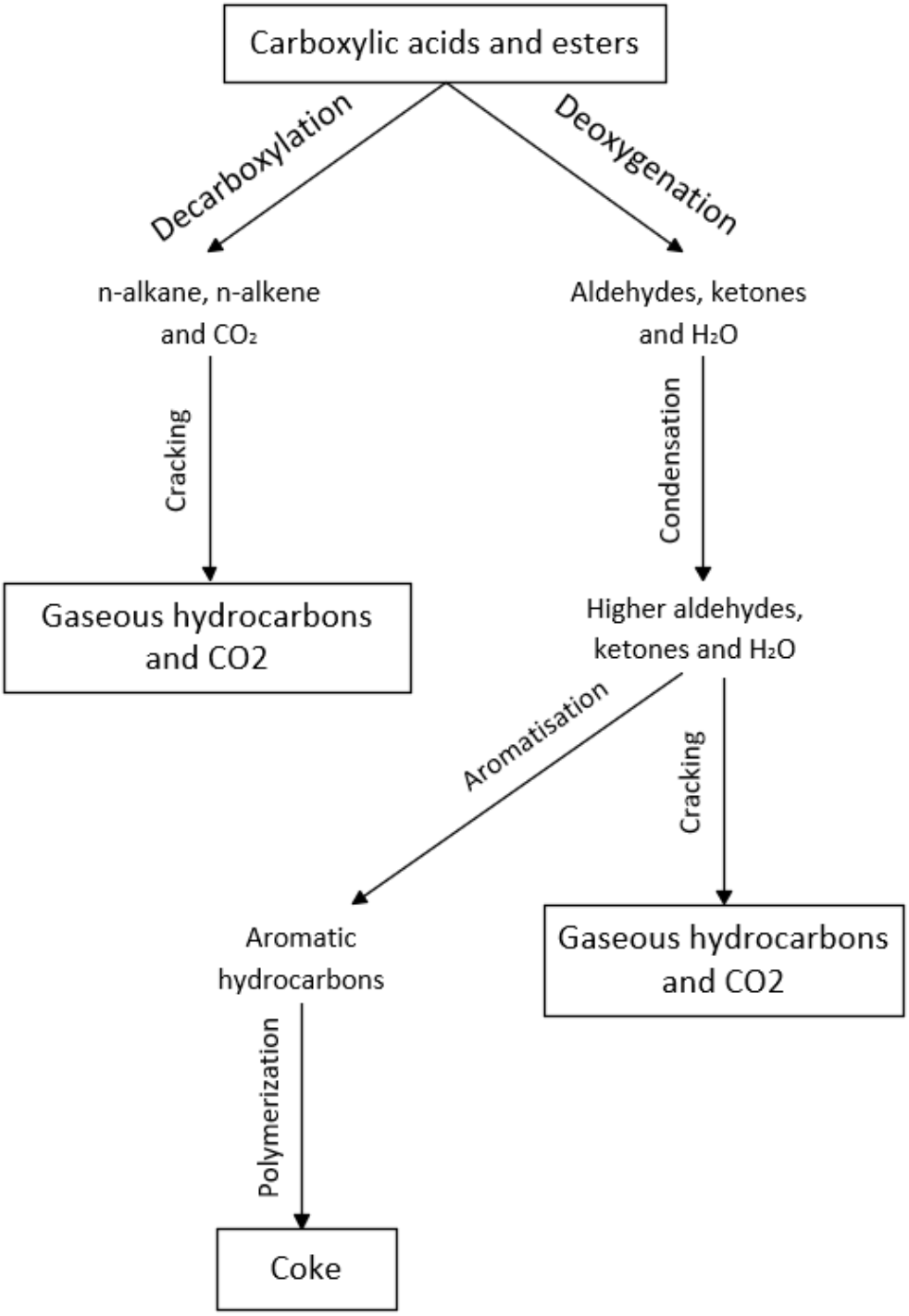

Figure 9: Biooil cracking, redrawn and adapted from [30]

From these two reaction pathways, it can be seen that, in addition to a higher yield of gaseous hydrocarbons and coke, the cracking of bio-oils also leads to the production of carbon dioxide and water. Since carbon dioxide is formed exclusively during decarboxylation, while water production is to be expected in addition to an increased gas yield during deoxygenation, conclusions could be made about the dominant reaction mechanism on the basis of the products.

6 FCC PILOT PLANT

There are currently two FCC pilot plants located at the Technische Universität Wien, an older and smaller one, utilizing approximately 10 kg of catalyst and a newer and bigger plant with a higher feeding rate, a bigger amount of catalyst and a more versatile design with catalyst sampling points, cones to maintain the desired catalyst to oil (C/O) ratio among other improvements.

The first FCC pilot plant was designed and built in 1996 by Reichhold [67]. It utilizes an internal circulating bed with a riser/reactor section in the middle. An advantage of the concentrical design of riser/reactor and regenerator and cooler is the strong thermal coupling between the endothermal riser/reactor and the exothermal regenerator section. The design was improved by Bielansky [68] in 2010 in the shape of a new plant, pilot plant B. A schematic of the second pilot plant is depicted in the following figure.

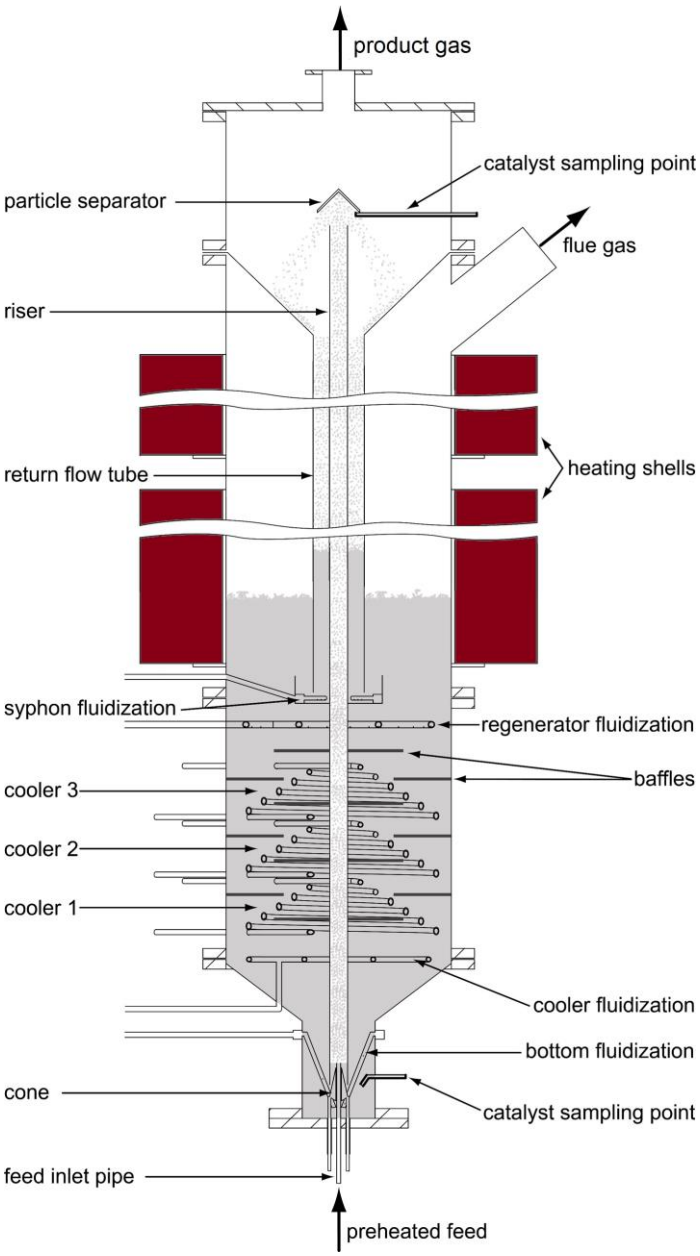

Figure 10: Pilot plant B

6.1 FCC Pilot plant B

The FCC plant is divided into the areas of reactor (riser), regenerator and cooler. The actual cracking process takes place in the riser. In the regenerator zone, the catalyst is reactivated by oxidizing the coke deposit, and in the cooler zone, the catalyst is cooled down again to reaction temperature. All process areas are located in one casing. This integral structure of the individual zones makes the plant very compact, but it also results in the thermal coupling of the individual reaction zones.

Key data of pilot plant B, such as feeding rate, maintainable C/O ratios, residence time, cracking temperature etc. can be found in the following Table 3.

Table 3: Key data pilot plant B

Overall height	3200	mm
Riser diameter	21.5	mm
Riser length	2505	mm
Riser residence time	ca. 1.1	s
regenerator diameter	330	mm
catalyst mass	50-70	kg
feed rate	ca. 2.5	kg/h
C/O ratio	15-60	-
Catalyst circulation rate	0.5 – 5	kg/min
Riser temperature	420-650	°C
regenerator temperature	500-800	°C
operating pressure	ca. 1	atm

A visualization of the individual process steps is depicted in the simplified block flow diagram in the following Figure 11.

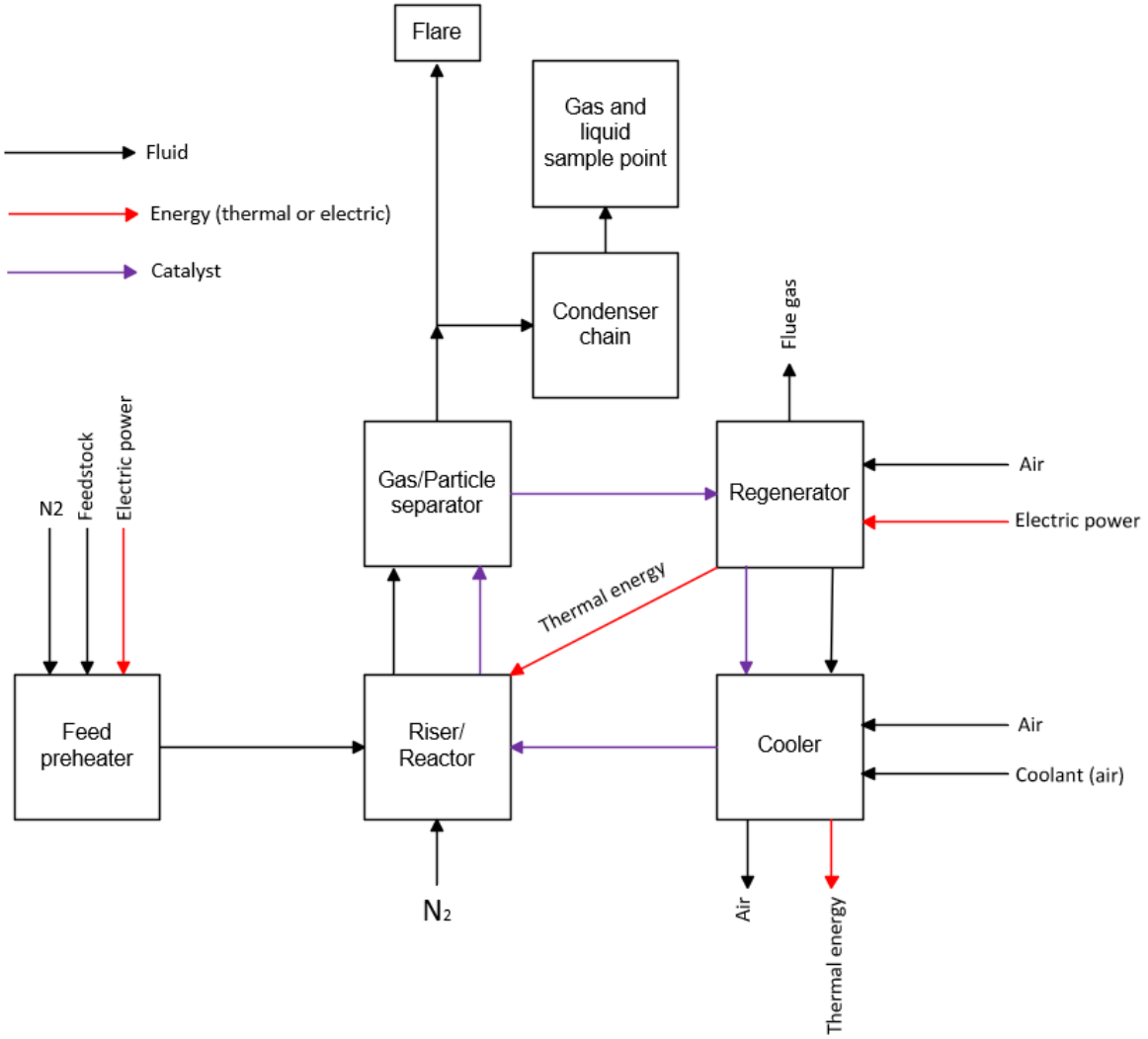

Figure 11: Block flow diagram FCC pilot plant B

6.2 High level overview on the operation procedure of the pilot plant

General remark: It's important to mention that the durations provided are generic and may vary depending on the specific experimental setup and requirements.

A typical experimental day consists of the following processes:

1. ***Heating phase: Approximately 3 hours***

   During this phase, the system is heated to the desired operating temperature. The purpose is to bring the system to the required temperature range for the experiment.

   As the pilot plant is a thermally inert system, it required an average preheating time of 3 hours at the beginning of each experimental day. This time is necessary to bring the system to operating temperature (ranging from 530 to 670 °C depending on the plant section). Additionally, it takes a certain amount of time to stabilize the various temperature ranges due to fluctuations caused by catalyst circulation and gas supply points at different temperatures. During this heating and stabilization phase, the feed is also preheated and mixed (if needed).

2. ***Preparation of measurement instruments and reaching a steady-state operating point: Approximately 3 hours***

   In this phase, the online analyzers are set up and calibrated. At the same time, the system is operated to establish a stable and consistent steady-state operating point.

   After the heating and preparation phase, feeding the feedstocks to the plant begins. During this phase, a steady-state operating point is established by balancing feeding and cooling rate to obtain the required mass flow to the plant whilst maintaining a thermic equilibrium (or steady state) in all plant sections.

3. ***Steady-state operation of the plant, sampling of the products: approximately 3 hours***

   The pilot plant is kept in steady-state mode and samples are taken.

   During steady-state operation several product samples are taken. For details on the sampling point refer to the figure above or the PFD in the ANNEX (Figure 89). Usually, the aim was to obtain a sampling time of 15 min for each of the 3 to 4 samples. For some experiments the number of samples and the sampling time was reduced due to difficulties in plant operation or due to the low amount of feedstock available. These shortcomings, if they are valid for an experiment, are pointed out individually in the corresponding section.

4. ***Analysis of the gas phase through 2-4 sampling points: Approximately 4 hours***

   During this phase, samples of the gas phase are collected from 2 to 4 sampling points. These samples are then analyzed to gather information about the composition and characteristics of the gas.

   Cleaning and regeneration of the system: Approximately 3 hours

   After the experiment and data collection, the system undergoes a cleaning and regeneration process. This ensures that the system is ready for subsequent experiments and maintains its optimal performance.

5. ***Analysis of the liquid samples***

   The filtration of the liquid samples and their injection into the “Simulated Distillation” gas chromatograph is carried out on the following day. This process involves filtering the liquid samples to remove any solid particles carried-over and then injecting the filtered samples into the gas chromatograph for analysis.

6.3 Sections of the pilot plant

6.3.1 Feed preheater

The feedstocks (VGO, canola oil, UCO and pyrolysis condensate) were prepared in a beaker, heated to approx. 80 °C and stirred. The feed was conveyed by a heated gear pump and preheated to approx. 350 °C in a tube furnace before being fed into the riser to ensure its abrupt and complete evaporation on contact with the hot catalyst.
During start-up of the plant, nitrogen was added to the feed stream between the pump and the tube furnace as a supporting fluidization. The purpose of this is to enable a more stable operation of the plant. This is necessary because the feed stream (especially VGO) tends to coke at the riser inlet. The difficulties encountered are discussed in the corresponding chapter.

6.3.2 Riser/Reactor

As can be seen in Figure 10, the centrally located riser tube forms the reactor section of the plant. At the lower end, preheated feed (VGO, canola oil, UCO and pyrolysis condensate) is mixed with hot catalyst, whereby the reactants evaporate abruptly.
The increase in volume due to evaporation and the cracking processes cause the pneumatic transport of the catalyst with the feed and the cracking products upwards through the riser (residence time ~1 s), whereby the cracking reactions with the gaseous hydrocarbons continue along the length of the reactor.

The product spectrum can be influenced by the operating parameters in the riser e.g. residence time, cracking temperature, C/O ratio among others.

The temperature in the riser predominantly influences the cracking reaction and therefore the product yields of the plant. Because the catalytic cracking reactions are endothermic, meaning that they absorb thermal energy from the catalyst and the walls of the riser tube. The heat transfer from the riser tube walls is not sufficient to retain a certain reaction temperature resulting in a temperature decline of the mixture of catalyst particles and feedstock/precursor products. To account for the different temperature levels at the bottom and the top of the reactor the mean cracking temperature was introduced. By calculating a mean temperature according to the following equation the cracking temperature was introduced as one of the defining parameters for the process.

$$\bar{T}_{Riser} = \frac{\frac{T_{Riser,in\,1} + T_{Riser,in\,2}}{2} + T_{Riser,out}}{2} \tag{9}$$

Another important parameter in the riser is the catalyst to oil ratio (C/O ratio). The C/O ratio is measured by an indirect method developed by Reichhold [67] by means of switching off the fluidization in the syphon temporary. The measurement of the changing pressure in the regenerator during this time can be seen in the following figure. The switching off of the syphon leads to an accumulation of used catalyst in the catalyst return pipe upstream of the regenerator and thereby a decreasing catalyst bed height and a pressure drop in the regenerator section. The circulation rate is a function of the measured pressure drop.

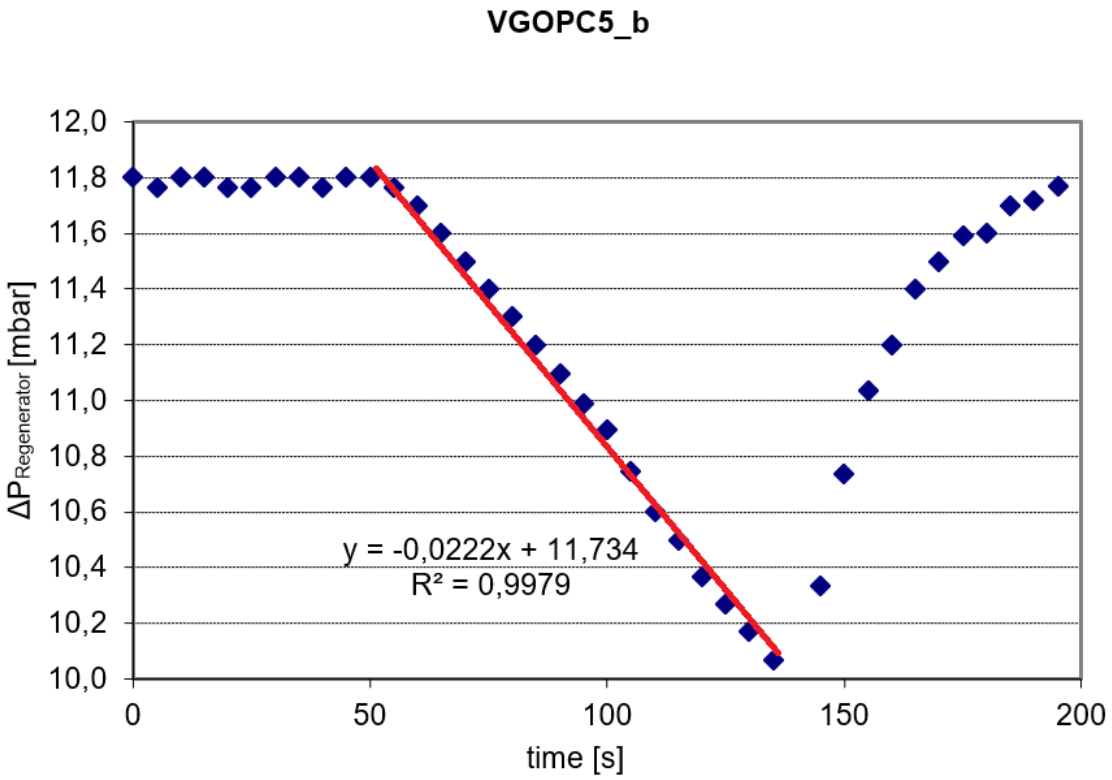

Figure 12: Pressure drop in regenerator section during measurement of the circulation rate (shown for the VGOPC5_b sample)

The mass flow of the catalyst can then be approximated based on the following equation.

$$\dot{m}_{catalyst} \approx \frac{A_{Regenerator}}{g} \cdot \frac{\Delta(\Delta p_{Regenerator})}{\Delta t_U} \tag{10}$$

The C/O ratio is defined as the ratio between the mass flow rate of the catalyst through the riser related to the mass flow rate of the feedstock.

$$\frac{C}{O}\ ratio = \frac{\dot{m}_{catalyst}}{\dot{m}_{feed}} \tag{11}$$

For details on the basics in fluid mechanics and their application in fluidized bed system leading to this calculation method refer to Weinert [69].

6.3.3 Regenerator

The catalyst, which is separated from the product gas by a continuously operating solid-gas separator, is loaded with coke after the reaction. This must be removed by controlled burning in the fluidized bed of the regenerator area. Regeneration takes place at approx. 620 °C [8]. For this reason, fluidization of the aerated bed in this area is carried out with compressed air. Care must be taken that the oxygen saturation in the exhaust gas does not become too low. Otherwise, a progressive deactivation of the catalyst could occur, caused by unburnt coke. This would be indicated by carbon monoxide emissions in the exhaust gas.

6.3.4 Cooler

In order to maintain the temperature at the riser inlet, there are three cooling areas below the regenerator fluidization with their own cooling coil and deflector plates. This enables a broader spectrum of operating conditions with the experimental plant. Air and deionized water can be used as cooling medium. However, air cooling was sufficient in this test series.
Apart from the amount of coolant, the cooling capacity can also be controlled by the cooler fluidization, where an increasing degree of turbulence increases the cooling effect of the coils.
The setting of the riser temperature can be controlled by the cooling capacity.

6.3.5 Condenser chain, gas and liquid sample point

Most of the resulting product is immediately burnt in the flare. Only during sample collection at stable and stationary operation, product gas flows through the condensation chain and the sampling point for a precisely defined period . By measuring via gas meter, the extracted gas volume flow can be determined.

The sampling procedure is divided into the following parts:

- Product gas extraction:
  Product gas flows through the sampling line of the system over a precisely defined period of time, usually 15 minutes. Due to shortage of the feedstock a shorter sampling time was chosen for the experiment with 100 %wt syncrude derived from plastic waste feedstock.

- Product gas measurement:
  For CO, CO_2 and O_2 measurement in the product gas, the product gas flow is diverted to the two Rosemount NGA2000 gas analyzers immediately after sampling.

- Measurement of the circulation rate of the catalyst.

7 FLUIDIZED BEDS

7.1 Fluid mechanical basics

A fluidized bed consists of particles through which a fluid flows against a settling/depositing force. Different types of fluidized beds are distinguished. The classification is made based on the flow velocity of the fluid. This flow velocity, also called empty tube velocity, results from the continuity equation:

$$u = \frac{\dot{V}}{A} \tag{12}$$

Here $\dot{V}$ stands for the volume flow that flows through the cross-sectional area A.

At low empty pipe velocities, the sum of hydrodynamic drag force and hydrostatic buoyancy force is not sufficient to lift the particle against gravity. However, if the flow velocity is successively increased, the fixed bed begins to expand. In the process, the point of equivalence of the weight force and the sum of the buoyancy force and the drag force is reached. This process represents the transition point, generally called the loosening point, from the fixed bed to the fluidized bed. A characteristic feature of this is, that the expansion of the bed increases the porosity ε. It is defined by:

$$\varepsilon = \frac{Interparticular\ volume}{Total\ volume} \tag{13}$$

If the fluid speed is increased further, the fluidized bed begins to form bubbles in the case of gaseous fluidization. As the gas velocity continues to increase, it turns into a turbulent fluidized bed and subsequently into lean phase fluidization as seen in the following figure.

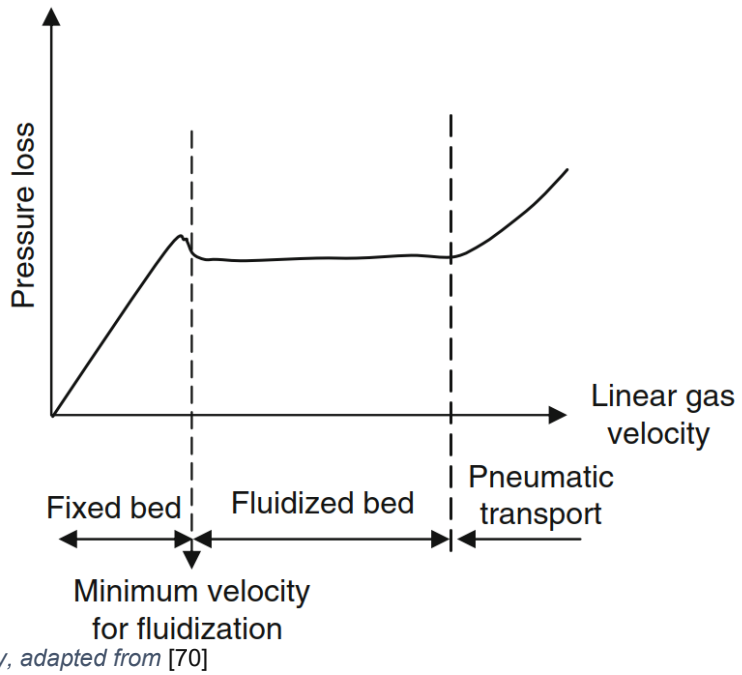

Figure 13: fluid velocity, adapted from [70]

The different stages of fluidized beds are also depicted in the following figure, where the transition from a fixed bed to a fluidized bed at the loosening point with a minimum fluidization

gas velocity can be seen. An increasing gas velocity causes bubbling in the fluidized bed and with further increasing of the gas velocity slugs start to form. When the gas velocity exceeds a certain limit dilute phase conveying of the particles is reached.

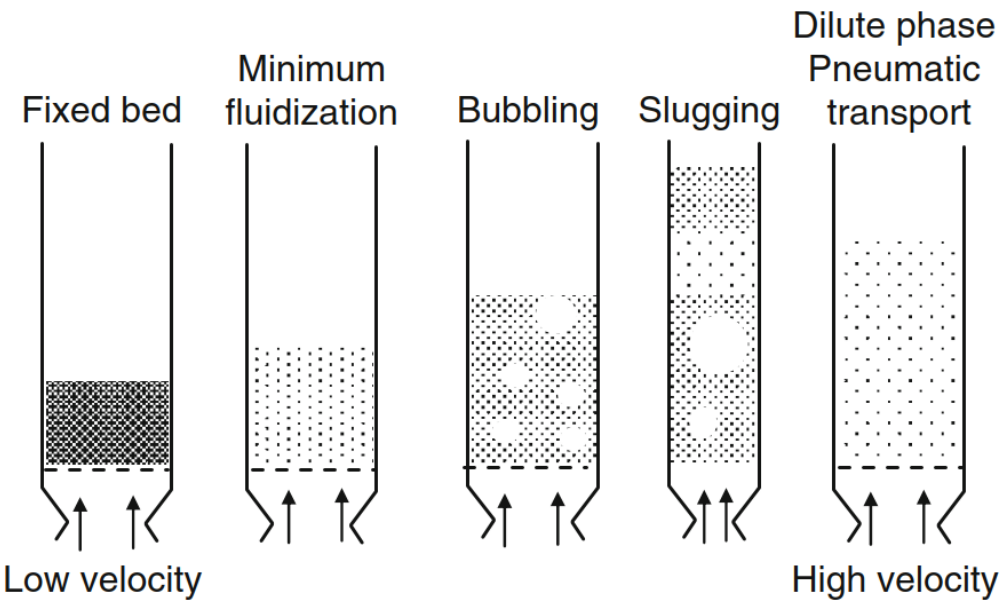

Figure 14: fluidized bed regimes, adapted from [70]

7.2 Pressure drop in fixed beds

To quantify the pressure loss in the fixed bed, the model consideration of cross-sectionally variable parallel channels through which the fluid flows is often used.
Depending on the Reynolds number, different equations have proven to be practical. The Reynolds number can be defined as follows:

$$Re = \frac{U \cdot \rho_g \cdot d_{sv}}{\mu} \tag{14}$$

In the range of low Reynolds numbers (Re<1), the Carman-Kozeny equation is often applied:

$$\frac{\Delta p}{H} = 180 \cdot \frac{(1-\varepsilon)^2}{\varepsilon^3} \cdot \frac{\mu \cdot U}{{d_{sv}}^2} \tag{15}$$

In the range of intermediate Reynolds numbers (1<Re<1000), turbulent behavior occurs more frequently, which is why the semi-empirical Ergun equation has proven itself:

$$\frac{\Delta p}{H} = 150 \cdot \frac{(1-\varepsilon)^2}{\varepsilon^3} \cdot \frac{\mu \cdot U}{{d_{sv}}^2} + 1{,}75 \cdot \frac{1-\varepsilon}{\varepsilon^3} \cdot \frac{\rho_g \cdot U^2}{d_{sv}} \tag{16}$$

Depending on the prevailing flow regime, the first part (fully laminar, Re<1) or the second part of the equation (fully turbulent, Re>1000) is dominant.

7.3 Minimum fluidization velocity

The minimum fluidization velocity represents the transition between the fixed bed and the fluidized bed. For very narrow particle size distributions this point is well-defined and distinct, however for more broadly distributed particle collectives, which are by far more common, the situation corresponds to a more gradual transition. To determine the loosening velocity first-hand, the gas velocity is gradually reduced starting from the area of the fluidized bed and the pressure profile is recorded during this time.

The minimum fluidization velocity is calculated using the following equation:

$$u_L = \frac{\mu}{\rho_g \cdot d_{sv}} \left[\sqrt{33{,}7^2 + 0{,}0408 \cdot Ar} - 33{,}7 \right] \tag{17}$$

Where Ar is the dimensionless Archimedes number. It is defined as the ratio of gravitational forces in relation to the viscous forces.

$$Ar = \frac{\rho_g \cdot {d_{sv}}^3 \cdot (\rho_p - \rho_g) \cdot g}{\mu^2} \tag{18}$$

7.4 Pressure drop in fluidized beds

The at section 7.1described equilibrium of forces can be written in the following way, where the pressure loss equation also represents the fundamental fluidization condition.

$$\Delta p = H_L \cdot (1 - \varepsilon_L) \cdot (\rho_p - \rho_g) \cdot g \tag{19}$$

This also means that the pressure drop, as a result of the drag force on the particle collective, is proportional to the sum of the mass of the individual particles of the fluidized bed. Since the pressure drop is independent of velocity, it remains constant in the fluidized bed (between the minimum fluidization velocity and the pneumatic transport velocity).

7.5 Hover velocity

The upper limit of a fluidized bed represents the "hover speed". The magnitude of forces acting on a suspended particle, including the buoyancy force (FA), drag force (FW), and gravitational force (FG), determine the particles movement. At the equilibrium point the particle hovers on the fluid stream. When the flow velocity is increased beyond this point, the particle is pneumatically transported with the fluid stream and dragged from the fluidized bed region.

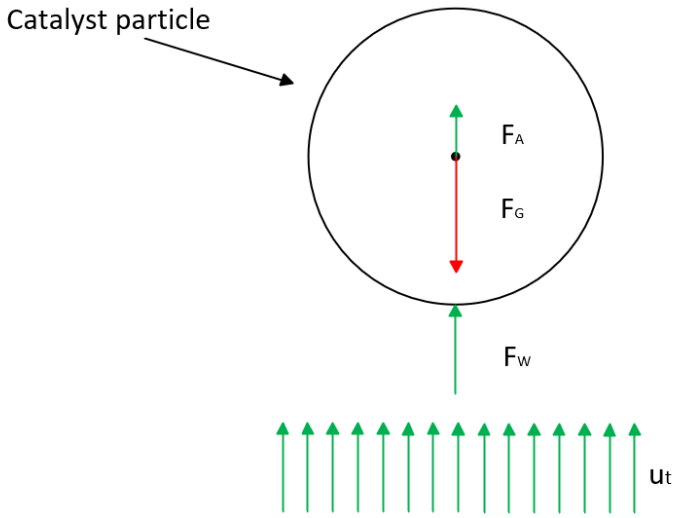

Figure 15: Forces on a single particle in a fluidized bed

For hovering of a spherical particle the following condition must apply:

$$\frac{\pi}{6} \cdot {d_k}^3 \cdot (\rho_p - \rho_g) \cdot g - c_W \cdot A_p \cdot \frac{\rho_g \cdot u^2}{2} = \frac{\pi}{6} \cdot {d_k}^3 \cdot \rho_p \cdot \frac{du}{dt} \quad (20)$$

Once the particle reaches its terminal velocity $u = u_t$ (21), the acceleration disappears

$\frac{du}{dt} = 0$ (22), which leads to $\frac{\pi}{6} \cdot {d_k}^3 \cdot \rho_p \cdot \frac{du}{dt} = 0$ (23), resulting in the following relationship for

the hover speed:

$$u_t = \sqrt{\frac{4}{3} \cdot \frac{\rho_p - \rho_g}{\rho_g} \cdot \frac{d_k \cdot g}{c_W}} \quad (24)$$

The term c_W in the equation above thereby depends on whether a laminar or turbulent flow regime is present.

For:

Re<0.2 (laminar flow, Stokes flow) is $c_W = \frac{24}{Re}$ (25) and $u_t = \frac{\rho_p - \rho_g}{18} \cdot \frac{{d_k}^2 \cdot g}{\mu}$ (26)

0.2<Re<1000 is $c_W = \frac{24}{Re} \cdot \frac{4}{\sqrt{Re}} + 0{,}4$ (27) and the hovering velocity can be calculated numerically

Re>1000 (turbulent flow) is (for spherical particles) $c_W = 0{,}43$ (28) and $u_t = \sqrt{\frac{4}{3} \cdot \frac{\rho_p - \rho_g}{\rho_g} \cdot \frac{d_k \cdot g}{0{,}43}}$ (29)

7.6 Fluidization characteristics of the pilot plant

The pilot plant utilizes different types of fluidized beds in the plant sections. All of them have their individual advantages and disadvantages and were chosen in order to optimize plant operation and to resemble industrial size FCC units as much as practicable. For more detailed information refer to the work of Bielansky [68].

The *bottom*, the *syphon* and the *regenerator section* operate in a bubble-forming fluidized bed. This ensures an optimal distribution of the fluidizing gas in the catalyst and thereby optimizes heat transfer and burning of the coke deposited on the catalyst particles.

To ensure optimal cooling of the catalyst and to minimize the formation of bypasses through the cooler a moving bed flow regime is used in the cooler section.

In the riser/reactor a short but intense contact between the feedstock and the catalyst is necessary. To reduce the contact time between the gas and the catalyst, the gas velocity is increased. In the riser this is done to a degree where the terminal velocity of the fluidized bed is exceeded. At this point the fluidized bed changes to a lean phase fluidization, pneumatically transporting the catalyst particles upwards to the particle separator.

8 ANALYTICS

8.1 The lump model

In the FCC process, a wide variety of hydrocarbon compounds are formed. Analyzing each individual compound would be an enormous and impractical task. Therefore, the products are divided into classes of compounds, known as "lumps". The following table shows the concept of these lumps, where the compounds are grouped together into different fractions with similar boiling ranges. This approach allows for a more manageable analysis and characterization of the product, focusing on the major classes of compounds rather than individual components.

Table 4: The lump model

Fraction	Lump	Composition/ Boiling Range	Analysis method
Gaseous	Carbon oxides	CO / CO_2	Infrared
	Gas	C1 - C4	Gas chromatography
	Gasoline	C5, C6	Gas chromatography
Liquid	Gasoline	< 215 °C	Gas chromatography (SimDist)
	Light Cycle Oil	215 °C < LCO > 320 °C	Gas chromatography (SimDist)
	Residue	> 320 °C	Gas chromatography (SimDist)
	Water		Gravimetric
Solid	Coke		Infrared, Paramagnetic

The boiling range of the gasoline lump was chosen to comply with the upper boiling temperature for gasoline stated by the “Ottokraftstoff” datasheet of the GESTIS database. [71]

A benchmark of the economic efficiency of an FCC plant is the so-called conversion, also called Total Fuel Yield (TFY). This relates the amount of desired lumps (usually gases and gasoline) produced to the amount of feed used. The ratio can be calculated via the following equation:

$$TFY = \frac{\dot{m}_{Gas} + \dot{m}_{Gasoline}}{\dot{m}_{Feed}} \tag{30}$$

8.2 Analytics of gases

The sample collected in the gas sampling tube consists mainly of short-chain hydrocarbons, nitrogen, and carbon monoxide/carbon dioxide. Immediately after sample collection, 50 µl of the sample were injected into a Shimadzu GC17A gas chromatograph using a syringe. The analysis involves two analysis channels. The first channel is used to determine the hydrocarbon composition, while the second channel is used to determine the nitrogen content in the product gas. The hydrocarbon content is detected using a flame ionization detector, while a thermal conductivity detector is used for nitrogen quantification. The following table shows the key parameters of the gas chromatography analysis:

Table 5: Characteristics and parameters of the gas chromatography

	Organic sample	N_2 (contained in the sample)
Injector	Splitless (50 µl)	
Heating program	50 °C to 200 °C, dwell time approximately 30 min	
Separation column	Varian CP-AL_2O_3/Na_2SO_4	CP CarboPLOT P7
Stationary phase	100% Polydimethylsiloxane	Carbon Porous Layer
Dimensions	50 m x 0.25 mm ID x 4 µm d_f	27.5 m x 0.53 mm ID x 25 µm d_f
Mobile phase	Hydrogen	Helium
Detector	Flame ionization detector FID	Thermal conductivity detector TCD

For the analysis of the CO, CO_2, and O_2 content of the product gas, a product gas analysis is performed online immediately after sampling. The gas analyzer Rosemount NGA2000 is utilized for this investigation. It measures the exhaust gas composition both during normal operation and during the product gas sampling process. Information on the online gas analyzers can be found in the following table:

Table 6: Characteristics of the online gas analyzers

Manufacturer	Emerson process management
Type	Rosemount NGA 3000 MLT3
Analysis methods	O_2: Paramagnetic CO_X: NDIR
Substances	CO, CO_2, O_2

8.3 Analytics of liquids

The condensable fractions of the product stream are collected at the two condensation columns and the liquid separator. The condensers operate in a countercurrent flow with either cooling water (first condenser, 7 to 12 °C) from the municipal water network or ethanol (second condenser, -20 °C) from a cryostat. After the second condenser, a liquid separator is used to remove residual condensate from the gas stream. The three fluid streams are combined after sampling.

The liquid samples are filtered (filter pore diameter <2 µm) to remove catalyst residues. The obtained organic sample is then injected into a second Shimadzu GC17A gas chromatograph. The analysis method employed is known as simulated distillation (SimDist). It aims to determine the boiling curve of the sample to determine the gasoline, light cycle oil (LCO), and residue content. Prior to analysis, the gas chromatograph is calibrated using external standards of n-alkanes.

Table 7: Characteristics and parameters of the SimDist gas chromatography

	SimDist
Injector	Split 30:1; 1.5 µl at 200 °C
Heating program	35 °C to 350 °C, linear ramp profile, dwell time 22 min
Separation column	Zebron ZB-1
Stationary phase	100% Polydimethylsiloxane
Dimensions	30 m x 0.32 mm ID x 0.25 µm d_f
Mobile phase	Hydrogen
Detector	Flame ionization detector FID

The obtained SimDist diagram depicts the recorded boiling curve plotted against the mass percent of the sample, along with the classification of different boiling ranges. The gasoline cut is defined with a boiling temperature of up to 215 °C, while the LCO (light cycle oil) cut is defined as having a boiling temperature ranging from 215 to 320 °C. The following figure illustrates an exemplary representation of the determined boiling curve, specifically for the liquid product obtained from the 100 %wt VGO base case experiment.

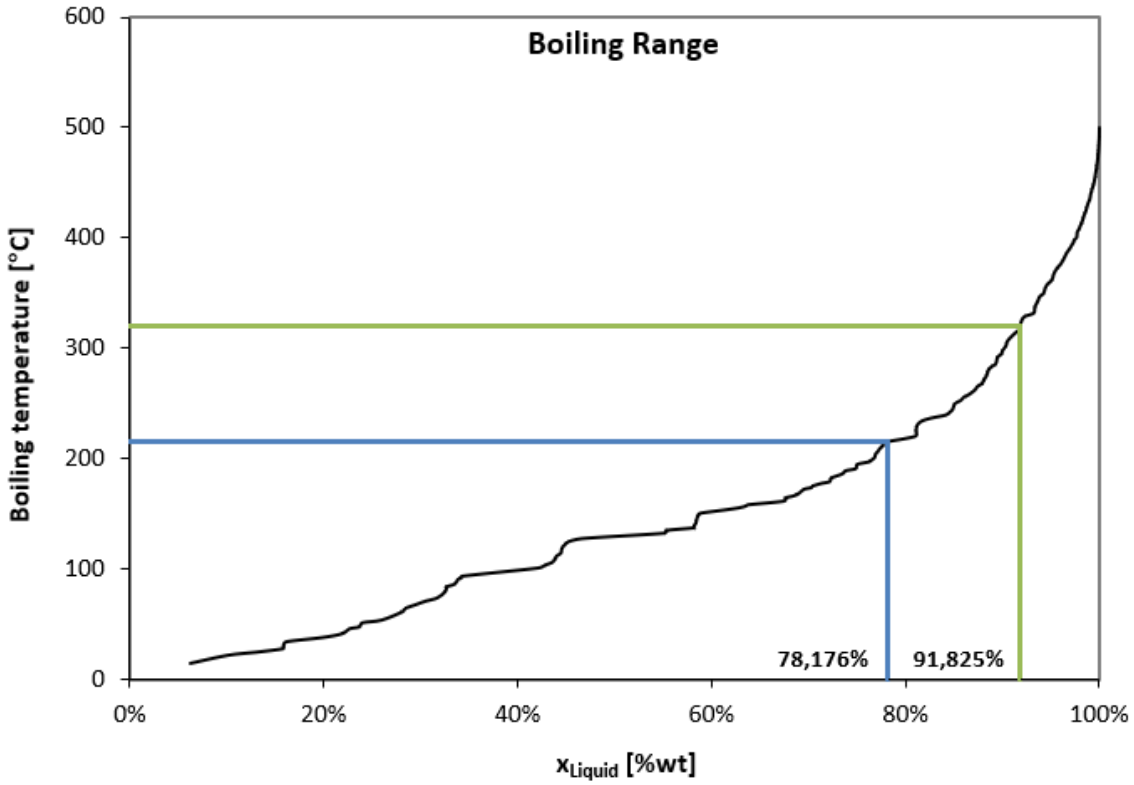

Figure 16: SimDist diagram of the VGOBASE2 experiment

8.4 Analytics of solid products

Solid cracking products in the FCC process typically consist of highly condensed aromatic hydrocarbons that deposit as coke on catalyst particles. The determination of the coke content is achieved by online measurement of the CO, CO_2, and O_2 levels in the exhaust gas, followed by back-calculation using a combustion calculation. The NGA 2000 online analyzers, as mentioned earlier, are used as the measuring instruments for this purpose. This analyzer

provides real-time analysis of the gas composition, allowing for accurate determination of the coke content based on the measured concentrations of CO, CO_2, and O_2. The combustion calculation involves applying stoichiometric principles to relate the measured gas concentrations to the amount of coke present in the cracking process.

8.5 Conradson Carbon residue

The conradson carbon residue test (also called CCR test) is used as a rough estimation of the coke-forming tendencies of hydrocarbons (in the course of this experimental work from: petroleum fractions, syncrude derived from plastic waste and bio lipids). The CCR number is the ratio between a certain amount of hydrocarbon liquid (the amount depends on the expected CCR, for the experiments described here 10 g of liquid were used) to the residue that persists in the ceramic beaker after the liquid's thermal decomposition. The procedure is specified in the international standard ASTM D189. [72]

The CCR test has certain shortcomings, such as a low reproducibility, it is labor intense and it measures thermal coke formation instead of catalytic coke formation. The CCR test was nevertheless chosen because it is inexpensive and simple. The lack of reproducibility was countered by reproduction of the test of at least 3 times. The results of the conducted CCR tests are depicted in the following figure.

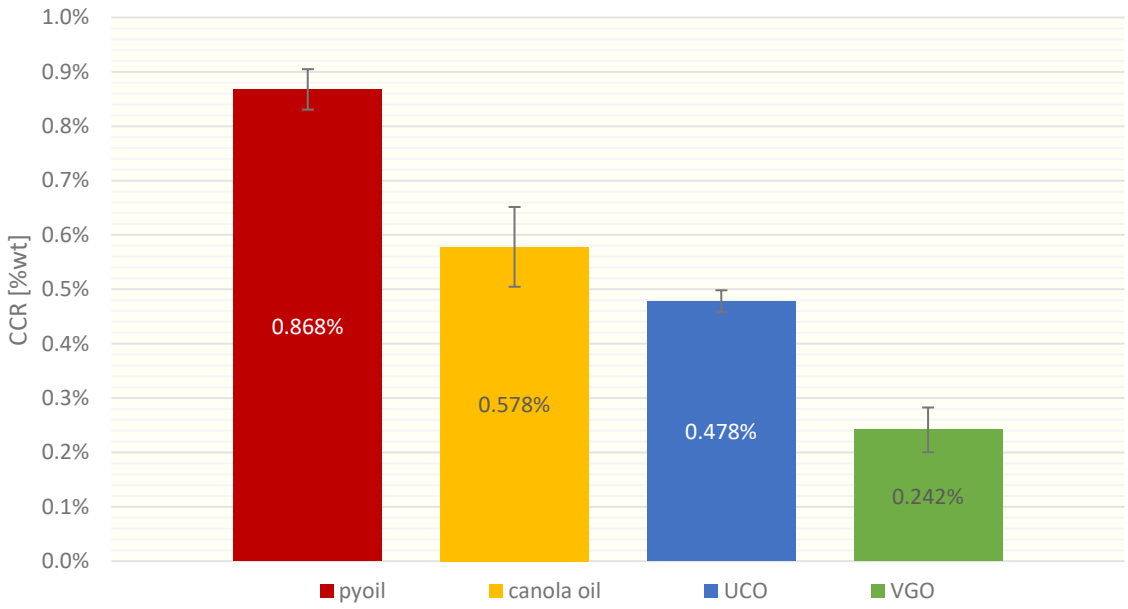

Figure 17: CCR values of the feedstocks

The CCR values of the feedstocks are low and relatively close together. They indicate no difficulties regarding coking during FCC pilot plant operation.

8.6 Inorganic ash content

One important parameter for conducting experiments in the FCC pilot plant at TU Wien is the ash content. A high amount of ash could possibly lead to blocking in numerous locations as observed in previous tests with other feedstocks. [26]
The ash content was analyzed by placing a ceramic beaker in a furnace and heating it for four hours to a maximum temperature of 775 °C. The temperature level was kept for another four hours before letting the samples cool down. The still relatively hot crucibles were placed in a

desiccator filled with fresh silica gel to obtain dry samples. After cooling to room temperature the remains inside the crucibles were analyzed gravimetrically. The results are depicted in the following table.

Table 8: Inorganic ash content of the feedstocks in comparison to the collected precipitation

Feed	Inorganic ash content	
VGO	virtually ash-free	%wt
Canola oil	virtually ash-free	%wt
UCO	0.0049	%wt
PC	0.0076	%wt
Pyoil	0.561	%wt

9 MATERIALS AND METHODS

9.1 Catalyst

All experiments were conducted using the same olefin-optimized mixture of catalysts. As previously mentioned, todays modern catalysts can be optimized to maximize either propene or LPG/butene yields. By mixing a propene and a butene boosting catalyst the best of both worlds could be combined.
The used catalyst is an equilibrium catalyst, meaning that the catalysts initial very high activity was reduced ("equalized") over time in a commercial scale FCC unit before usage in the FCC pilot plant at TU Wien. The usage of equilibrium catalyst is key to ensure first comparability with industrial scale FCC units and second reproducibility of the individual experiments. The equilibrium catalyst is not keen to major changes in its characteristics such as its selectivity or activity, especially not inside the pilot plant with its relatively short accumulated yearly operation time.

The following table gives an overview on some parameters of the used catalyst.

Table 9: Key parameters of the used catalyst

Total surface area	173	m^2/g
Unit cell size	24.29	Å
Average bulk density	0.84	g/cm^3
Pore volume	0.39	cm^3/g
Nickel content	609	ppm
Vanadium content	105	ppm
Sodium content	0.22	%wt
Iron content	0.3	%wt
Rare earth oxides (RE_2O_3) content	1.75	%wt
Cerium oxide (CeO_2) content	-	%wt
Lanthanum oxide (La_2O_3) content	-	%wt
Aluminum oxide (Al_2O_3) content	47.70	%wt
Phosphor pentoxide (P_2O_5) content	2.52	%wt
Silicon oxide (SiO_2) content	-	%wt
Titanium content	-	%wt

9.2 Feedstock

9.2.1 VGO

Vacuum gas oil is the top product of the vacuum distillation unit. It resembles the "light heavies" of the petroleum fraction. The vacuum distillation unit uses the relatively heavy bottom product of the upstream atmospheric distillation as a feedstock, meaning that the light product fractions have already been removed from the feedstock. This results in a relatively high boiling range of the VGO beginning at approximately 430 °C topping out at approximately 565 °C. [70]
Depending on the purpose of the refinery (energy, lubricant or petrochemical oriented) there can be multiple VGO fractions, such as light VGO (LVGO) or heavy VGO (HVGO) which can be split again as required by refinery operation. [73]

The used VGO is a hydrotreated LVGO with a boiling range of approximately 310 to 550°C. Hydrotreating generally lowers sulfur, nitrogen and heavy metals level, which improves both, product quality as well as operability of the FCC unit and catalyst life cycle time. For more details on VGO parameters refer to the following table.

Table 10: Key parameters of the used VGO

Density at 15 °C	0.89	g/cm³
Viscosity at 100 °C	6.25	mm²/s
Sulfur content	214	mg/kg
Nitrogen content	143	mg/kg
Vanadium content	2	mg/kg
Nickel content	2	mg/kg
Total aromatics content	32.6	%wt
Ash content	below limit of detection	%wt
Conradson carbon residue	0.16	%wt

The boiling curve is depicted in Figure 18 in comparison to the boiling curve of the used pyrolysis condensate derived from pyrolyzed municipal plastic waste in the following section.

9.2.2 Pyrolysis oil derived from municipal plastic waste

The used pyrolysis oil (“pyoil”, also called syncrude or, due to the type of used pyrolysis process, pyrolysis condensate) is derived from municipal plastic waste from an Austrian and German municipal collection system for recyclable material often referred to as “der Gelbe Sack” or “the yellow bag”. For a more detailed description of the used plastic waste feedstock for the pyrolysis reactor refer to the specifications 05/2012 and 08/2018 for mixed plastic waste feedstocks from “Der Grüne Punkt”. [74], [75]

The pyrolysis process used to produce the pyoil includes a screw reactor with hot pyrolysis gas filtration at atmospheric pressure. The pyrolysis process was developed at the Karlsruhe Institute of Technology at the institute for Technical Chemistry. The plastic waste has an average residence time of 30 minutes in the screw reactor at an average cracking temperature of approximately 500 °C. The gaseous pyrolysis products leaving the reactor are hot filtered via ceramic filters before being condensed to obtain liquid pyrolysis oil. Solid products and char are removed from the reactor via a solid outlet. For further information about the reactor refer to the publications of Tomasi Morgano et al. [76], [77]

Since the used pyoil is a mixture of the product of numerous experimental runs from the mentioned pyrolysis pilot plant the following table shows an approximation of the used plastic types.

Table 11: Approximation of the components of the feedstock for the pyrolization pilot plant

LDPE	35	%wt
HDPE	17.5	%wt
PP	17.5	%wt
PS	10	%wt
ABS	5	%wt
PVC	7.5	%wt
PET	7.5	%wt

This variation in the feedstock and experimental conditions of the pyrolysis pilot plant also results in uncertainties in the characteristics of the pyoil depicted in the following table. These values are good approximations, but deviations can apply. However, all experimental runs of this thesis were conducted by merging the product charges of the plant to one unified pyoil feedstock, which ensures comparability between experimental runs.

Table 12: Key parameters of the used pyoil

Density at 15 °C	0.875	g/cm³
Viscosity at 40 °C	10 - 15	mm²/s
Carbon content	82.3	%wt
Hydrogen content	10.7	%wt
Oxygen content	4.5	%wt
Sulfur content	<100	mg/kg
Nitrogen content	<1	%wt
Chlorine content	310	mg/kg
Water content	0.5	%wt
Olefins content	15.7	%wt
Paraffins content	28.3	%wt
Cyclo-paraffins	5.1	%wt
Cyclo-olefins	3.3	%wt
Total aromatics content	34.9	%wt
Ash content	$7.6 \cdot 10^{-3}$	%wt
Conradson carbon residue	0.868	%wt

The table gives some information on density, ash content and aromatics content, which are in the same order of magnitude for pyoil as well as VGO. However, pyoil introduces a certain amount of oxygen into the feedstock in comparison to the virtually oxygen-free VGO. Although both, inorganic ash content and CCR, are elevated compared to the benchmark of VGO no issues regarding processability in the FCC pilot plant related to these still moderate values is to be expected.

It is worth to mention that the used feedstock for the obtained pyoil contains a relatively high amount of polyvinyl chloride, a plastic type especially problematic due to its high chloride content. This can be problematic because it is a catalyst poison for e.g. steam crackers downstream of the FCC unit, can lead to corrosion in equipment downstream of the pyrolysis reactor and requires either treatment of the pyoil or the final products in order to be removed.

Current approaches to mixed plastic waste feedstocks are often to remove high-value fractions (e.g. PP rigids, PP flexibles, HDPE, LDPE, PET) in order to be recycled mechanically. The

residual waste is then cleansed to remove PVC from the feedstock of downstream chemical recycling units.

The following figure compares the boiling curves of VGO and pyoil, indicating a significant lighter composition of the pyoil.

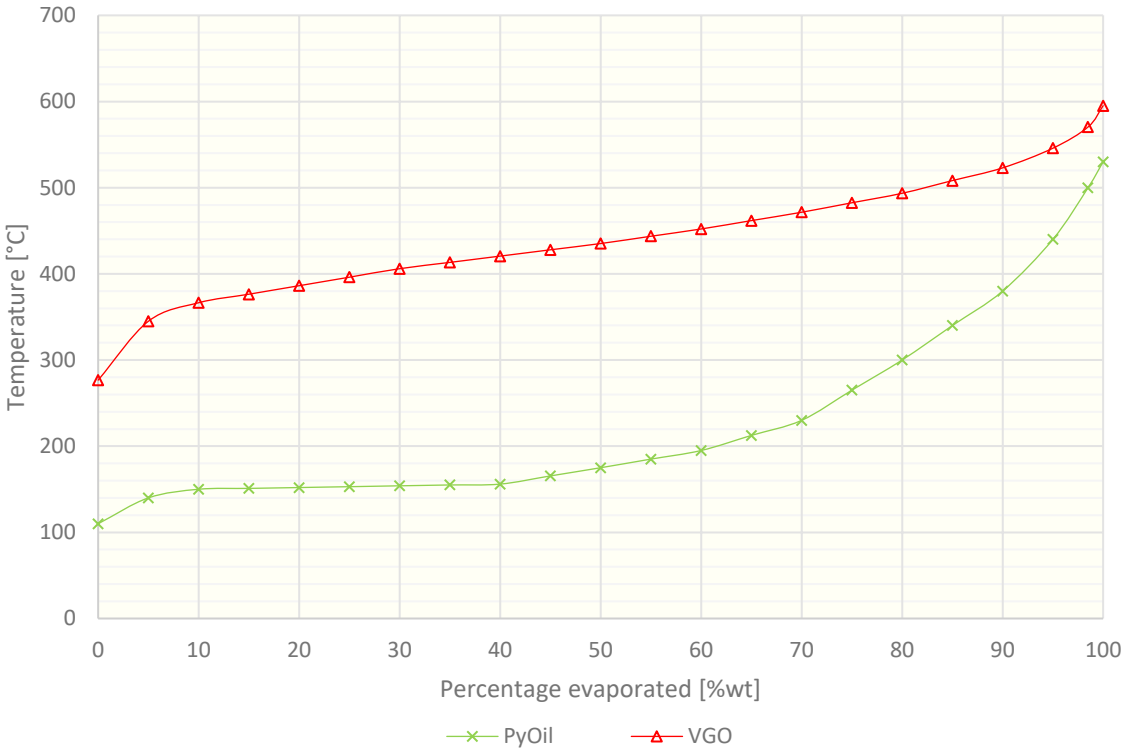

Figure 18: Boiling range of the pyoil in comparison to the used VGO

9.2.3 Canola oil

The canola oil used to introduce a bio-approach is commercially available food-grade canola oil. The following table gives an indication on the characteristics of the used oil. Because the shelf life of used canola oil was expired for a few years the peroxide number was relatively high (pristine food grade oils have a peroxide number <6). The smoke point marks the temperature at which the free fatty acids in the canola oil disintegrate and start to produce visible smoke. From the smoke point onwards more and more triglycerides start to break up, meaning that the canola oil will evaporate/crack instantly when entering the very hot riser/reactor. [30]

Table 13: Key parameters of the used canola oil

Density at 15 °C	0.915	g/cm³
Viscosity at 40 °C	35.9	mm²/s
Smoke point	190 to 230	°C
Carbon content	77.5	%wt
Hydrogen content	11.6	%wt
Oxygen content	10.9	%wt
Acid number	0.15	mg KOH/g
Peroxide number	8.73	meq
Water content	<0.1	%wt
Ash content	below limit of detection	%wt
Conradson carbon residue	0.578	%wt

9.2.4 Used cooking oil (UCO)

The used cooking oil was collected from a municipal waste cooking oil collection system/infrastructure called "NÖLI". According to the collection guidelines issued by the lower Austrian government [78] the UCO consists of:

- Used oil for frying
- Oil from pickled foods
- Clarified butter (mainly from deep-frying)
- Expired cooking oils

There are certain oils and fats prohibited from collection by means of the NÖLI system, which include:

- Lubricants
- Other liquids and chemicals
- Sauces
- Leftovers

Due to the restrictions of the collection system and the rather vague specification of the oil no details on the composition can be given. However, the widespread infrastructure includes restaurants as well as domestic households and ensures a maximum in diversity regarding the oils and fats collected. Prior to usage the oil was filtrated to remove contaminants such as food residues and suspended solids. A small amount of water was present as a second phase at the bottom of the beaker and was removed before feeding the oil to the pilot plant.

To get more information about the used UCO two different tests to evaluate the degree of rancidity of the oil were conducted.

Peroxide value

The PV gives an indication on the extent the oil has undergone oxidation. It is conducted by measuring the amount of iodine formed by the reaction of peroxides with iodide ions. The peroxide value is expressed in units of milliequivalents (meq), which corresponds to the amount of a substance that reacts with an arbitrary amount of another substance. In this case it is defined as "milliequivalent of active oxygen per kilogram of oil/fat". The test is standardized in the DIN EN ISO 27107:2010-08. [79]

A peroxide value < 6 meq indicates flawless refined oils and fats whereas peroxide values < 10 meq indicate flawless native (unrefined) oils and fats. [80]

The measured peroxide values of samples of the used UCO and canola oil feedstocks are depicted in the following diagram. The rather high peroxide value of the UCO indicates a high degree of rancidity and underlines the non-suitability for food purposes. The elevated peroxide value of the canola oil reflects the age of the used canola oil, which has expired its shelf life significantly (> 2years).

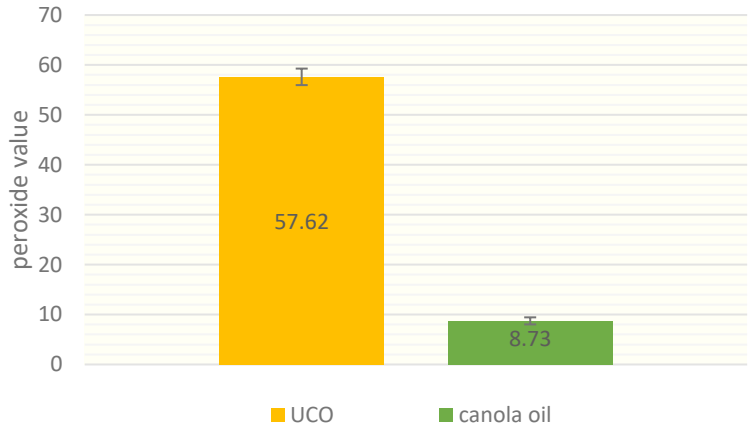

Figure 19: Peroxide value of the used biogenic oils

Acid value

The acid value (AV) is used to quantify the acidity of an oil or fat. It can be used to determine the amount of free fatty acids (FFA) contained in an oil or fat sample. It is measured by the amount of potassium hydroxide (in mg) needed to neutralize the FFAs contained in 1 g oil or fat sample. The test is conducted by dissolving the sample in a sufficient solvent and titrating it with an ethanolic or methanolic solution of potassium hydroxide. It is standardized in the DIN EN ISO 660:2020-12. [81]

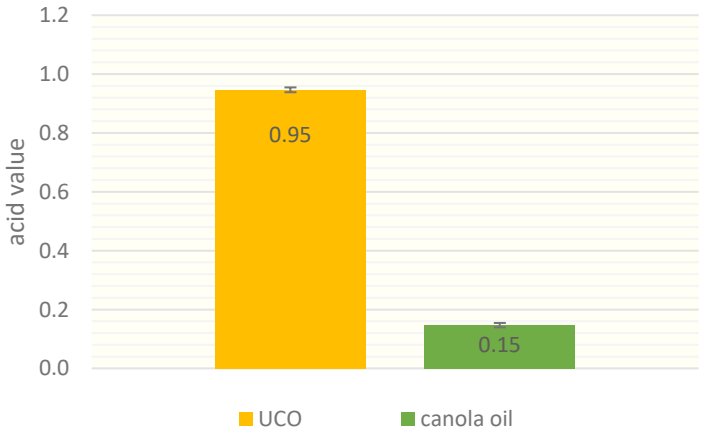

Figure 20: Acid value of the used biogenic oils

An acid value of < 0.6 indicates flawless refined oils or fats (< 4.0 for native or unrefined oils and fats). The elevated AV of UCO indicates a certain (and expected) degree of fat deterioration and the resulting FFA. The AV of the expired canola oil indicates that it is pristine oil with no thermal damage detectable with this test.

10 EXPERIMENTAL WORK

10.1 Pre-experiments

Before the feedstocks where fed to the pilot plant the polymerization and precipitation-forming tendencies were shortly investigated.

10.1.1 Polymerization tendencies of pyoil admixtures with VGO or canola oil

To investigate the polymerization tendency, samples of VGO and canola oil where mixed with 10 and 50 %wt pyoil. After mixing, the samples where transferred to a drying oven. The samples were stored at a constant temperature of 100 °C for 24, 48 and 72 hours. After the residence time, the samples where taken out and cooled to ambient temperature. The increased viscosity was noticed by stirring the cooled samples.

The polymerization tendency was dependent on the admixture rate as well as the temperature.

At 10 %wt admixture rate of pyoil to either canola oil or VGO and a residence time of

- ***< 48 h***
  The mixture increased its viscosity to a moderate, still pumpable level.
- ***> 48 h***
  No further increasing viscosity was observable.

At 50 %wt admixture rate of pyoil to either canola oil or VGO and a residence time of

- ***< 48 h***
  The mixture increased its viscosity to a relatively high level.
- ***> 48 h***
  The mixture had a very high, gel-like viscosity.

All samples showed partially thixotropic behavior. The viscosity lowered, sometimes from almost solidity, to a low viscosity during stirring.
After the stirring, the samples were stored at ambient temperature. After approximately another 48 h, the samples where investigated again. The samples regained some of their viscosity, but not to the same extent as before.

10.1.2 Precipitation

After the feedstock preparation and during mixing and pre-heating of the feedstock (VGO is paste- or gel-like at ambient temperature) to approximately 80 °C a black and highly viscous precipitation formed shown in the following figure.

Figure 21: Precipitation of the VGO/UCO/canola oil and pyoil admixtures

The precipitation accounted for approximately 0.97 %wt (in case of VGO) of the prepared feed and had a relatively high ash content of 0.56 %wt, compared to 0.0078 %wt of the used pyrolysis oil, and 0.0049 %wt for UCO and the virtually ash free VGO and canola oil.

An explanation for this could be the coagulation of normally dispersed, very heavy hydrocarbons or a mild polymerization reaction formed the black and viscous precipitation. By maintaining

constant and rigid agitation through magnetic or mechanic stirrers, the precipitation of the deposit could be avoided.

10.2 Experiments on the pilot plant

The experimental work conducted follows a certain logic with the aim to work on a:

- Partial substitution of fossil petroleum fractions as a feedstock for FCC by pyrolysis oil derived from municipal plastic waste
- Lowering the fossil carbon intensity of the overall process by adding biogenic oils to the feedstock
- Biogenic feedstocks for defossilization of the FCC process – a short comparison of the base cases
- Further lowering the fossil carbon intensity by substituting VGO with canola oil
- Reducing the impact on food chains by substituting food-grade canola oil by UCO
- Investigating the effect of elevated cracking temperatures on the gas and olefin yield of the partially “circularized and decarbonized” process
- Feeding 100 %wt Pyoil to the plant

10.2.1 Partial substitution of fossil petroleum fractions as a feedstock for FCC by pyrolysis oil derived from municipal plastic waste

Introduction

As described earlier, chemical recycling of plastic waste fractions unsuitable for other, energetically more beneficial, recycling techniques can be a key feature on the long way to a circular economy. The utilization of pyrolyzed municipal plastic waste in an FCC unit to tap a source of circular carbon and bring it back into the value chain fulfills exactly this purpose. The FCC process could be a versatile intermediate step, which itself produces a significant amount of petrochemical buildings blocks directly. The integration of petrochemical precursor products, such as naphtha, into the existing petrochemical infrastructure is an approach currently investigated by many refiners, FCC licensors and FCC catalyst manufacturers. This is also reflected in the number of publications coming forward with data and concepts for such an approach.

The experimental work presented in this section has been presented before at the DGMK online conference on “Chemical Recycling – Beyond Thermal Use of Plastic and other Waste” in 2021. [82]

Experimental setup

To investigate the effects of pyoil co-processing in the FCC pilot plant four feedstock mixes were prepared. The first feedstock was pure VGO to produce a base case to compare the results of the other experiments to. The following three feeds were admixtures of VGO and pyoil in rising admixture rates from 5 %wt to 20 %wt. Due to lacking industrial applicability no higher admixture rate than 20 %wt was investigated during these experiments.

Table 14: Admixture rates of VGO/pyoil experiments

Experiment ID	VGO content	Pyoil content	
VGOBASE2	100	0	%wt
VGOPC5	95	5	%wt
VGOPC10	90	10	%wt
VGOPC20	80	20	%wt

Results

The feedstock mixes described in the above table are fed to the pilot plant at a mean feeding rate of 2.5 kg/h (the measured feeding rate was 2.49 kg/h). The mean cracking temperature was chosen at 550 °C (549.4 °C was measured for all experiments). At these conditions the C/O ratio was 29.

Overall, the changes in product yields were minor, considering the relatively high admixture rate of maximum 20 %wt. The detailed changes are depicted in the following figure.

The hydrocarbon gases and the gasoline are shown alongside the total fuel yield in the following figure 22. While the gasoline yield decreases from 42.8 to 40.0 %wt, the hydrocarbon gases increase from 41.7 to 42.4 %wt. This decreases the total fuel yield slightly from 84.5 to 82.4 %wt.

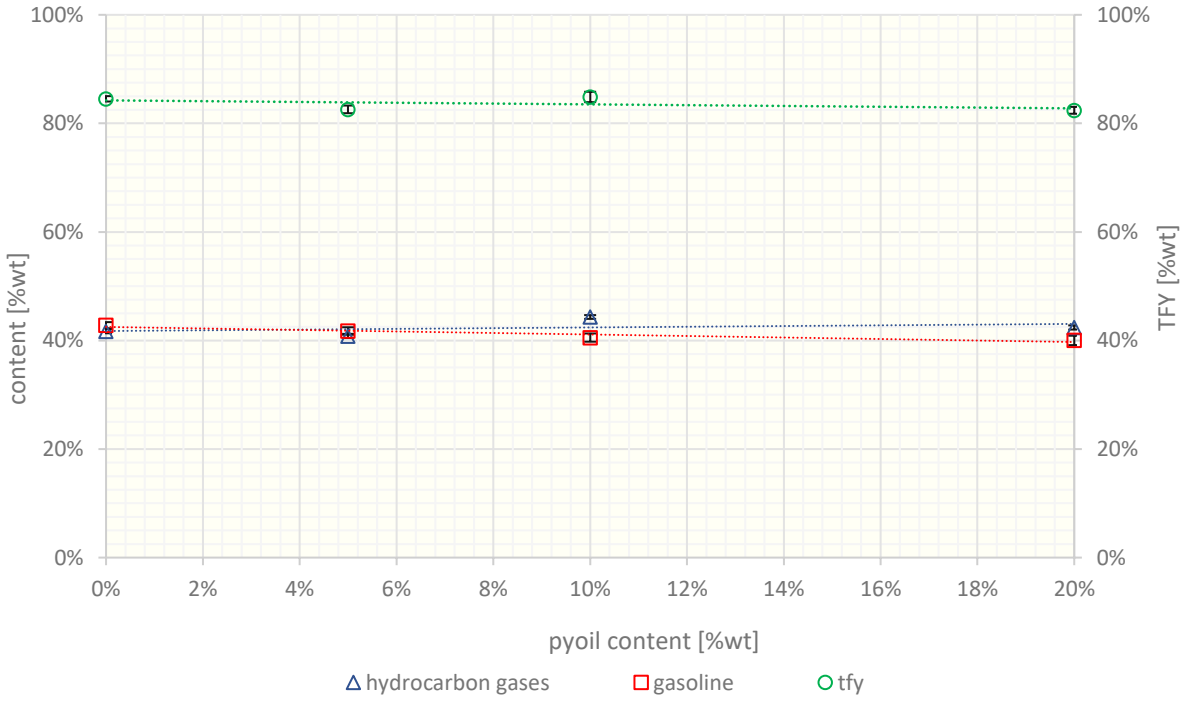

Figure 22: Hydrocarbon gases, gasoline yield and TFY of VGO/pyoil admixtures

The following figure 23 shows the yields of the lower-value heavier hydrocarbons such as LCO, residue and coke and additionally the valueless water fraction. The LCO yield is relatively constant, rising from 5.5 to 6.0 before falling to 4.8 and rising to 5.6 %wt. The same applies to the produced residue, which rises from 3.5 to 4.0 before decreasing to 2.8 and rising again to almost its initial value and reaching 3.2 %wt. The, for thermal equilibrium important, coke yield shows almost no variation by slightly changing from 6.3 to 6.4%wt.
A more remarkable outcome is the expectably increasing water yield. By introducing a feedstock containing a significant amount of oxygen the production of water is to be expected, rising from 0.0 for the virtually oxygen free pure VGO to 2.1 %wt at the experimental run with 20 %wt pyoil admixture rate.

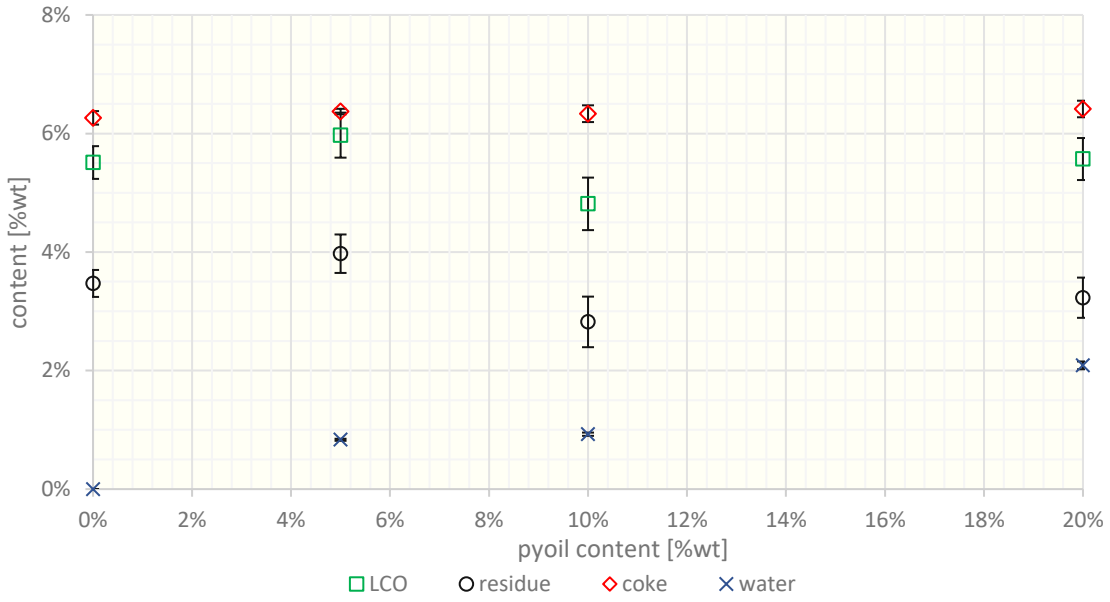

Figure 23: LCO, residue, coke and water yield of VGO/pyoil admixtures

The highly valuable olefins and the produced saturated hydrocarbon gases (alkanes) are depicted in the following figure 24. FCC cracking of pyoil significantly increases propene and butene yields. The produced amount of propene increases from 14.7 to 15.8 %wt whilst the yield of butenes (1-butene, isobutene, trans-2-butene and cis-2-butene) increases from 8.8 to 9.7 %wt. Both, the propene and the butene production reach a maximum at 10 %wt pyoil admixture rate before falling slightly at the 20 %wt admixture rate experiment.
The ethene production almost stagnates, dropping from 3.4 to 3.2 %wt. The yield of saturated hydrocarbons, which are often referred to as “dry gas” or “fuel gas”, show a slight lowering trend with a certain variation, starting at 14.8 and reducing to 13.9 before rising again to 14.8 and falling ultimately to 13.8 %wt.

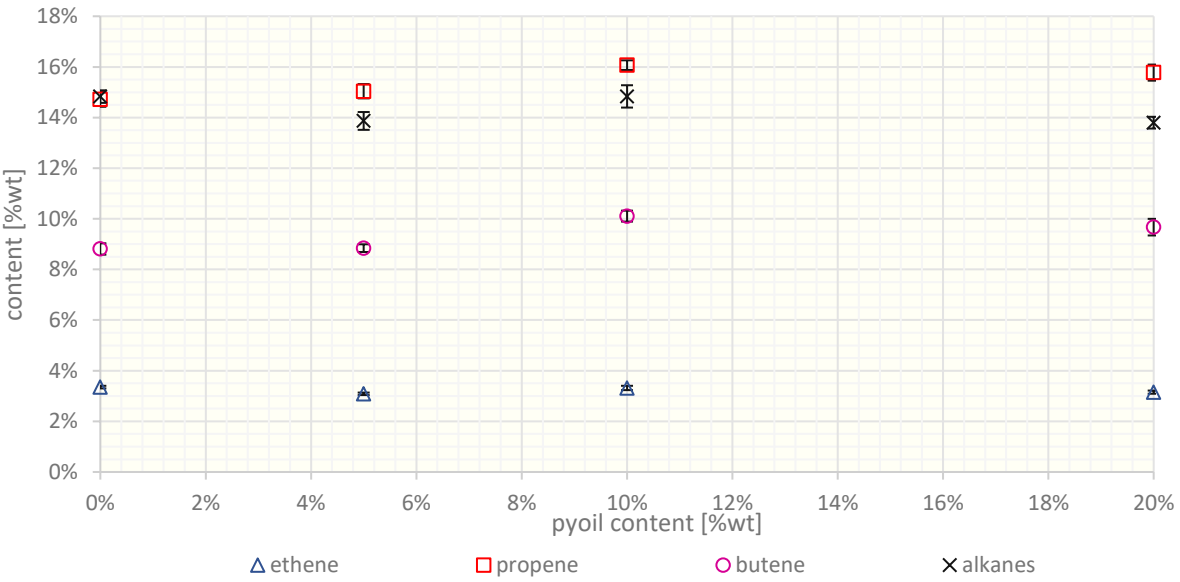

Figure 24: Ethene, propene, butene and alkane yield of VGO/pyoil admixtures

To get a clearer picture on the gas composition, the values from the above figure are set into comparison to the overall gas yield in the following figure 25. The addition of pyoil increases the yields of the olefins propene and butenes significantly. Propene rises from 35.1 to 37.0 %wt and the butenes rise from 21.0 to 22.7 %wt. These gains come at cost of the ethene and the alkane

yield. Ethene is reduced from 8.0 to 7.4 %wt and alkanes from 35.4 to 32.3 %wt. Carbon oxides are almost constant at 0.6 to 0.7 %wt.

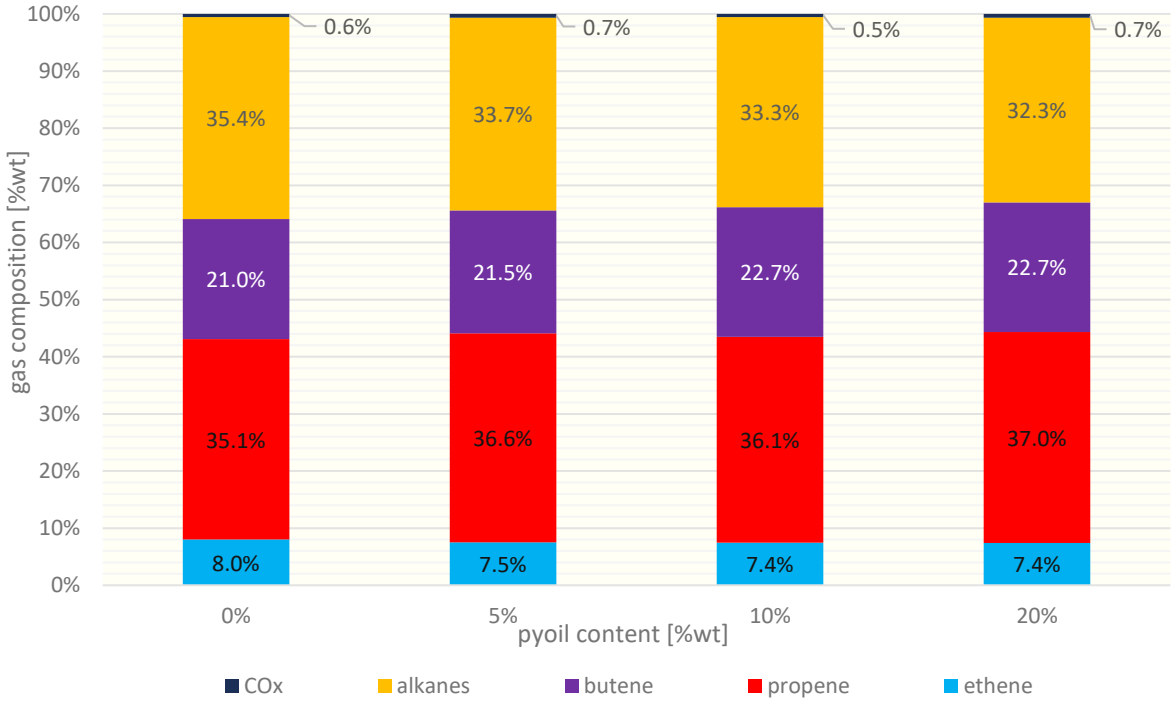

Figure 25: Gas composition of VGO/pyoil admixtures

The individual yields of the butenes are depicted in the following figure 26. All butenes increase slightly, in the case of 1-butene from 1.7 to 1.9 %wt. Isobutene rises from 3.3 to 3.5 %wt. Cis-2-butene and trans-2-butene rise from 1.6 to 1.8 and from 2.2 to 2.5 %wt. It is worth to mention that the butene yield shows a maximum at 10 %wt pyoil admixture rate and the yields drop slightly when the pyoil content in the feedstock is raised. This is contrary to the relative maximum of the ethene and propene yield in the previous figure. They reach a relative maximum at 5 %wt admixture rate, drop slightly at 10 %wt before rising again at 20 %wt.

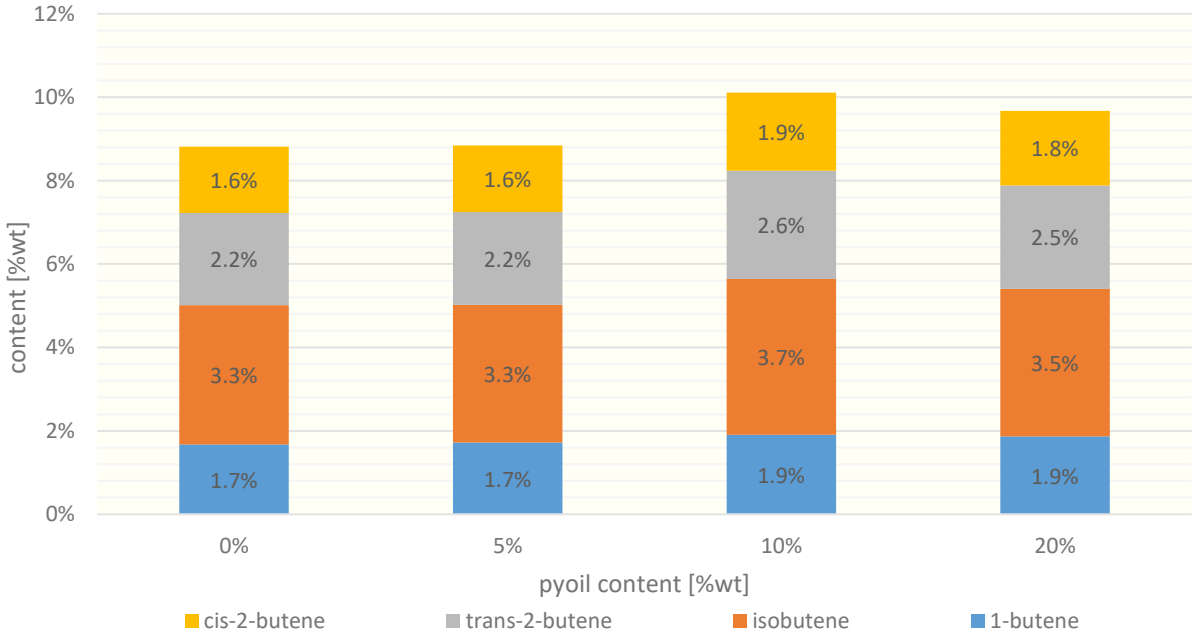

Figure 26: Butene yield of VGO/pyoil admixtures

In the next figure the alkanes and CO_X yields are depicted. Methane and ethane yields stay relatively stable at 1.1 respectively 0.6 %wt with small deviations at higher admixture rates. The propane yield decreases from 3.1 to 2.7 %wt, the isobutane yield also decreases from 8.6 to 8.1 %wt but shows an intermediate maximum of 8.7 %wt at 10 %wt admixture rate. The n-butane yield in comparison stays relatively stable with initial 1.5 and final 1.3 %wt. The figure contains additional information on the produced carbon oxides in the product gas. Carbon monoxide and carbon dioxide both stay relatively constant. CO production increases from 0.1 to 0.1 %wt and CO_2 production increases from 0.1 to 0.2 %wt.

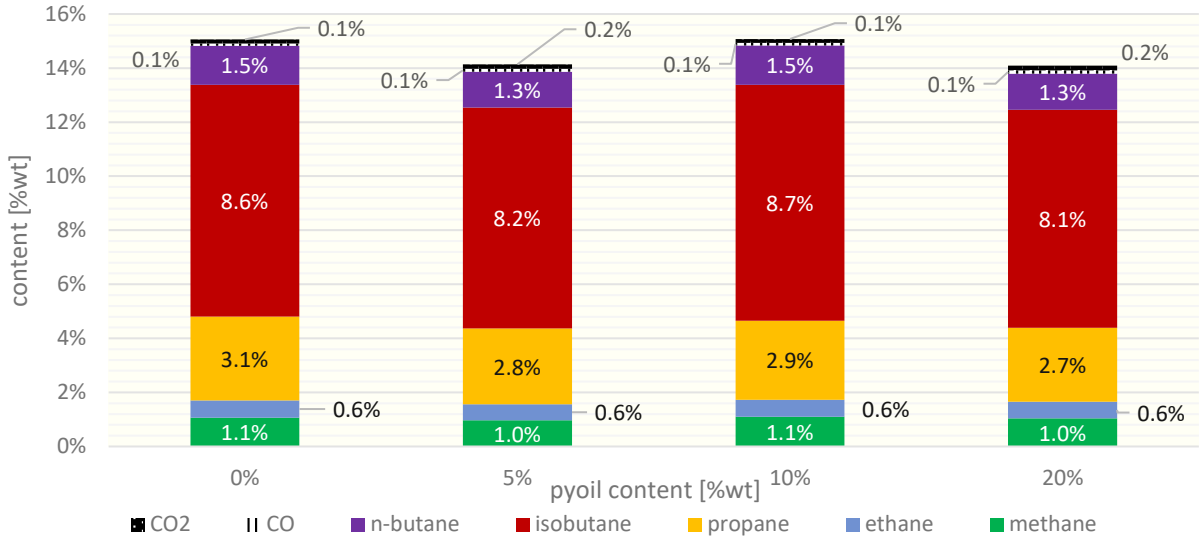

Figure 27: Alkane and CO_X yield of VGO/pyoil admixtures

Discussion

Plant operation

In a nutshell, pyrolyzed municipal plastic waste-derived pyoil is a viable raw material for a pilot-scale FCC (fluid catalytic cracking) plant. Certain challenges related to plant operation that came up such as small blockings, increased cooling and increased water production can be addressed by implementing common practices used in full-scale industrial FCC plants, such as employing hot filtration techniques to remove impurities and precipitates. Another requirement could be the slight adaption of the autothermal profile of the plant to cope with lighter boiling curve of the pyoil and, thus, the higher C/O ratio. The oxygen content goes hand in hand with a significant water production in the riser.

Products

The inclusion of pyoil as a co-feed led to a reduced production of gasoline. This outcome can potentially be attributed to the lower boiling range of pyoil compared to VGO (Vacuum Gas Oil). The aromatic contents in both feedstocks are similar (34.9 %wt for pyoil versus 32.6 %wt for VGO), leading to similar amount of uncrackable aromatics in the liquid product, resulting in a similar aromatic gasoline fraction. The variable (non-aromatic) part of the gasoline is indeed influenced by the boiling curve of the feedstock. Therefore a lighter feedstock blend will result in lighter products if the cracking parameters remain untouched due to over cracking of the feedstock.

The reduced gasoline production is compensated by the increased gas production, especially the olefin production. The significant higher C3 and C4 olefin yields increase the amount of

directly usable petrochemicals, elevating the ratio of directly recycled pyoil. An explanation for the high olefin yields could be the high ratio of polyolefins contained in the feedstock for pyoil production. The long chain paraffinic structures react readily with the catalyst to produce olefins. At the same time C3 and C4 alkane production is decreased. An explanation could be the catalyst. The catalyst is designed to increase the production of C3 and C4 olefins. The higher olefin production could simply be the result of the catalyst's selectivity. Another explanation could be the amount of oxygen contained in the pyoil. The oxygen predominantly forms water in the riser, reducing the available hydrogen for other reactions in the riser.
The water production bears some challenges for co-processing of pyoil in industrial sized FCC units. Industrial sized FCC units are commonly fluidized with steam, meaning that a high amount of steam is expected to be part of the product gas fraction. However, equipment downstream of the FCC riser needs to be re-evaluated for suitability of the increased steam (and after condensation water) flow rate.

Two notable outcomes are CO_X and coke production, which both stay relatively constant. The constant CO_X production implies that the oxygen contained in the feedstock is almost entirely transferred to water. The possible production of oxygenates could not be investigated due to missing analyzation capabilities.
The constant coke production is indeed remarkable because the CCR value implied an elevated coking tendency, which was not observed during the test runs.

10.2.2 Lowering the carbon intensity of the overall process by adding biogenic oils to the feedstock

Introduction

The two challenges, defossilization of industrial processes and establishing a circular economy, need to go hand in hand to achieve a sustainable industry and society. Implementing chemical recycling by utilizing pyoil obtained from municipal plastic waste into refinery operations can only be one small step into this direction. Another small step could be to decarbonize the process by introducing biogenic feedstocks in addition to pyoil in order to lower the overall carbon intensity of the process.

Because biogenic feedstocks bear a lot of challenges to FCC plants a ready-to-use feedstock was chosen, namely canola oil. It is clear that pristine food-grade canola oil cannot be the solution to all of our problems in regard to FCC, but it can be a first step into the right direction.

Experimental setup

To investigate the effects of pyoil co-processing combined with canola oil co-processing in the FCC pilot plant three feedstock mixes were prepared. The first feedstock was pure VGO to produce a base case to compare with the results of the other experiments. The following two feeds were admixtures of VGO, pyoil and canola oil from overall 10 %wt (5 %wt pyoil and 5 %wt canola oil) to 20 %wt (10 %wt pyoil and 10 %wt canola oil).

Table 15: Admixture rates of VGO/canola oil/pyoil experiments

Experiment ID	VGO content	Pyoil content	Canola oil content	
VGOBASE2	100	0	0	%wt
VGORAPSPC10	95	5	5	%wt
VGORAPSPC20	80	10	10	%wt

Results

The feedstock mixes described in the above table are fed to the pilot plant at a mean feeding rate of 2.5 kg/h. The mean cracking temperature was chosen at 550 °C (549.7 °C was measured for all experiments). At these conditions the C/O ratio was 28.5.

The introduction of a recycled and a biogenic feedstock at the same time reduces the gasoline yield from 42.8 to 37.8 %wt and increases the gas yield marginally from 41.7 to 42.0 %wt. The rise of the gas yield is not high enough, compared to the significant drop of the gasoline production rate, to stabilize the total fuel yield. This causes the conversion (TFY) to drop from 84.5 to 79.8 %wt.

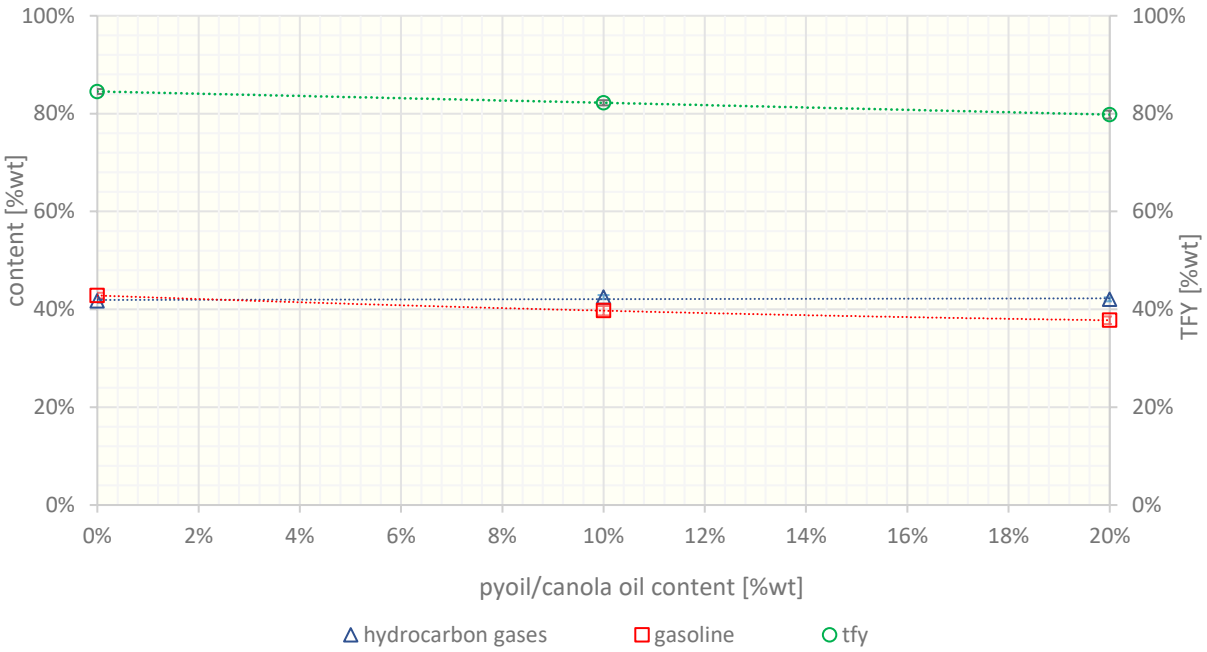

Figure 28: Hydrocarbon gases, gasoline yield and tfy of VGO/canola oil/pyoil experiments

The before mentioned drop in the conversion, caused by the reduced gasoline yield, can be related to the rising of LCO, coke and water, depicted in the following figure 29. The liquid product LCO increases from 5.5 to 6.0 %wt whilst coke increases from 6.3 to 6.8 %wt. The heaviest liquid product, residue, stagnates at 3.5 respectively 3.4 %wt. Due to the increased oxygen content of the mixed feedstock the produced water increases from a starting 0.00 %wt to 3.2 %wt.

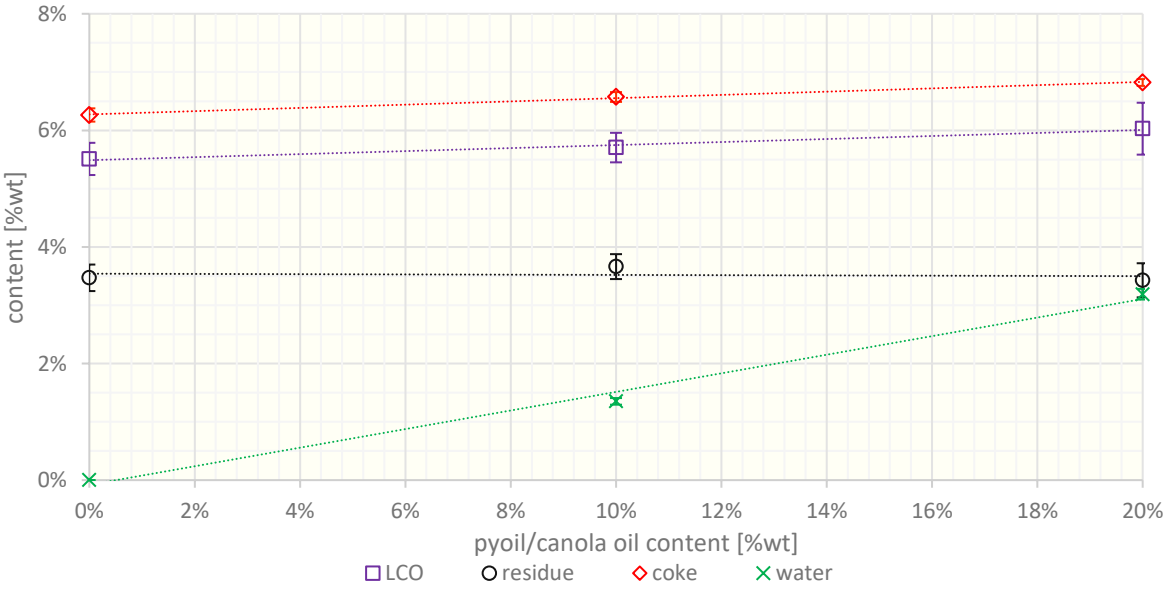

Figure 29: LCO, residue, coke and water yield of VGO/canola oil/pyoil experiments

In the following figure 30, a more detailed gas composition is depicted. The propene production increased by co-processing of pyoil and canola oil. Whilst at 0 %wt admixture rate 14.7 %wt propene are produced, 10 %wt admixture of pyoil and canola oil elevate production to 15.8 %wt. For 20 %wt admixture rate this value drops slightly to 15.7 %wt. The production of butenes also

increases from originally 8.8 to 9.8 %wt. At the same time, the ethene production almost stagnates, falling slightly from 3.4 to 3.2 %wt. The gains in the valuable olefins come at cost of the alkanes. The overall alkane production drops from 14.8 to 13.3 %wt. However, the significant increase of the overall olefin yield still increases the overall gas yield of the process, which is especially interesting regarding the amount of valuable petrochemical precursors/products.

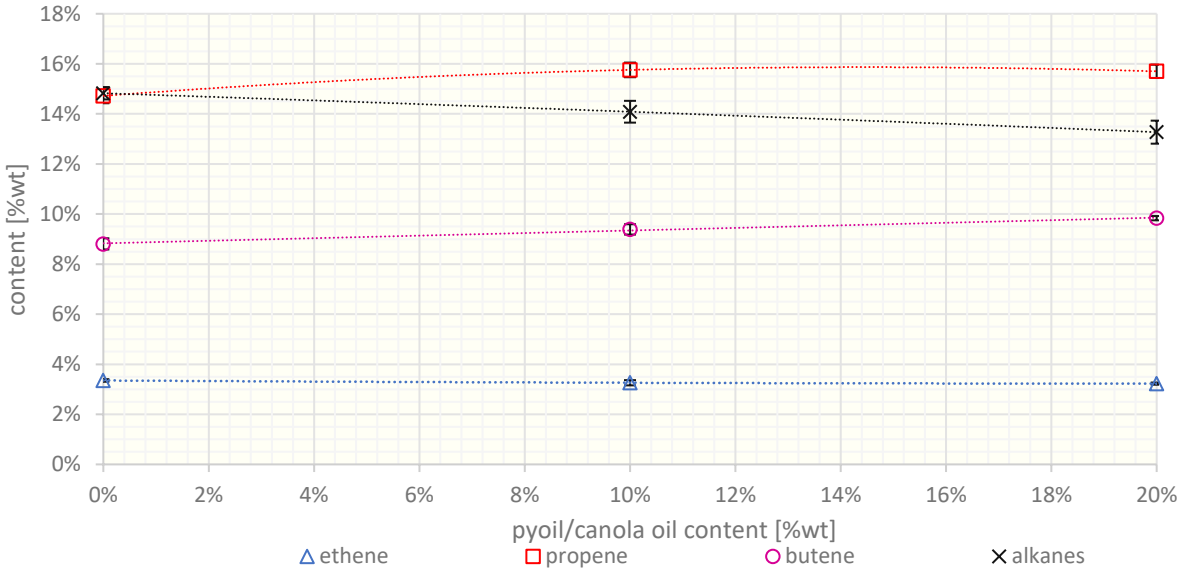

Figure 30: Ethene, propene, butene and alkane yield of VGO/canola oil/pyoil experiments

The more detailed composition of the gaseous products is depicted in the following figure 31. The values shown are set into relation to the overall gas yield. This illustrates the changes in the gas composition with the rising admixture rate. The most prominent gaseous product is propene. The propene yield rises with rising admixture rate, starting at 35.1 %wt for pure VGO and ending at 36.7 %wt for overall 20%wt admixture rate. Similar developments can be seen in the butene yield. The yield rises from initially 21.0 %wt to 23.0 %wt. These rises are countered by the drop of alkane and ethene production. The ethene yield is lowered from 8.0% to a final 7.5 %wt. The alkene production decreases from 35.4 %wt to 31.0 %wt. The carbon oxide production increases from 0.6 to 1.7 %wt.

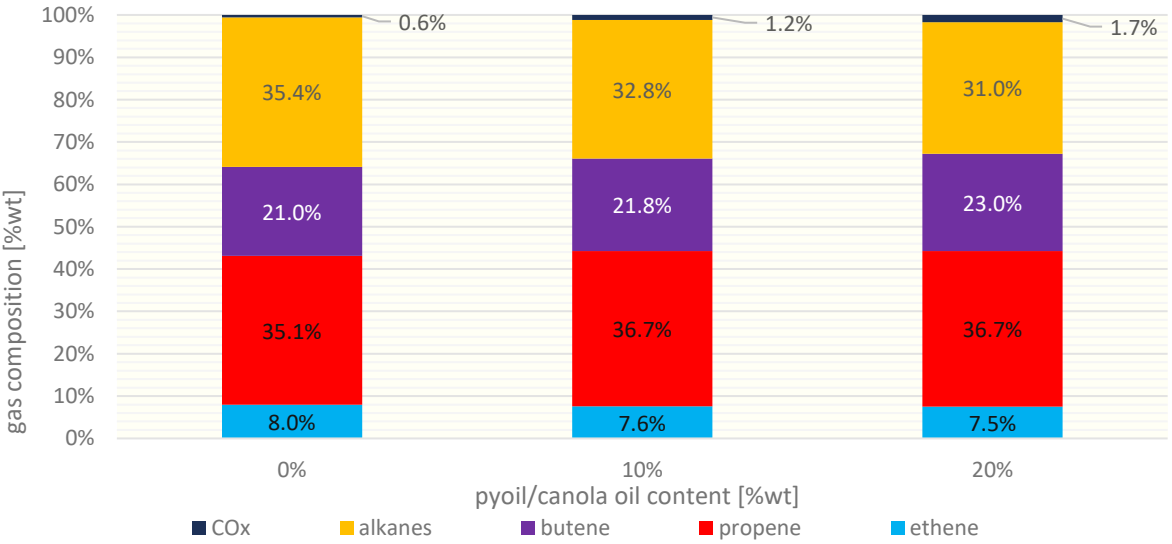

Figure 31: Gas composition of VGO/canola oil/pyoil experiments

The butene composition depicted in the following figure 32 reflects the gain in overall yield of the butenes. 1- butene increases from 1.7 to 1.8 %wt, isobutene rises from 3.3 to 3.6 %wt. Similar to this trans-2-butene increases from 2.2 to 2.6 %wt and cis-2-butene rises from 1.6 to 1.8 %wt.

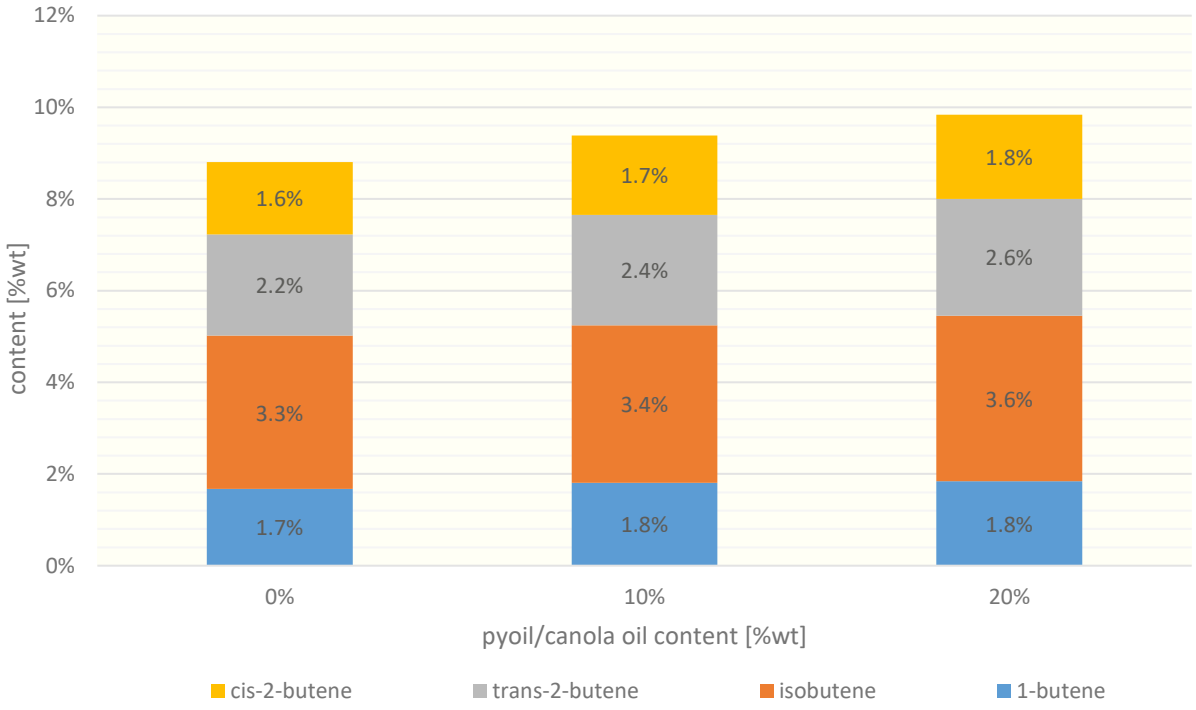

Figure 32: Butene yields of VGO/canola oil/pyoil experiments

The overall reducing saturated gas yield is depicted in the following figure 33. Methane stays almost constant and varies from 1.1 to 1.0 %wt. The same applies for ethane at 0.6 %wt. Propane shows a decreasing trend, dropping from initial 3.1 to 2.7 %wt. Similar to this the isobutane and n-butane yield decrease from 8.6 to 7.6 %wt respectively from 1.5 to 1.3 %wt. The implementation of the two co-processed feeds increases the carbon oxide production. CO rises from 0.1 to 0.5 %wt. CO_2 increases from 0.1 to 0.3 %wt.

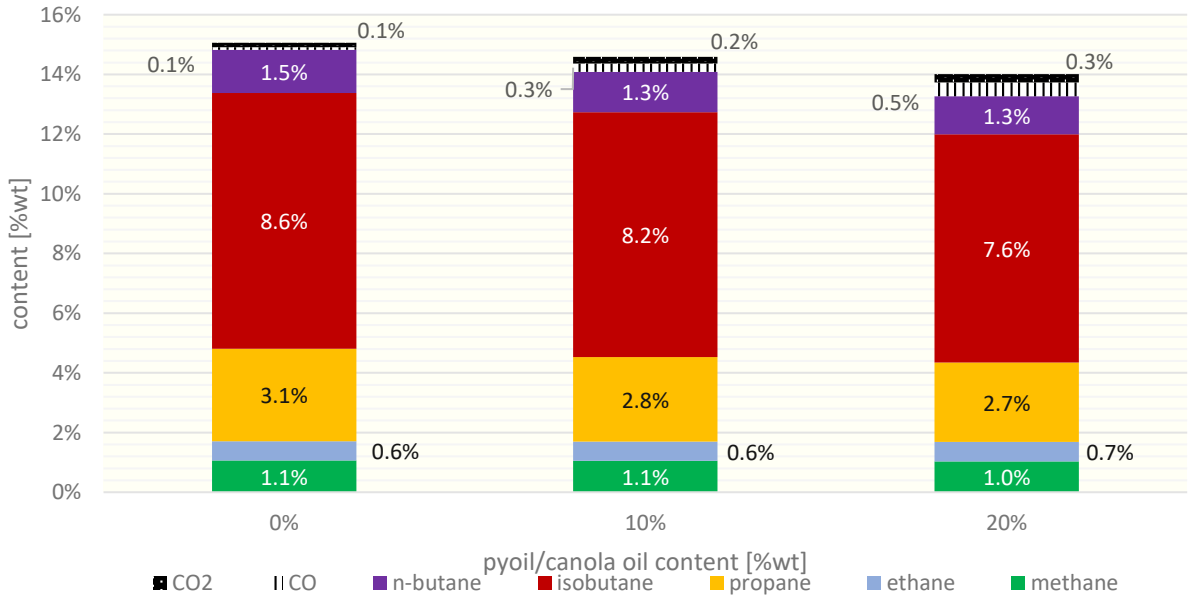

Figure 33: Alkane and CO_X yields of VGO/canola oil/pyoil experiments

Discussion

Plant operation

To obtain industrial-scale co-processing the mixture of multiple feedstocks of diverse origins needs to be considered. Finding synergies between these feedstocks will be a challenge to the process experts and future operators. Multi-dimensional feedstock strategies will require extensive testing to find synergetic and antagonistic effects to circumvent such feedstock combinations.

The utilized feedstock admixtures where easily feedable to the FCC pilot unit. Apart from an (expected) increased cooling demand no challenges regarding plant operation arose during the experimental runs.

Products

One challenge regarding the business case of industrial size FCC units is the dropping gasoline lump size. A drop of more than 5 %wt bears an enormous loss in profitability of the process. This can be explained by the increasing hydrocarbon gas yield, LCO and residue yield as well as by the valueless byproducts water and carbon oxides. Although LCO and residue are not valueless they are predominantly fed back into the FCC unit or act as blending components and don't bear the degree of value creation inherent to high-octane FCC gasoline. Although the overall gas yield stagnates, the quality of the gas improves. The yield in olefins increases significantly, not only in relation to the gas yield but also in absolute numbers.

The produced water bears always challenges to downstream equipment. The considerations regarding the produced water can be found in the previous discussion chapter on pyoil integration into FCC units.

The rising amount of produced carbon oxides in the product gas are characteristic to biogenic oils such as canola oil in FCC units. High admixture rates of canola oil lead to high CO contents. For pure canola oil, a CO content of 2.0 %wt and a CO_2 content of 0.6 %wt can be reached easily. The challenges born out of this are even higher than for the elevated water content in the product gas. Industrial sized FCC units are fluidized with steam, meaning that the downstream equipment is designed to handle high amounts of water. Removing high amounts of carbon oxides is in comparison a major challenge and requires extensive gas scrubbing and treatment.

10.2.3 Biogenic feedstocks for defossilization of the FCC process – a short comparison of the base cases

The base case of canola oil (and subsequently of UCO) should first and foremost be compared to the standard FCC feed VGO.
UCO as a feedstock for the FCC plant can be compared to FCC cracking VGO as the standard feedstock and to the results of a chemically more similar pure canola oil.

As seen on the following figure 34, the introduction of biogenic lipid-based feedstocks reduces the hydrocarbon gas yield and the gasoline yield at an average rate of approximately 3.7 respective 6.3 %wt. Biogenic oils also produce on average approximately 1.8 %wt less residue. At the same time they boost LCO (plus 2.0 %wt on average) and slightly coke (plus 0.4 %wt on average) production.
Regarding olefins a slight rise can be seen with a plus 0.4 %wt on ethene, a stagnant propene and plus 0.5 %wt butene yield.
The valueless carbon oxides rise on average approximately 2.3 %wt. Water is produced on an average rate of 7.1 %wt with biogenic oils as a feedstock.

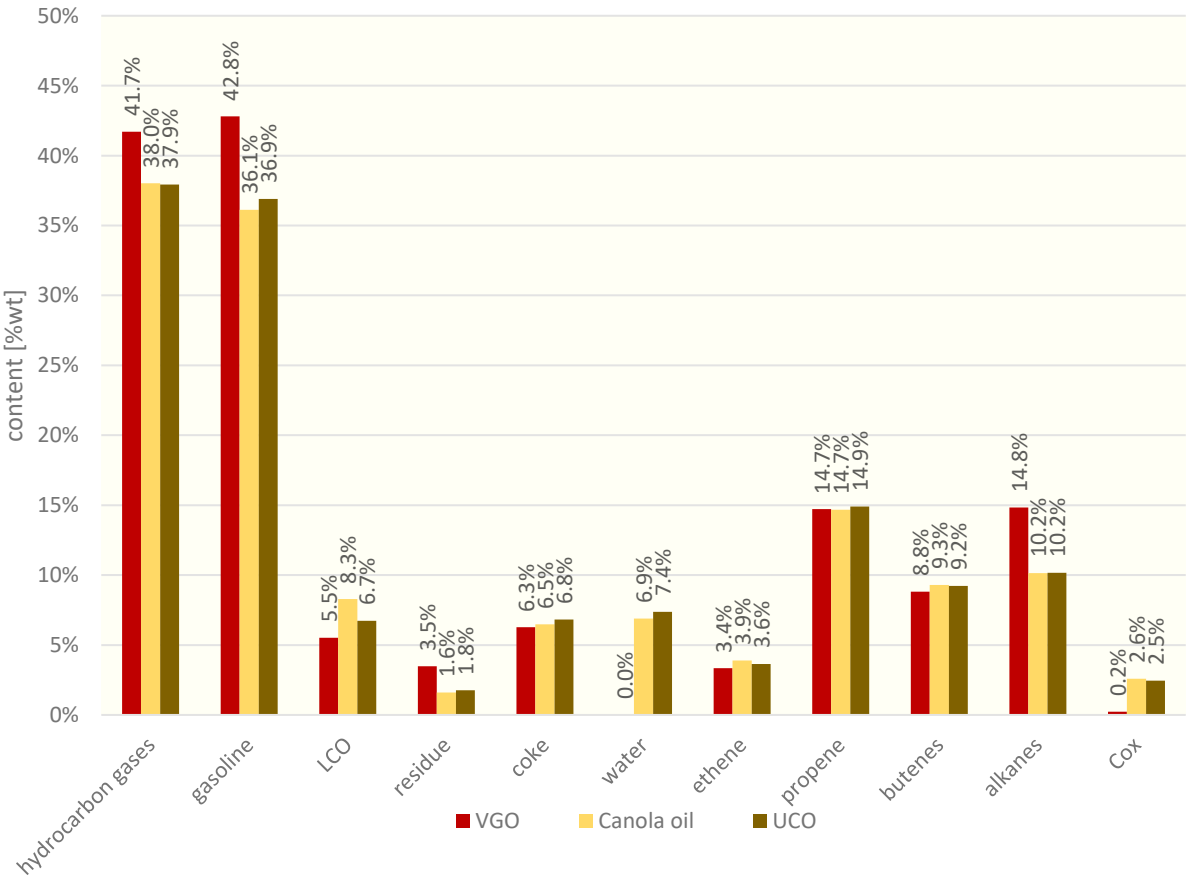

Figure 34: Short product yield comparison between VGO, canola oil and UCO

All of these developments mean a drop in conversion of approximately 10.0 %wt on average. The utilized C/O ratio almost doubles. For VGO a C/O ratio of 25.5 is realized. The in section 5.2.1 mentioned catalytic cracking reactions of biogenic oils, namely the deoxygenation and decarboxylation reaction, produce as by-products water and CO_2. This increases the volume of the oil additionally when it encounters the hot catalyst. As a result, the mean C/O ratio of canola oil is very high 43.4 and the C/O ratio for UCO is exceptionally high at 56.8.

10.2.4 Further lowering the carbon intensity by substituting VGO with canola oil

Introduction

Substitution of a part of VGO by pyoil may contribute to a small degree to a circular economy, but this comes at a cost. The combination of emissions related to energy and emissions arising from byproducts of the chemical and petrochemical industry account for 5.8 % of the global greenhouse gas emissions. [83]
Cutting back in production in this vital industrial sector is no option, considering the value creation, the economic merit of this sector and the global demand for plastics.

Introducing renewable feedstocks into the FCC process, especially considering its versatility regarding feedstock and product spectrum could be a game changer for sustainable fuels and petrochemicals. The usage of a combination of biogenic feeds such as bio lipids, bio oils derived from pyrolyzed biomass and pyoil from plastic waste could be such a cesura.

By using canola oil as the base feedstock, replacing VGO entirely, and adding pyoil from plastic waste biogenic plastic recycling could be achieved. Replacing all fossil feedstocks for FCC units globally through canola oil is not realistic. Nevertheless, replacing as much as possible of the fossil feedstocks for FCC, combined with the reduced future demand for fuels such as gasoline or diesel, could do the trick.

The experimental work presented in this section has been published before in the journal “Chemical Engineering and Processing – Process Intensification” under the title “Municipal plastic waste recycling in fluid catalytic cracking units: Production of petrochemicals and fuel in a fluid catalytic cracking pilot plant from biogenic and recycled feedstocks” in 2022.[84]

Experimental setup

To investigate plant operation and product yield distribution four experimental runs have been conducted. The first feedstock used in the pilot plant was pure canola oil.
The following three experiments were conducted with increasing pyoil content, starting at 5 %wt followed by a 10 %wt admixture rate and ending on 20 %wt pyoil in the base feedstock canola oil. Higher admixture ratios were, although interesting from an academic point of view, not conducted due to scarcity of the pyoil feedstock.

Table 16: Admixture rates of VGO/canola oil experiments

Experiment ID	Canola oil content	Pyoil content	
RAPS100	100	0	%wt
RAPSPC5	95	5	%wt
RAPSPC10	90	10	%wt
RAPSPC20	80	20	%wt

Results

The canola oil and pyoil admixtures shown in the previous table 16 are fed to the pilot plant at a measured mean feeding rate of 2.5 kg/h. The mean cracking temperature was chosen at 550 °C (551.2 °C was measured for all experiments). At these conditions the C/O ratio was very high at 45.9. The high C/O ratio is a result of the relatively low smoking point of canola oil. Canola oil tends to evaporate explosively when it comes into contact with the very hot catalyst at the start of the riser. Additionally evaporation and thermal cracking in the preheating oven cannot be ruled out.

The following figure shows the impact of pyoil addition to the base feedstock canola oil, a feedstock by itself challenging for FCC units due to very high water and carbon oxide production.

Starting at 36.1 %wt the produced gasoline shows a small rising tendency with a maximum of 37.6 %wt at 10 %wt pyoil admixture rate before dropping to 36.4 %wt. Hydrocarbon gases drop from initially 38.0 to 35.6 %wt. The almost constant gasoline yield and the significant drop in gas production causes the conversion to drop from 74.2 to 72.1 %wt.

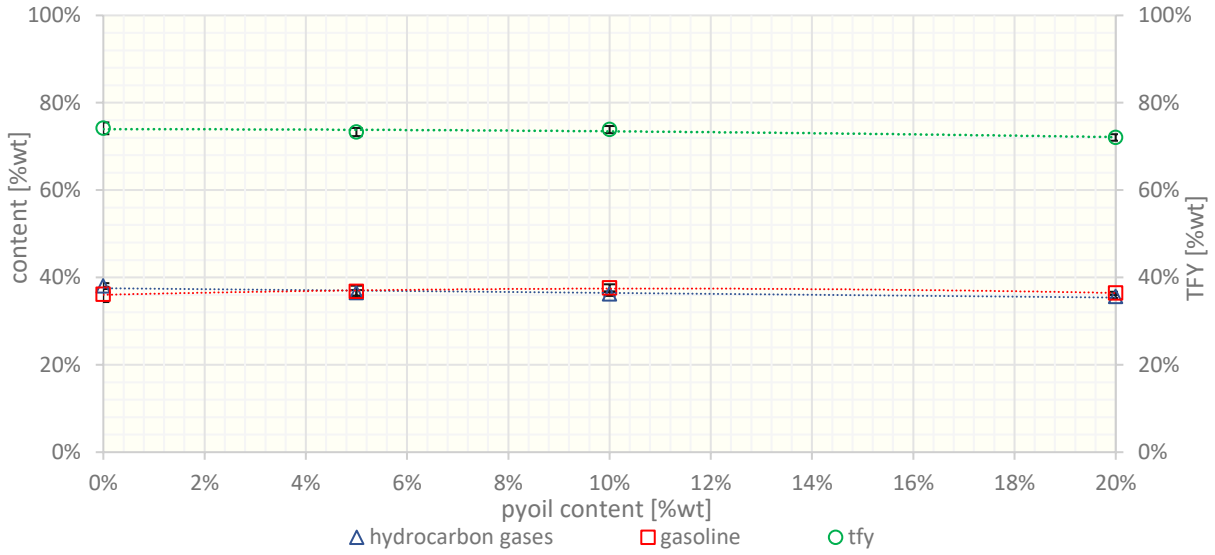

Figure 35: Hydrocarbon gases, gasoline yield and tfy of canola oil/pyoil experiments

The product yields of the lower-value products are depicted in the following figure. LCO decreases from initial 8.3 to 7.3 %wt. A drop in residue production from 1.6 to 1.3 %wt is also clearly indicated in Figure 35. In contrast to this is a rising coke production, increasing from a moderately high 6.5 to a high 7.3 %wt.

A remarkable development can be seen in the water production. The produced water increases from a very high 6.9 %wt to an outstanding 10.1 %wt.

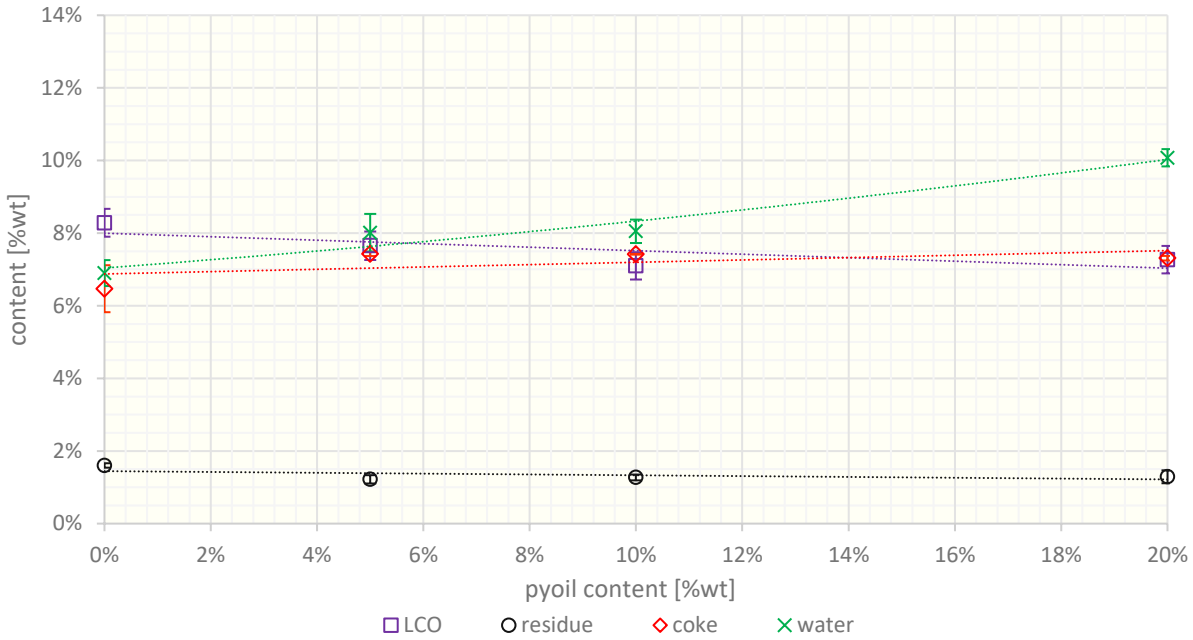

Figure 36: LCO, residue, coke and water yield of canola oil/pyoil experiments

As seen in the following diagram the propene yield increases by addition of pyoil to the feedstock. From initially 14.7 %wt the propene yield rises to a final 15.1 %wt with a maximum of 15.2 %wt at an admixture rate of 5 %wt pyoil. Butenes show no such clear trend, increasing slightly from 9.3 %wt to the local maximum of 9.5 %wt at 5 %wt admixture rate before dropping again to final 9.2 %wt. A clearly decreasing trend can be seen in the ethene production rate. The ethene yield drops from 3.9 to 3.0 %wt. A similar development can be seen for saturated hydrocarbons, the alkanes. Starting at 10.2 %wt the yield drops to 8.3 %wt.

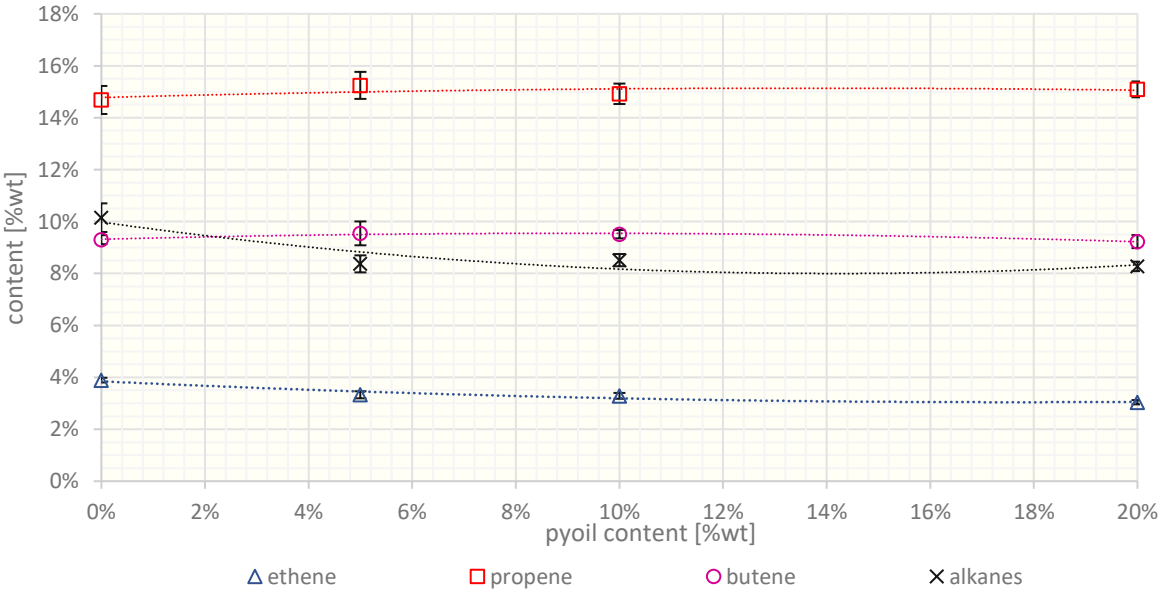

Figure 37: Ethene, propene, butene and alkane yield of canola oil/pyoil experiments

The gas composition shown in the following figure 38 supports the trend of a rising propene and butene production whilst the yields in other gas fractions drop. In relation to the overall produced hydrocarbon gas the propene yield rises from an already high value of 36.1 to 40.1 %wt. The yield in the group of the butenes rises from 22.9 to 24.5 %wt with a slight local maximum of 24.7

%wt at 10 %wt pyoil admixture rate. The dropping ethene production can also be seen in the relative values. Ethen production drops from 9.6 to 8.1 %wt. A significant drop can also be seen for the produced alkanes with a reduction from 25.0 to 22.0 %wt. The production rate of COx is reduced from 6.4 to 5.3 %wt.

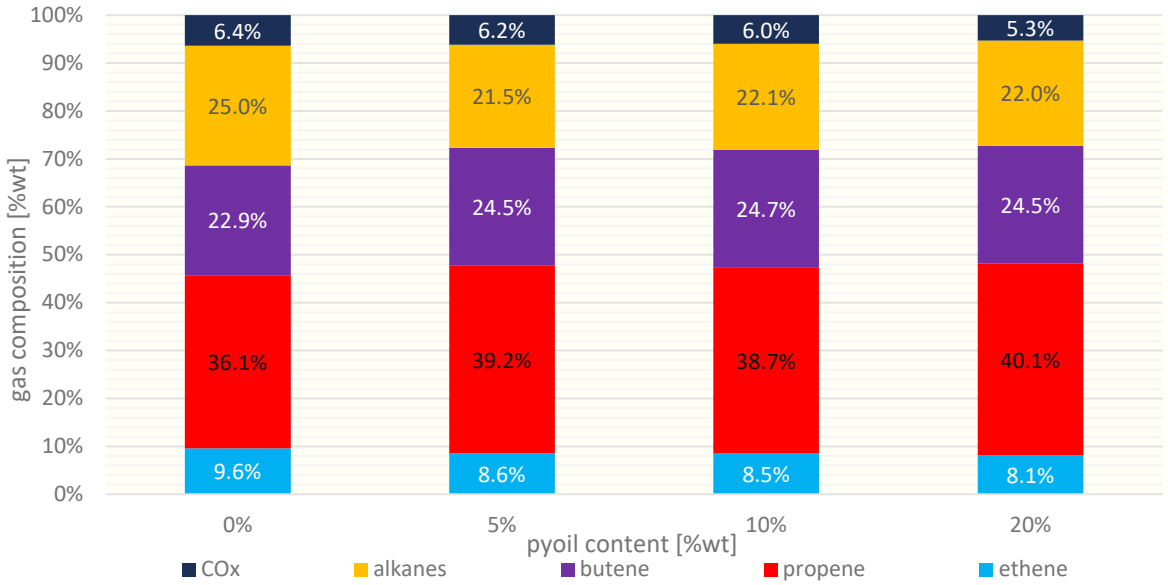

Figure 38: Gas composition of canola oil/pyoil experiments

Going into detail on the individual butenes in the following figure two different trends can be observed. A decreasing trend is depicted for isobutene, which yield reduces from 3.5 to 3.2 %wt. The other butenes show a relative maximum either at 5 or at 10 %wt admixture rate. 1-butene rises from 1.7 to 1.8 %wt. A slightly increasing trans-2-butene yield can be observed, increasing from 2.4 to a maximum of 2.5 %wt at 5 %wt admixture rate before decreasing again to 2.4 %wt in the end. The cis-2-butene production rate increases temporarily from 1.8 %wt to 1.9 %wt at 10 %wt pyoil content to a final 1.8 %wt at the highest feedstock admixture rate.

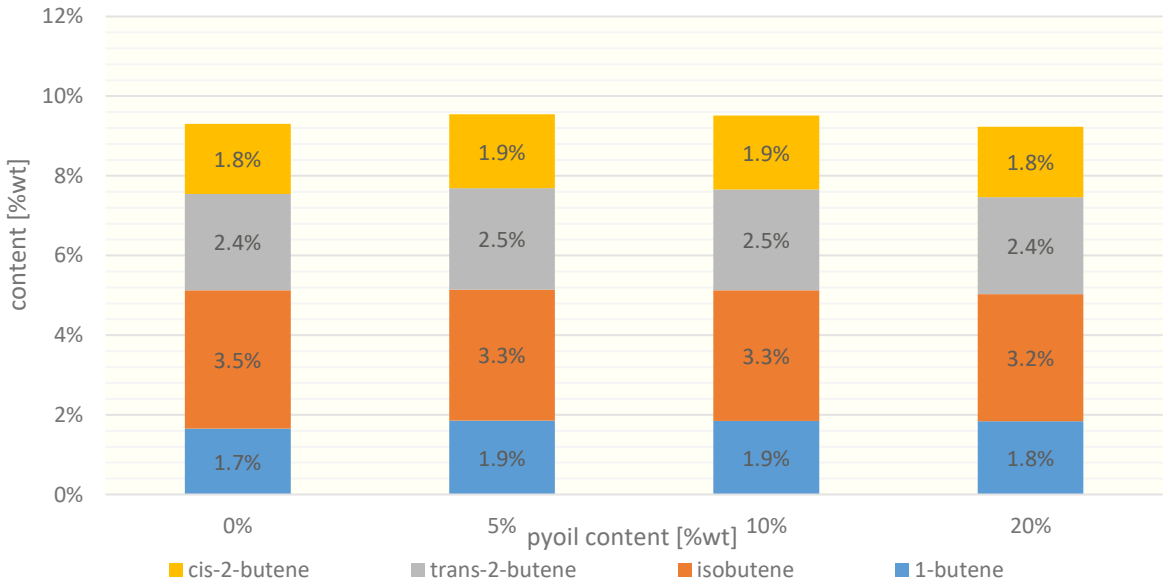

Figure 39: Butene yields of canola oil/pyoil experiments

The detailed composition of the alkanes and the carbon oxides is depicted in the following figure. A major part of the drop in the hydrocarbon gas yield can be attributed to the reduced alkane yield and the reduced carbon monoxide production rate. Starting at the smallest alkane, namely

methane, a slight reduction can be observed from initially 1.0 to 0.9 %wt. A similar behavior can be observed for the production rate of all other alkanes. Ethane drops from 0.7 to 0.6 %wt whilst propane decreases from 2.3 to 1.6 %wt. The same applies to isobutane and n-butane, decreasing from 5.2 to 4.5 %wt and from 1.0 to 0.7 %wt, respectively.

The trend of dropping yields includes carbon monoxide, going from initially 2.0 to 1.5 %wt. Carbon dioxide yield is almost constant with a production rate of initially 0.6 %wt, which insignificantly reduces to 0.5 %wt.

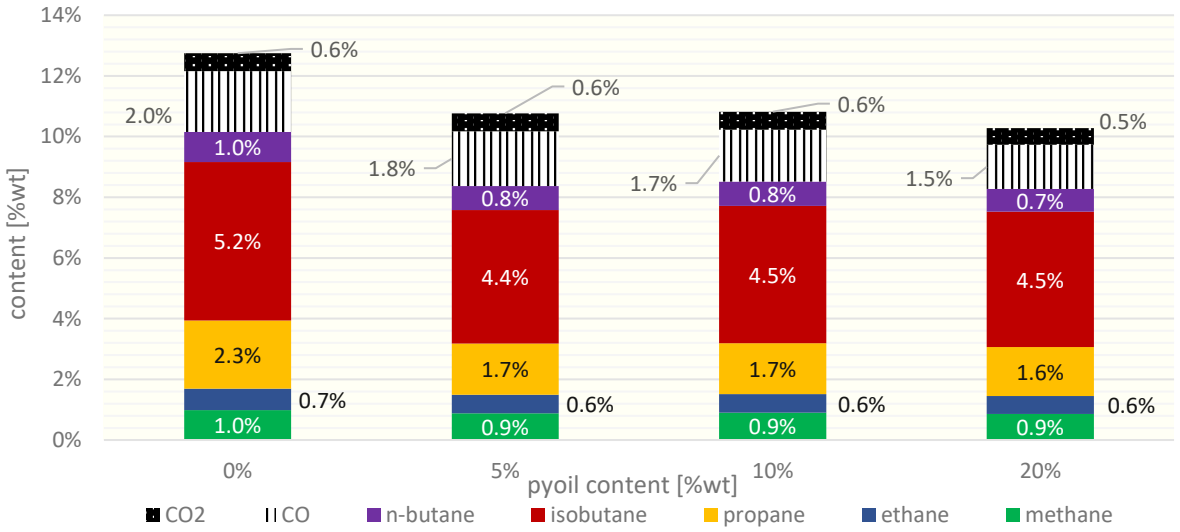

Figure 40: Alkane and COx yields of canola oil/pyoil experiments

Discussion

Plant operation

A remarkable outcome of the experiments is that co-processing of canola oil with pyoil is feasible, showing a technically, but maybe not economically, feasible way of biogenic plastic recycling.

As mentioned in section 10.2.3, introducing a feedstock such as canola oil to the FCC process is a challenge on its own.
A slightly increased coke production, compared to the standard feedstock VGO, and a high water production bear major challenges on the thermal management of the reactor and regenerator. Additionally very high production rates of carbon monoxide and carbon dioxide put additional loads on gas scrubbers downstream of the FCC unit. The addition of pyoil shifts these challenges slightly from high water and CO_X production to excessive water and lower CO_X production.

Products

The addition of pyoil changes the product spectrum, which can be seen, among other things, in the total fuel yield. The TFY behaves slightly nonlinearly, which can be described by the nonlinear development of the gasoline fraction. A reason for this could be the high content of aromatics in the syncrude. The aromatics present in the feedstock are very resistant to catalytic cracking (apart from any side chains that may be present) and therefore retain their boiling point, which can lead to an increased gasoline fraction. As the syncrude blending rate continues to increase, coke and water production increases, reducing the conversion rate of the feedstock to gasoline.

A more linear behavior can be observed for the hydrocarbon gas yield. The production rate of gas decreases with increasing admixture rate of pyoil. Similar to the gasoline production the reason for this can be found in the added aromatics, contained in the pyoil. With an increasing ration of pyoil to canola oil the amount of aromatics rises, increasing the amount of uncrackable feedstock.
Although gas production drops, propene production rises and butenes stay almost constant. This can be described by the long-chained polyolefins contained in the feedstock of the pyrolysis plant. These chains are keen to be catalytically cracked and readily form olefins as a product instead of alkanes. Additionally, these hydrocarbon chains are overall cracked to heavier gas components than the very linear-built highly saturated fatty acids of canola oil.

The reduced LCO and residue lump can be the outcome of the light boiling pyoil. Less heavy feedstock and less feedstock keen to coking (such as canola oil) means naturally less heavy hydrocarbon products.

The increased coke production means a tough challenge for FCC operators and process experts. The thermal profile of a given FCC unit needs to be adapted rigorously to cope with the high amount of thermal energy produced by the coke. All that given that the regenerator section can burn the increased amount of coke.

The reason for the high amount of water produced remains uncertain. The admixture of pyoil with its lower oxygen content than canola oil was expected to reduce water production. Due to the co-processing the overall oxygen content of the feedstock reduced from 10.9 to 9.6 %wt at 20%wt admixture rate. An explanation for this could be a suppressed formation of oxygenates, reducing solubility of water in the organic phase and thereby increasing the visible water. Another explanation for this behavior can be found when looking back to the VGO-pyoil experiments. Although the water yield rises with the pyoil ratio, no such trend could be seen there for the CO_X production rate. In the canola oil experiments such a development can be seen even clearer as a rising water production whilst at the same time CO_X production stagnates or even drops. This could be a hint that by adding pyoil to the feedstock the formation of water is favored over the production of CO and CO_2.

10.2.5 Reducing the impact on food chains by substituting food-grade canola oil by UCO

Introduction

Using pristine, food-grade canola oil perfectly fuels the tank vs. plate discussion. Using food needed elsewhere energetically or even for petrochemicals opens up ethical and political discussions. The usage of used cooking oil could lower the socioeconomical footprint of the biogenic base feedstock of the FCC plant compared to food grade oils such as canola oil.

Used cooking oil is currently predominantly used for the production of fatty acid methyl ester (FAME) or biodiesel. Biodiesel has the advantage of a lowered carbon footprint compared to fossil diesel but bears challenges to producers and users, such as a limited compatibility to engines, a low shelf life due to bio activity and a hygroscopic (water attracting) behavior. FCC units are perfectly suited to open up used cooking oil for the gasoline route whilst avoiding most disadvantages of FAME and producing a significant amount of olefins. The products of UCO in an FCC plant are chemically identical to the fossil-based products used for gasoline and olefins production.

Including pyoil from plastic waste to UCO as a base feed for the FCC takes advantage of biogenic and low carbon recycling of plastic waste. This could happen whilst producing a low carbon high-octane gasoline fuel or a naphtha fraction, suitable as a feedstock for steam crackers to help close the loop on plastic recycling.

Experimental setup

The experimental setup is identical to the canola oil experiments except for the base feedstock, which is used cooking oil from a municipal used cooking oil collection infrastructure.

Similar to the canola oil runs the investigation of plant operation and product yield distribution was done based on three experimental runs. The first feedstock used in the pilot plant was as usually a pure base feedstock, in this case UCO.
The following two experiments were done with an increasing pyoil content, starting at 5 %wt followed by 10 %wt admixture rate.

Table 17: Admixture rates of UCO/pyoil experiments

Experiment ID	UCO content	Pyoil content	
UCO100	100	0	%wt
UCOPC5	95	5	%wt
UCOPC10	90	10	%wt

Results

The gasoline yield of UCO pyoil admixtures declines slightly with increasing pyoil content, starting at 36.9 %wt and ending at 35.9 %wt at an admixture rate of 10 %wt. In contrast to this is a slightly rising hydrocarbon gas yield, starting at 37.9 %wt and ending at 38.5 %wt. The opposing trends almost compensate each other, causing only a marginal decrease in the conversion from 74.9 to 74.4 %wt.

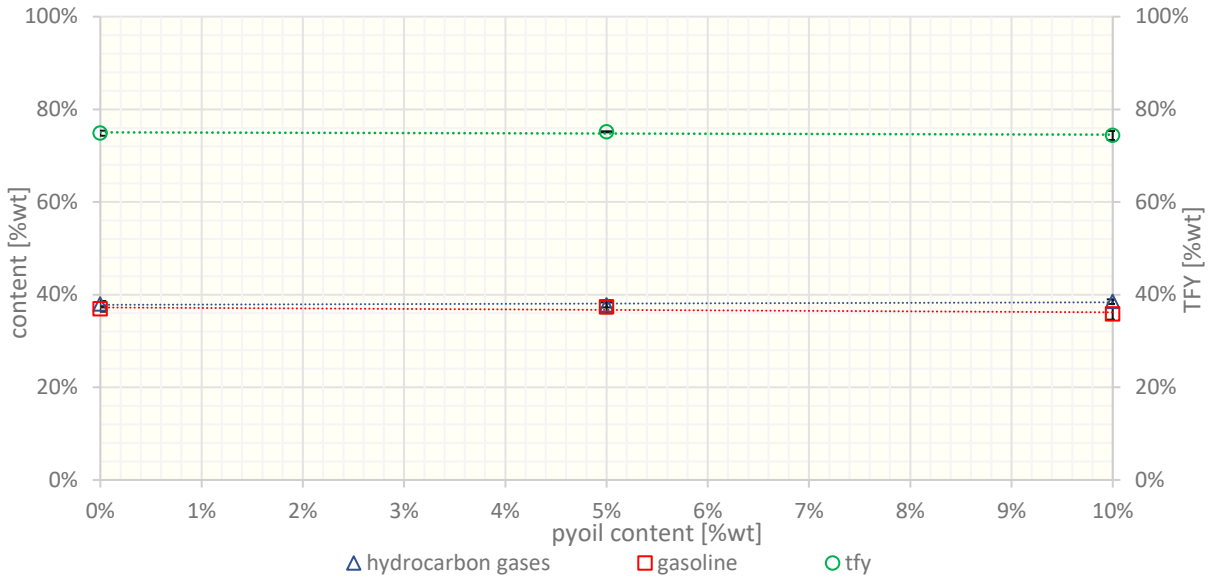

Figure 41: Hydrocarbon gases, gasoline yield and tfy of UCO/pyoil experiments

The lower-value product yields are depicted in the following figure 42. LCO is decreasing from 6.7 %wt at pure UCO feeding to 5.8 %wt at 10 %wt admixture rate. LCO also shows a local minimum of 5.5 %wt at 5 %wt pyoil admixture rate. The opposite can be observed for the coke production rate. Starting at 6.8 %wt it increases to 7.2 %wt with a local maximum of 7.6 %wt at 5 %wt admixture rate. The residue yield in comparison shows no such non-linearities, decreasing linearly and only slightly from 1.8 to 1.7 %wt.
The water production increases by admixture of pyoil. The already high amount at 0 %wt admixture rate of 7.4 %wt increases to 8.7 %wt at 10 %wt admixture ratio.

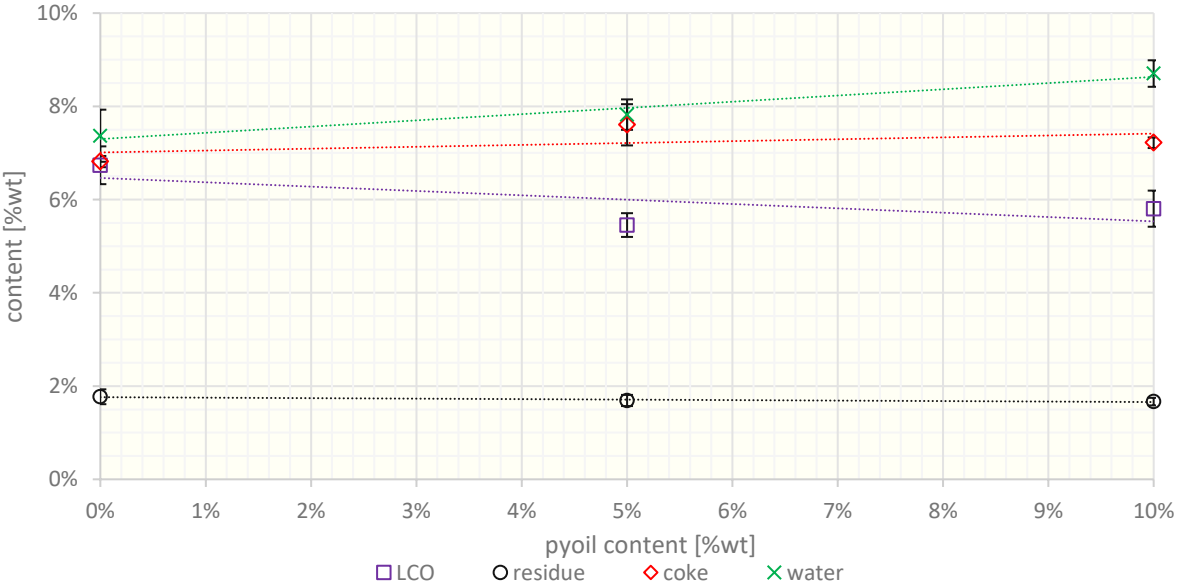

Figure 42: LCO, residue, coke and water yield of UCO/pyoil experiments

The important high value olefins are depicted in the following diagram 43. The propene yield increases from 14.9 to 15.9 %wt. The same applies to the butene production, increasing from 9.2 to 10.0 %wt. As seen in previous experiments, the ethene and alkane yield drop when pyoil is added to biogenic oils. Ethen drops from 3.7 to 3.5 %wt and the group of alkanes drop from 10.2 to 9.0 %wt.

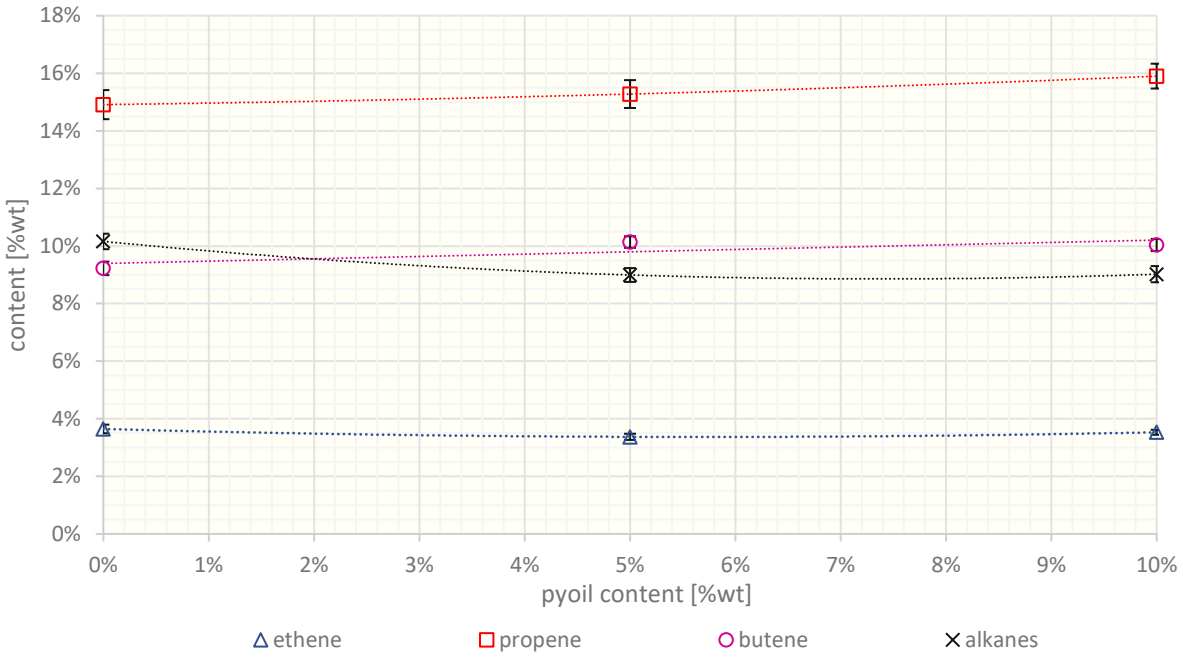

Figure 43: Ethene, propene, butene and alkane yield of UCO/pyoil experiments

The group of olefins is analyzed in more detail based on the overall gas yield in the next figure 44. The drop in ethene and alkane production can also be observed here. Ethene drops from 9.0 to 8.7 %wt. The alkanes reduce from 25.1 to 22.1 %wt content in the product gas. The opposite can be observed for the propene and the butene yield. Propene increases from 36.9 to 39.0 %wt and the butenes rise from 22.8 to 24.6 %wt. The COx production decreases from 6.1 to 5.5 %wt.

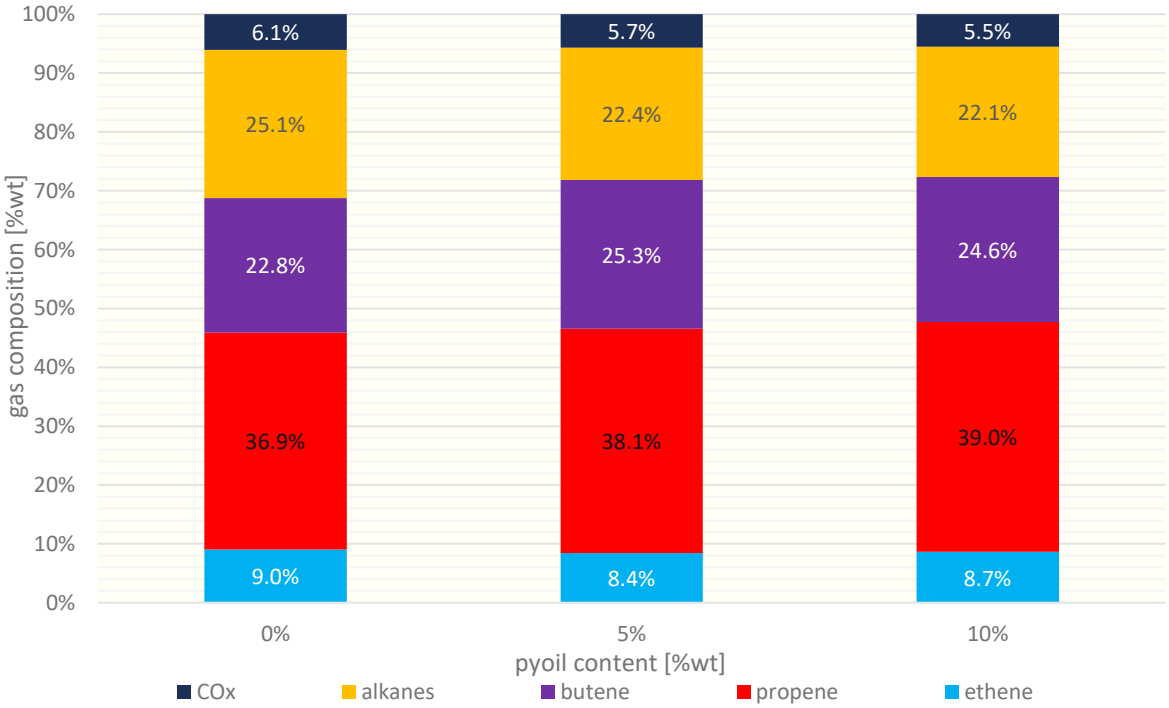

Figure 44: Gas composition of UCO/pyoil experiments

Details on the yield distribution in the group of the butenes are depicted in the following figure 45. The increased gas yield also includes gains in the butene group. 1-butene rises from 1.7 to 1.9 %wt whilst isobutene yield is increased from 3.4 to 3.5 %wt. Cis- and trans-2-butene rise from 1.7 to 1.9 %wt and from 2.4 to 2.7 %wt, respectively. Both show a maximum at 5 %wt admixture rate with 2.0 %wt for the cis-2-butene yield and 2.7 %wt for the trans-2-butene yield.

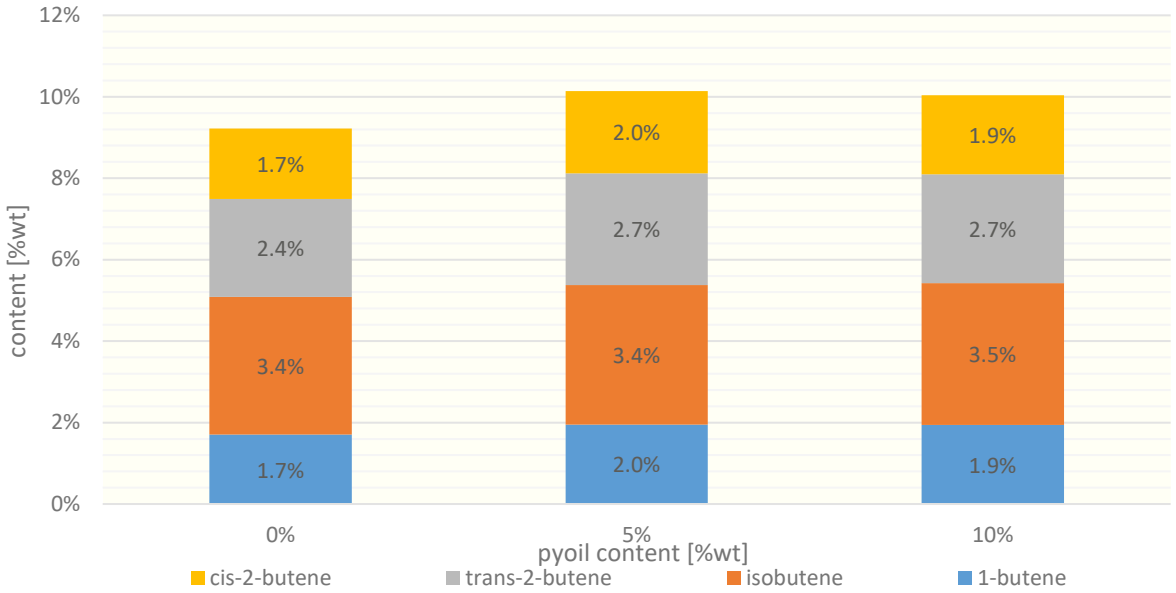

Figure 45: Butene yields of UCO/pyoil experiments

The overall produced alkanes are reduced with increasing co-feeding of pyoil as seen in the following figure. Contrary to the overall alkane production the methane yield stays almost constant at 0.9 and 1.0 %wt, respectively. Ethane drops insignificant from 0.7 to 0.6 %wt and propane from 2.1 to 1.8 %wt. The most significant drop can be observed for isobutane, decreasing from 5.4 to 4.8 %wt. N-butane drops slightly from 1.0 to 0.8 %wt.
A positive trend can be observed for CO_X production, which is reduced from 1.9 to 1.7 %wt for CO and for CO_2 slightly from 0.6 to 0.5 %wt.

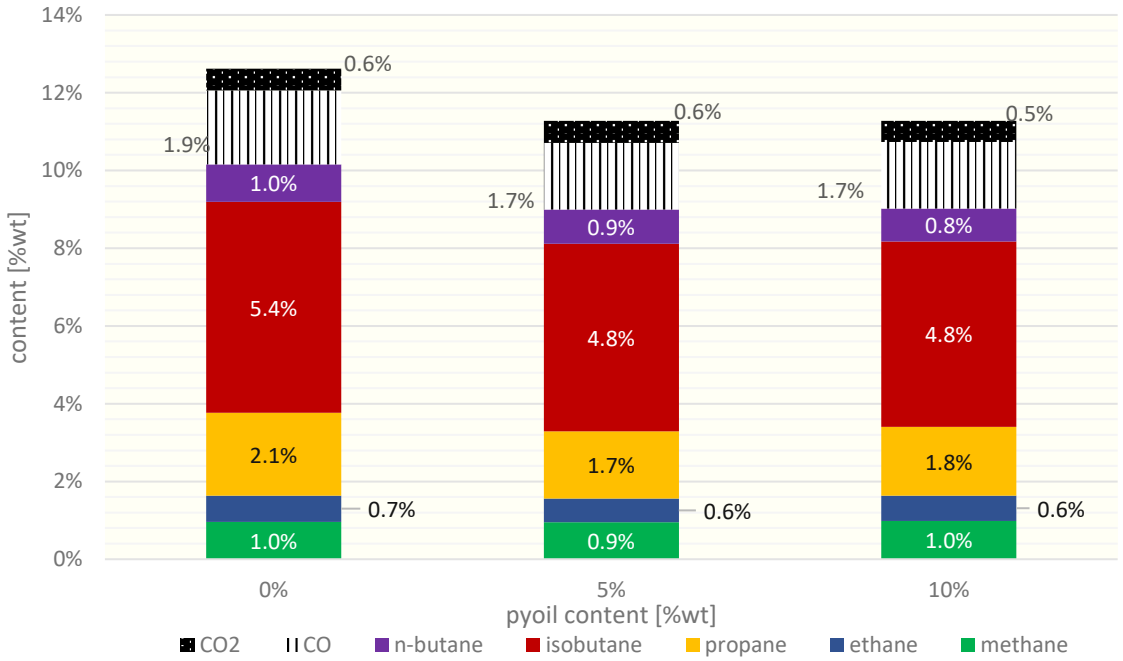

Figure 46: Alkane and CO_X yields of UCO/pyoil experiments

Discussion

Plant operation

Operation of an FCC pilot plant co-feeding UCO and pyoil can be challenging. UCO often contains contaminants such as water and food residues, which have to be removed before feeding it to the plant in order to prevent blocking due to coking and aggregating particles in feed and preheat lines.
Similar to canola oil the high oxygen content in UCO fuels water production and the higher C/O ration increases the thermal energy input into the riser. All of this results in higher temperatures of the riser/reactor if the thermal profile of the unit remains unadjusted to the feedstock.

Products

The results regarding the product yields of co-processing of UCO and pyoil are relatively positive. Co-processing improves the hydrocarbon gas yield whilst reducing gasoline only slightly. In the case of 5 %wt admixture rate the pyoil addition improved gasoline production compared to the benchmark whilst only reducing hydrocarbon gas yields insignificantly, meaning that the both feedstocks synergize to a certain degree.

Similar to the canola oil experiments the addition of pyoil boosted propene production. As previously stated, this can be explained by the changing feedstock composition, the amplitude of the boost is nevertheless remarkable. The same applies to the produced butene yield, which increases significantly, especially when the results are compared with the canola oil experiments.

The low value product yields stay constant or decrease whilst the yield of the valueless product water rises. The produced amount of the valueless byproduct CO_X decreases.

10.2.6 Investigating the effect of elevated cracking temperatures on the gas and olefin yield of the partially “circularized and decarbonized” process

Introduction

To close the circle on polymers the production of olefins from the FCC process needs to be maximized. An influence parameter, apart from catalyst and feedstock composition among others, is the cracking temperature. Increasing the temperature increases the severity of the process, potentially leading to increased gaseous products and lowering long chained product yields. All of this depends on the exact position of the temperature-dependent gasoline maximum. For detail on the temperature influence on product yields refer to the chapter 3.5.

To investigate the influence of elevated cracking temperatures on pyoil admixtures the temperature level was elevated from 550 °C to 570 °C.

Experimental setup

To ensure comparability the same feedstocks and feedstock admixtures already used in previous experimental runs have been chosen.

Details on the conducted experiments are shown in the following table 18. The values used for the experiments at 550 °C are identical to the previously shown values.

Table 18: Admixture rates of high temperature experiments

Experiment ID	Feedstock composition				Mean cracking temperature	
	VGO	UCO	PC			
VGO_570	100	0	0	%wt	570	°C
VGOPC10_570	90	0	10	%wt	570	°C
UCO_570	0	100	0	%wt	570	°C
UCOPC10_570	0	90	10	%wt	570	°C
VGOBASE2	100	0	0	%wt	550	°C
VGOPC10	90	0	10	%wt	550	°C
UCO	0	100	0	%wt	550	°C
UCOPC10	0	90	10	%wt	550	°C

Results

High severity cracking of VGO-based admixtures

Pure VGO at 570 °C

The first step of increasing the cracking temperature was done for the standard feedstock VGO. As depicted in the following figure 47.
Increasing the mean cracking temperature showed only very little effect on the product lumps gasoline and hydrocarbon gases. The gas production drops slightly from 41.7 to 41.1 %wt. The gasoline yield is almost constant at 42.8 and 42.9 %wt, respectively. This causes the conversion to drop slightly from 84.5 to 84.1 %wt.

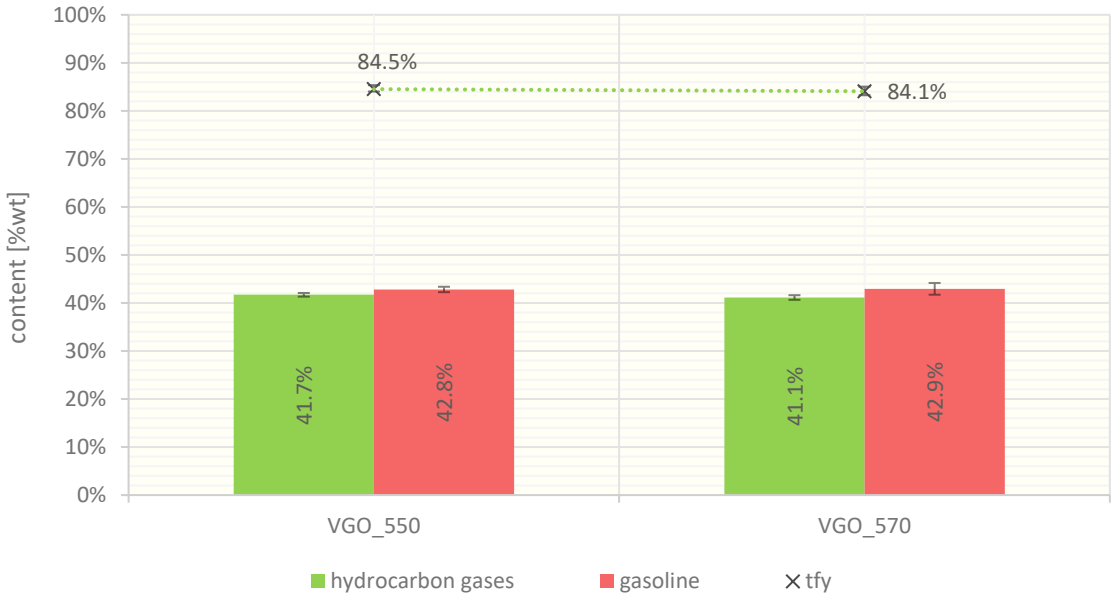

Figure 47: Hydrocarbon gases, gasoline yield and tfy of high severity cracking experiments with pure VGO

The lower value products depicted in the next figure show a similar behavior to the previous lumps. LCO stays almost constant with a slight raise from 5.5 to 5.6 %wt. The residue yield increases from 3.5 to 3.8 %wt. Coke production rate drops slightly from 6.3 to 6.1 %wt. Because pure VGO contains virtually no oxygen no water formation was observed for both temperature levels.

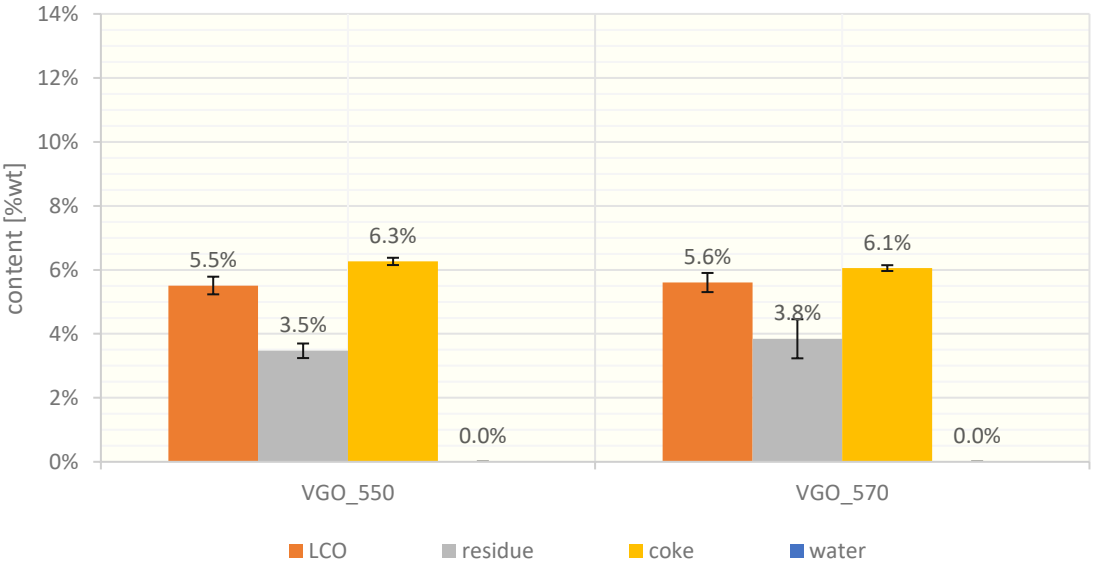

Figure 48: LCO. residue, coke and water yield of high severity cracking experiments with pure VGO

Increasing the mean cracking temperature increases the propene and butene production significantly as seen in the following figure. Although the overall gas production decreases, the propene yield rises from 14.7 to 15.8 %wt. The same applies to the production of butenes, which increases from 8.8 to 10.2 %wt. The ethene yield constant at 3.34 %wt.
In contrast to this are the alkane yields, decreasing from 14.8 to 11.8 %wt.

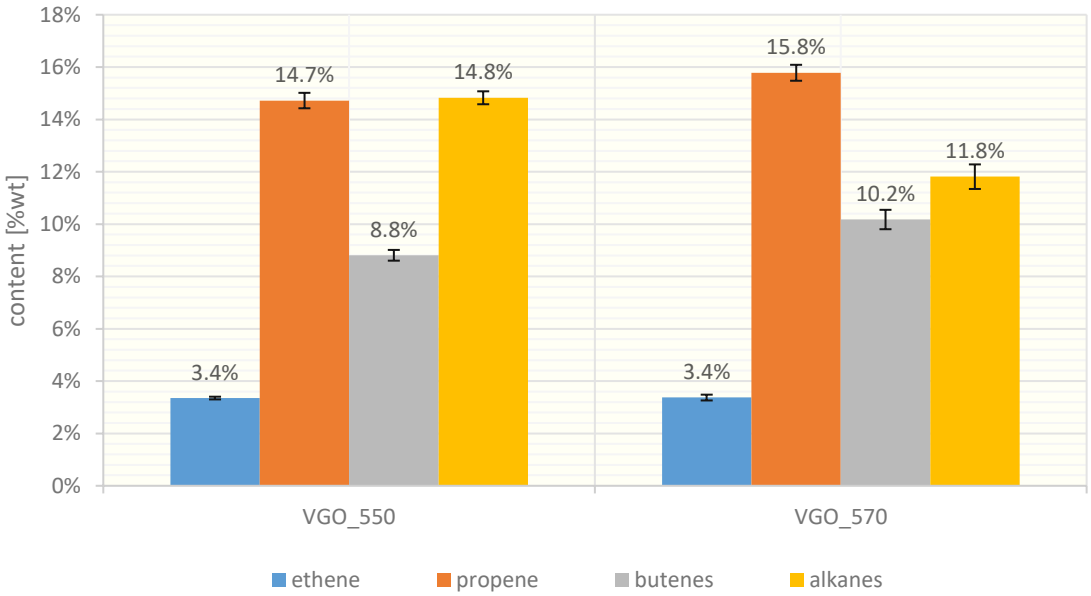

Figure 49: Ethene, propene, butenes and alkane yield of high severity cracking experiments with pure VGO

In relation to the overall hydrocarbon gas yield, the rise of the propene and butene yield are significant. Propene increases from 35.1 to 38.0 %wt. Butenes increase from 21.0 to 24.5 %wt. Ethene increases slightly from 8.0 to 8.1 %wt. These increases come at cost of the alkane yield, dropping from 35.4 to 28.4 %wt. COx increases from 0.6 to 1.0 %wt.

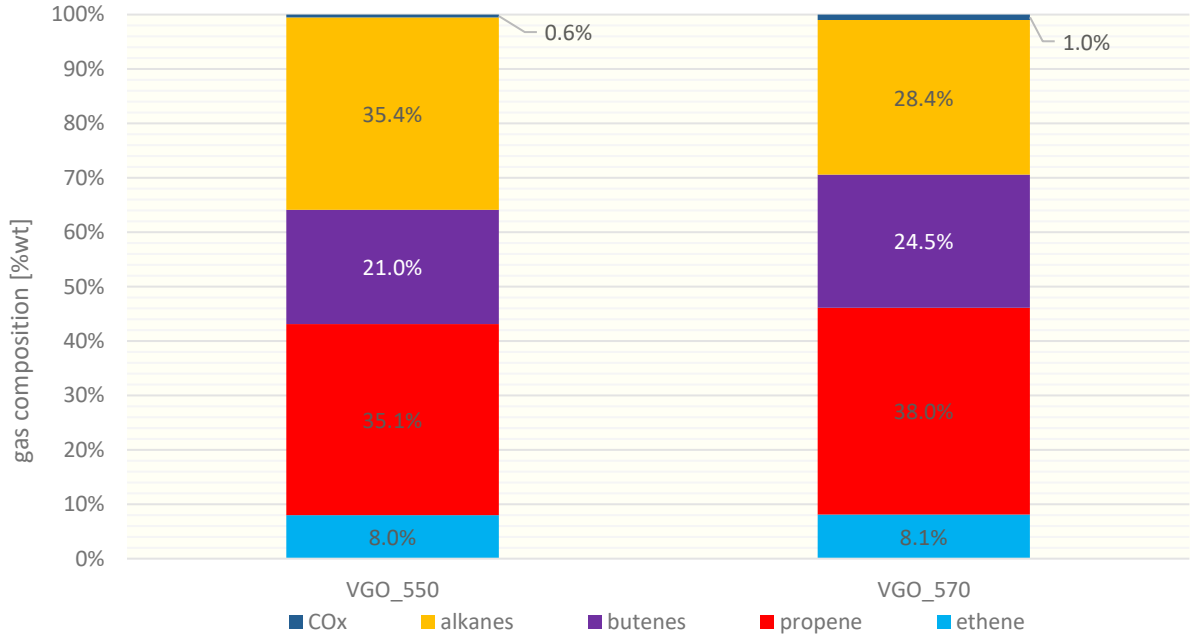

Figure 50: Gas composition of high severity cracking experiments with pure VGO

The increased temperature results in increased yields of all butenes, depicted in the following diagram 51. 1-butene increases from 1.7 to 1.9 %wt. Isobutene increases from 3.3 to 3.9 %wt. Trans-2-butene increases from 2.2 to 2.5 %wt and cis-2-butene increases from 1.6 to 1.8 %wt.

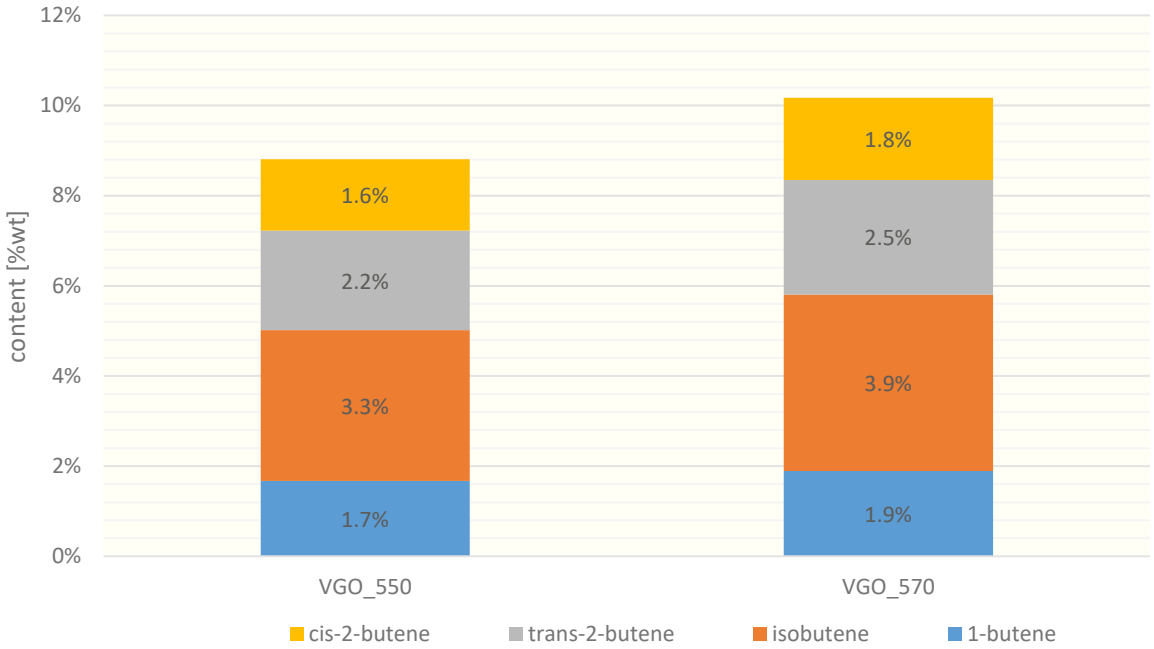

Figure 51: Butene yields of high severity cracking experiments with pure VGO

The composition if the remaining alkane gas fraction and the produced carbon oxides is depicted in the following diagram 52. The drop in alkane production rate includes all depicted fractions. Methane stays almost constant at 1.1 and 1.0 %wt, respectively. The same applies to ethane at 0.6. More significant is the drop of propane, decreasing from 3.1 to 2.5 %wt. The even bigger drop of isobutane starts at 8.6 %wt before decreasing to 6.5 %. N-butane decreases from 1.5 to 1.2 %wt.
The valueless carbon oxides stays constant at 0.1 %wt for carbon monoxide. Carbon dioxide increases slightly from 0.1to 0.3 %wt for carbon dioxide.

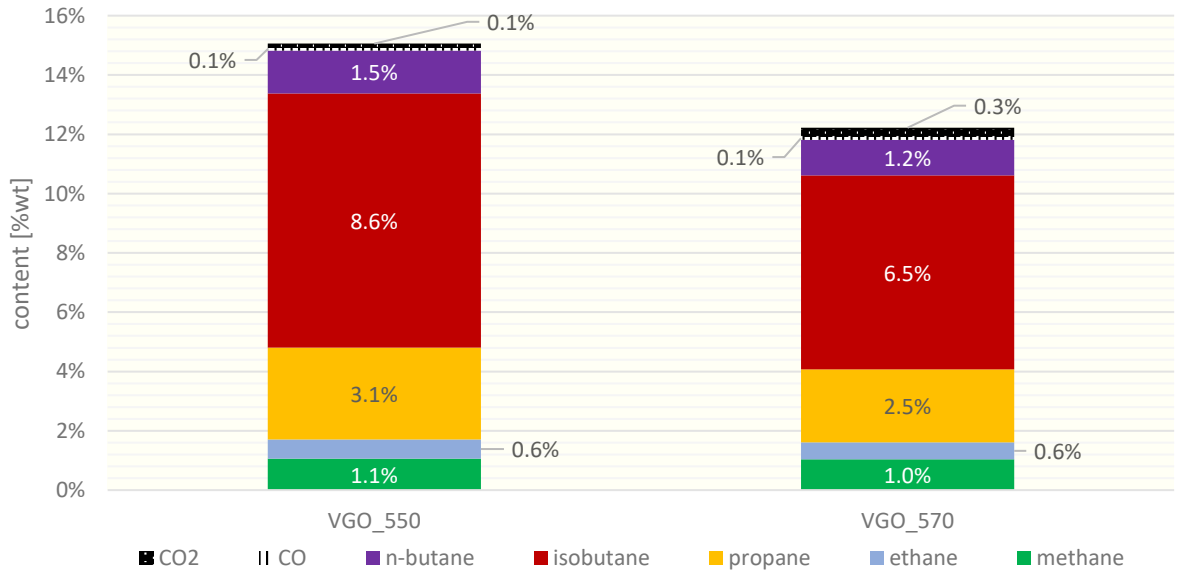

Figure 52: Alkane and COx yields of high severity cracking experiments with pure VGO

The addition of 10 %wt pyoil to VGO

Adding 10 %wt of pyoil changes the picture significantly. The production of hydrocarbon gases drops from initial 41.1 to 37.6 %wt and the gasoline production rate increases from 42.9 to 44.0 %wt. The relatively big drop of hydrocarbon gas production causes the conversion to drop from 84.1 to 81.5 %wt.

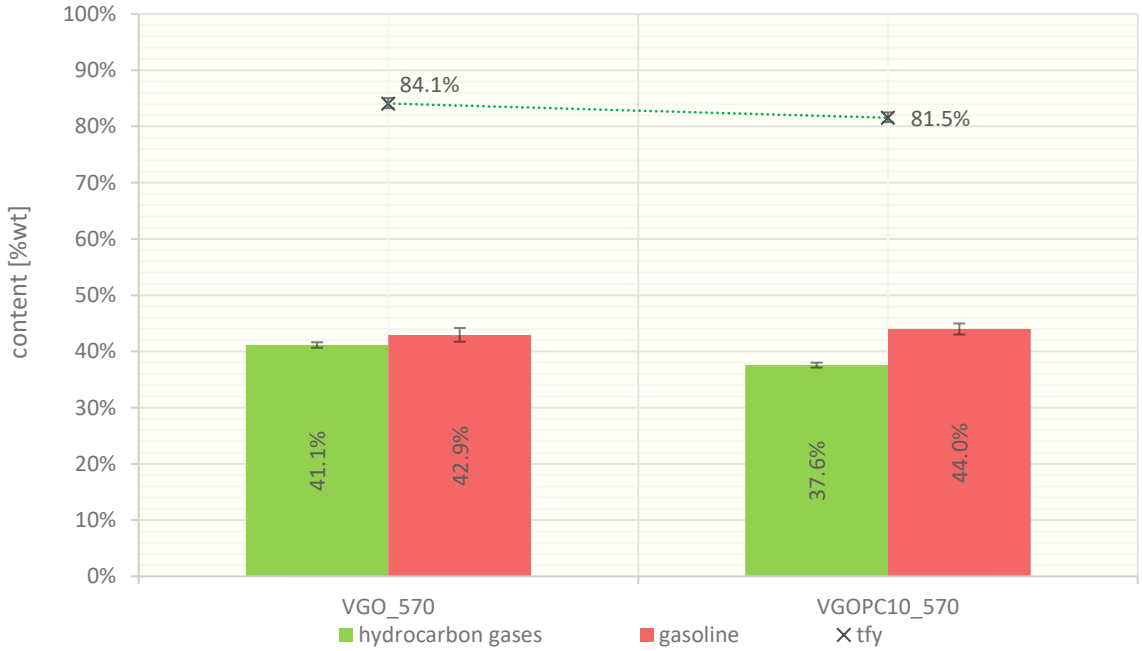

Figure 53: Hydrocarbon gases, gasoline yield and tfy of high severity cracking experiments with VGO and 10 %wt pyoil

The side products are depicted in the following figure 54. LCO increases from 5.6 to 6.6 %wt and residue increases from 3.8 to 4.5 %wt. Although the heavier product yields increase the production rate of coke stagnates at 6.1 %wt respectively 6.0 %wt. Due to the oxygen contained in pyoil the water amount in the product is at 0.9 %wt.

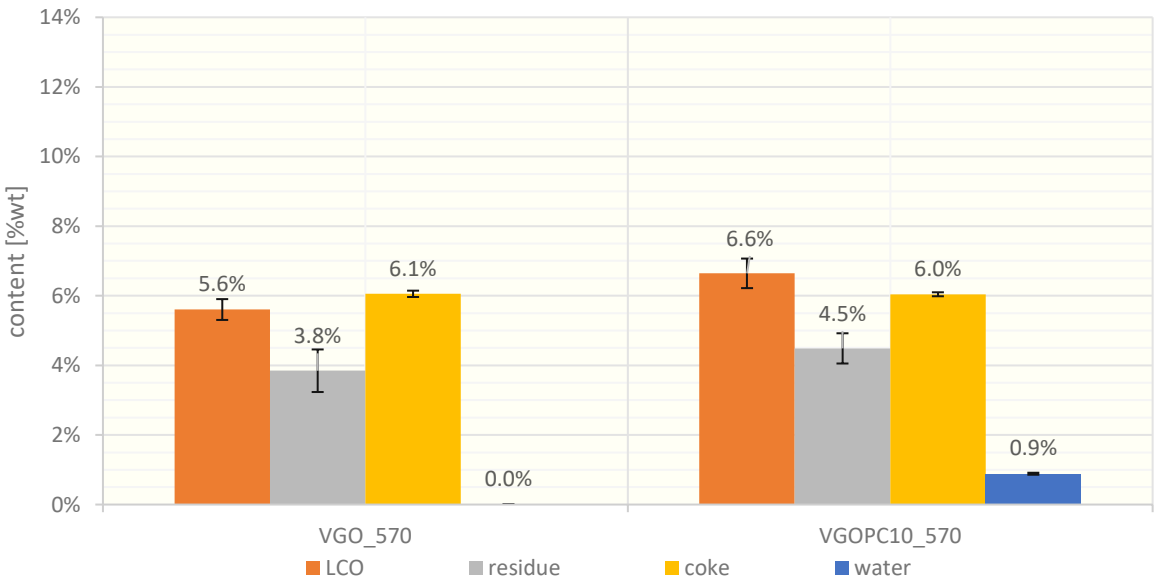

Figure 54: LCO, residue, coke and water yield of high severity cracking experiments with VGO and 10 %wt pyoil

Adding pyoil at high temperatures reduces the overall gas yield. This reduction includes all fractions of the hydrocarbon gases as shown in the following picture 55. Ethene is reduced from 3.4 to 2.9 %wt. The economically important propene yield is reduced from 15.8 to 14.7 %wt. The economically also important butenes drop from 10.2 to 9.3 %wt. The group of alkanes declines from 11.8 to 10.7 %wt.

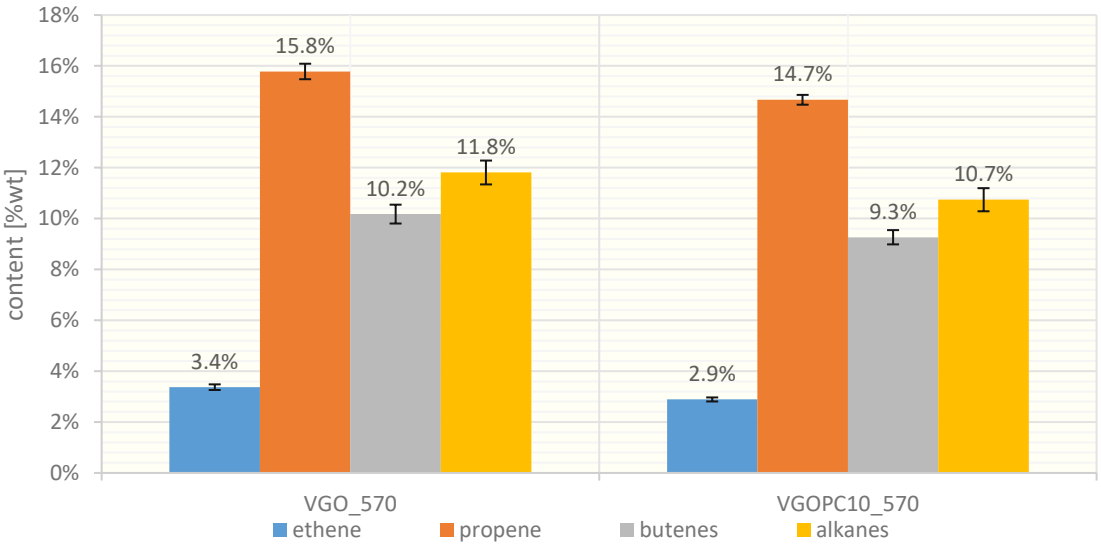

Figure 55: Ethene, propene, butene and alkane yield of high severity cracking experiments with VGO and 10 %wt pyoil

Although the absolute amount of propene drops, the relative amount increases from 38.0 to 38.6 %wt. Ethene drops in contrast to this from 8.1 to 7.6 %wt. The production of butenes stays almost constant at 24.5 respectively 24.4%wt. The ratio of produced alkanes drops slightly from 28.4 to 28.3 %wt. Carbon oxides are constant at 1.0 %wt.

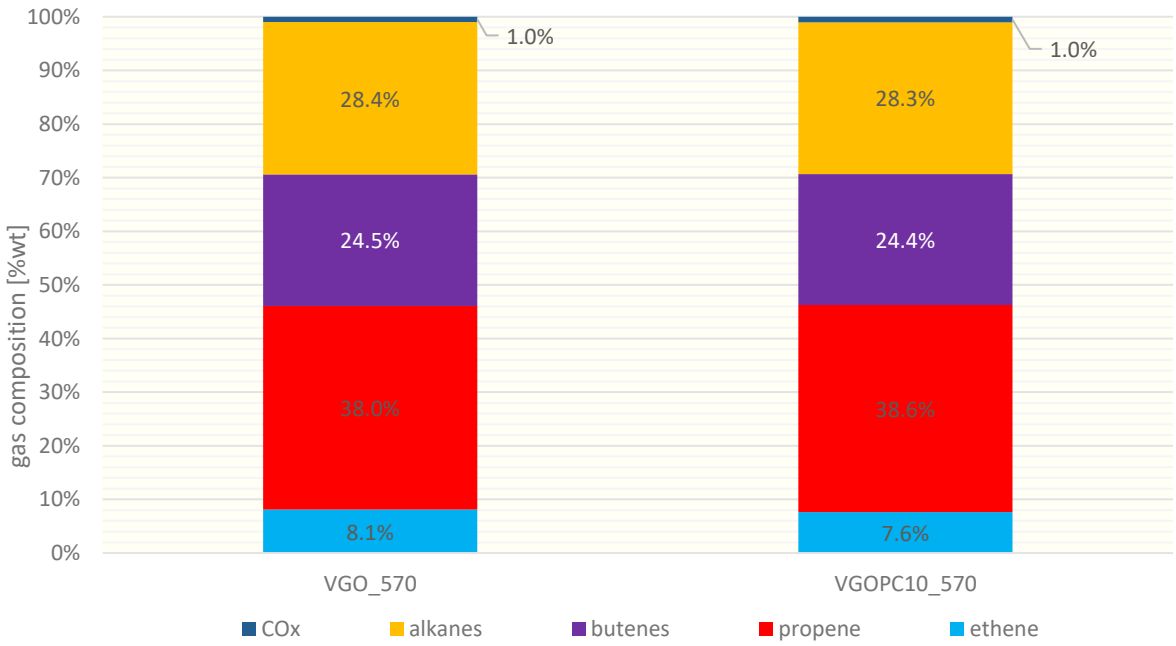

Figure 56: Gas composition of high severity cracking experiments with VGO and 10 %wt pyoil

The detailed view on the butenes shows a declining trend for all components. 1-butene reduces from 1.9 to 1.8 %wt. Isobutene drops from 3.9 to 3.5 %wt. Trans-2-butene declines from 2.5 to 2.3 %wt and cis-2-butene declines slightly from 1.8 to 1.7 %wt.

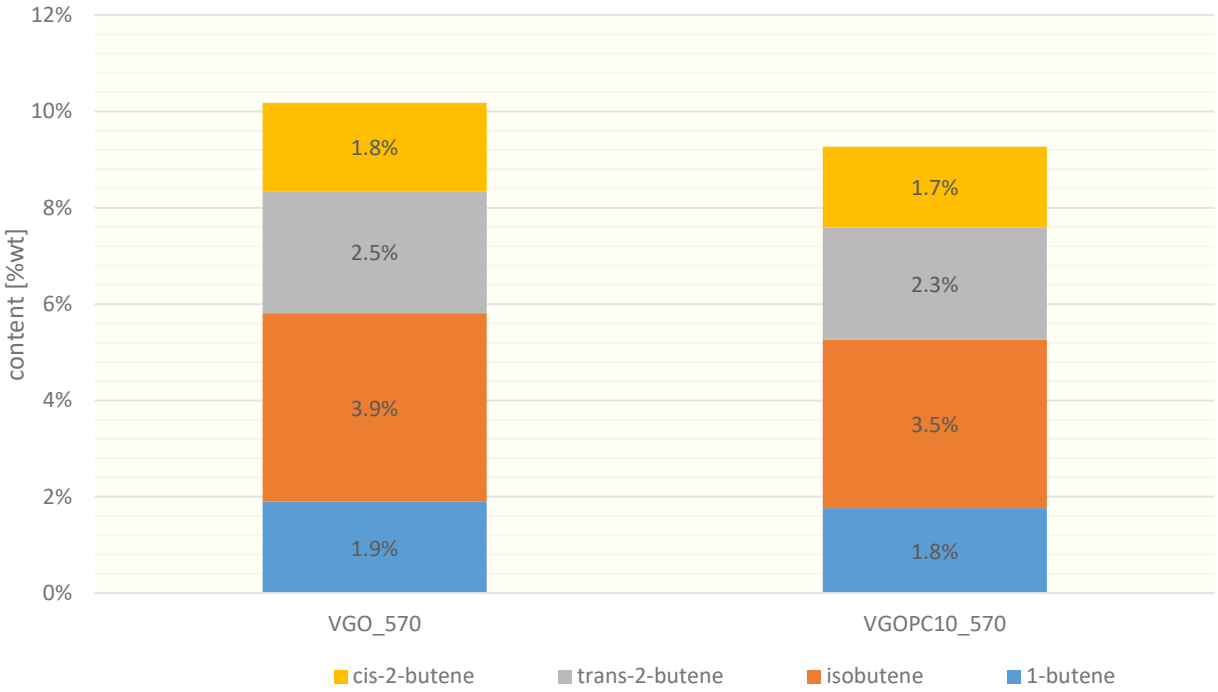

Figure 57: Butene yields of high severity cracking experiments with VGO and 10 %wt pyoil

The saturated hydrocarbon yields are reduced significantly by the raised cracking temperature. The methane yield drops slightly from 1.0 to 0.9 %wt, the same applies for the ethane yield from 0.6 to 0.5 %wt, respectively. Propane production rate reduces from 2.5 to 2.2 %wt. The same applies to isobutane and n-butane, dropping from 6.5 to 6.1 and from 1.2 to 1.1 %wt, respectively. Carbon oxide production stagnates at 0.1 %wt for carbon monoxide and 0.3 %wt for carbon dioxide.

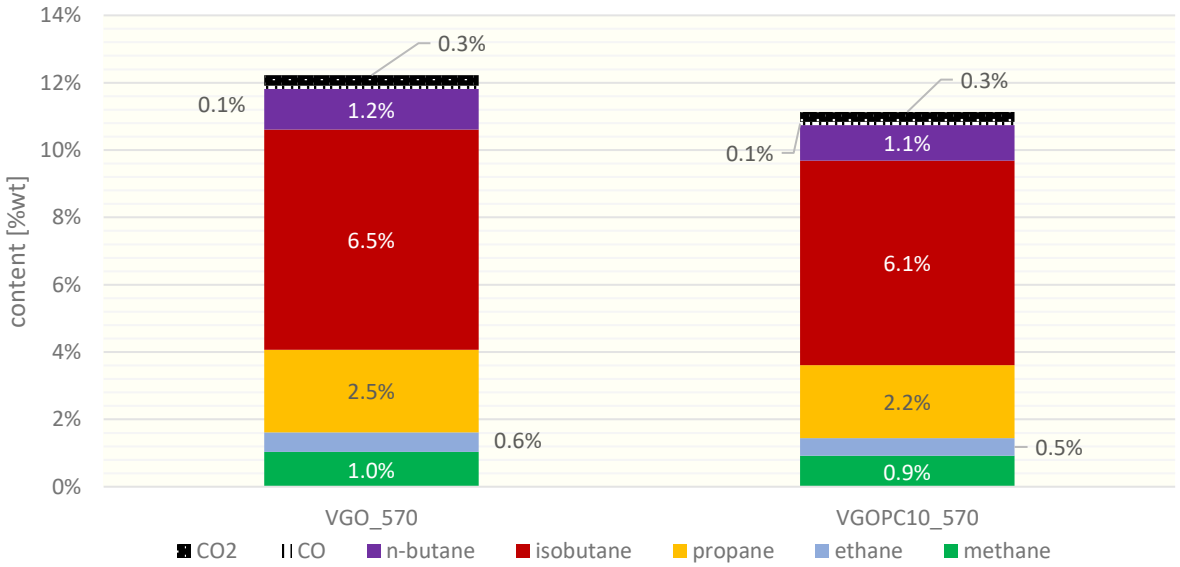

Figure 58: Alkane and COx yields of high severity cracking experiments with VGO and 10 %wt pyoil

VGO/pyoil co-processing at normal versus high severity cracking

The following figures show the direct comparison of a VGO/pyoil admixture at standard and elevated cracking temperature.

What can be seen in the following figure 59 is a decreasing hydrocarbon gas yield and an increasing gasoline yield. The gas production reduces from 44.3 to 37.6 %wt, gasoline increases in contrast from 40.5 to 44.0 %wt. The relatively big drop of the hydrocarbons gases outweighs the gains in gasoline production causing the conversion to drop from 84.9 to 81.5 %wt.

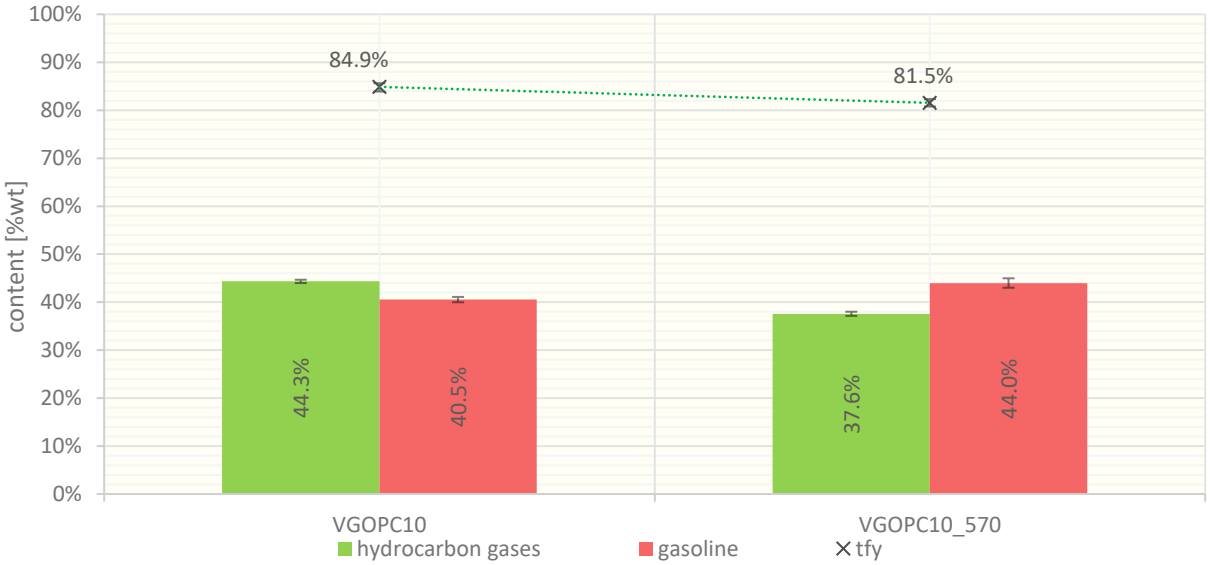

Figure 59: Hydrocarbon gases, gasoline and tfy of VGO/pyoil co-processing at normal versus high severity cracking

The low value product increase, in the case of LCO from 4.8 to 6.6 %wt. The residue yield is increased from 2.8 to 4.5 %wt. in contrast to this is the coke production, which drops from 6.3 to 6.0 %wt.
The water production stays constant at 0.9 %wt.

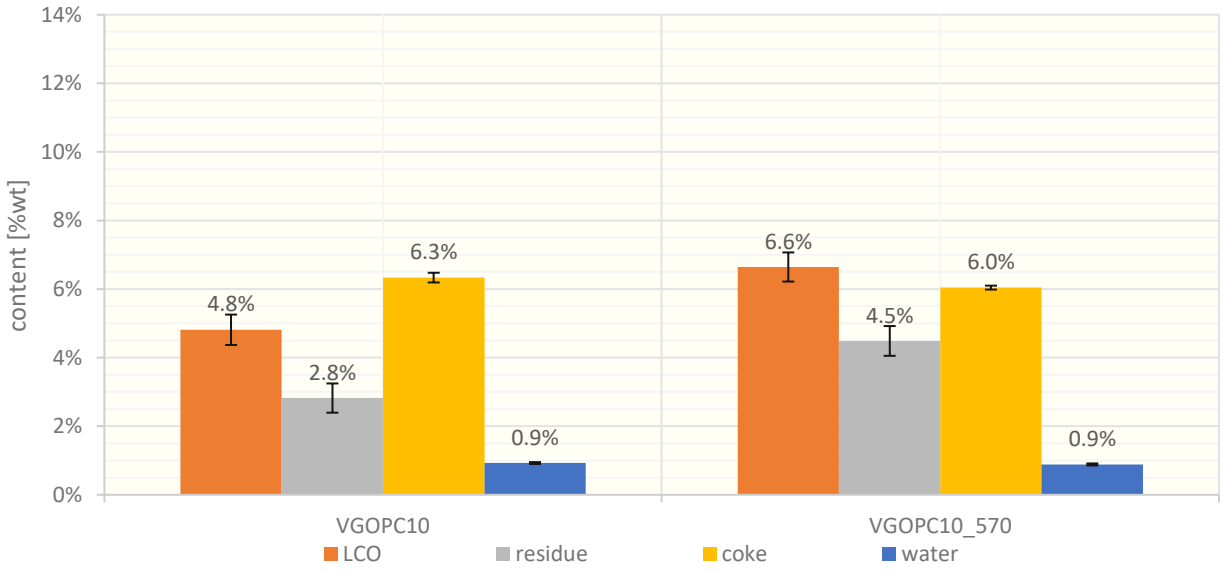

Figure 60: LCO, residue, coke and water yield of VGO/pyoil co-processing at normal versus high severity cracking

The more detailed gas composition is depicted in the following figure 61. Olefin production drops with an increasing cracking temperature. Ethene decreases from 3.3 to 2.9 %wt. A more significant drop can be observed at the propene production, decreasing from 16.1 to 14.7 %wt. A similar development can be seen at the butene yield, decreasing from 10.1 to 9.3 %wt. The alkanes decrease from 14.8 to 10.7 %wt.

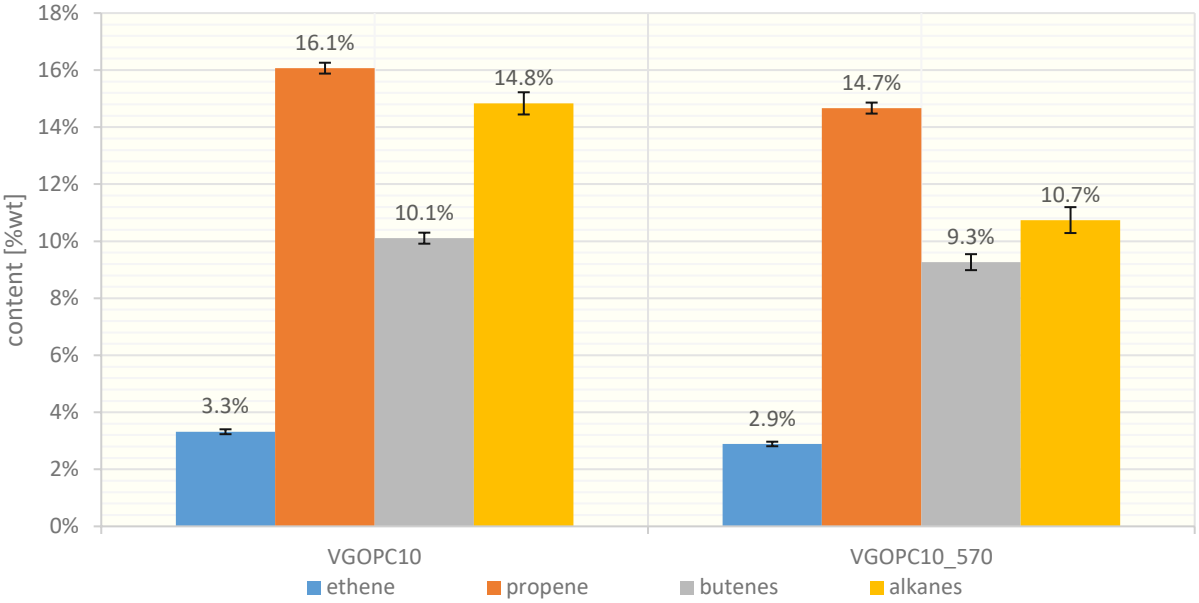

Figure 61: Ethene. propene, butene and alkane yield of VGO/pyoil co-processing at normal versus high severity cracking

The gas composition is depicted in the following figure 62. Ethene reduces in relation to the overall gas yield from 7.4 to 7.6 %wt. Propene and butenes ratio increases, from 36.1 to 38.6 %wt respectively from 22.7 to 24.4 %wt. Alkanes drop from a 33.3 %wt in the beginning to 28.3 %wt at the higher temperature. Carbon oxides production rises from 0.5 to 1.0 %wt.

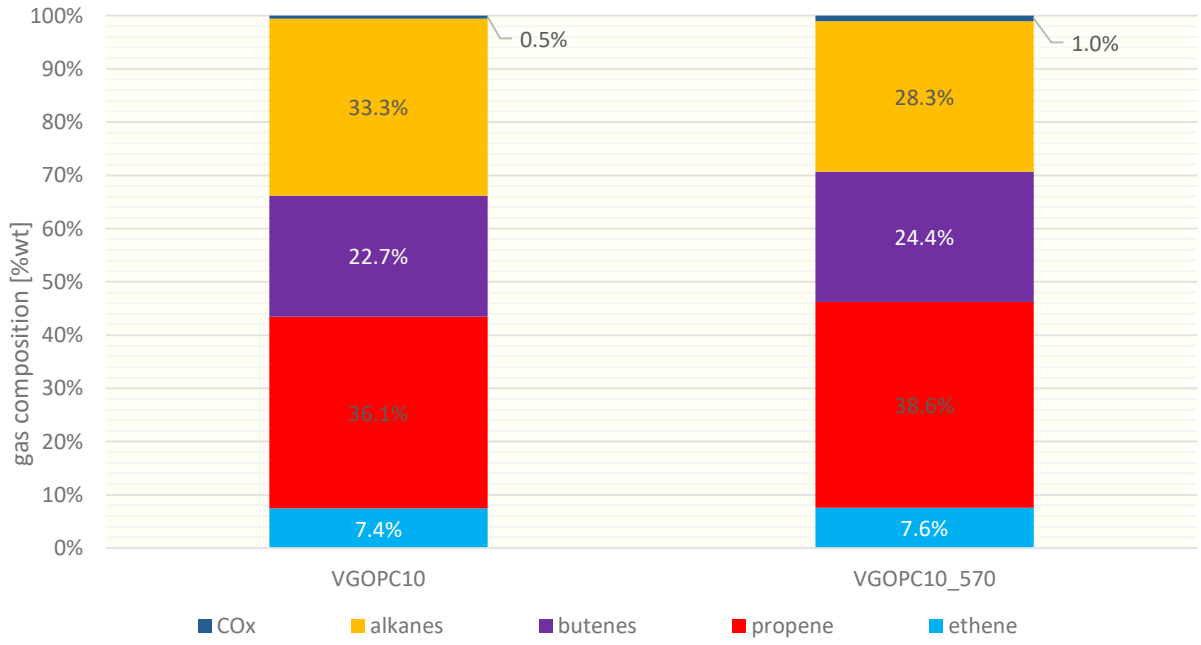

Figure 62: Gas composition of VGO/pyoil co-processing at normal versus high severity cracking

The individual butenes reduce analogous to the overall drop in the butene yield. 1-butene production declines from 1.9 to 1.8 %wt. Isobutene is reduced from 3.7 to 3.5 %wt. Trans-2-butene is reduced from 2.6 to 2.3 %wt and cis-2-butene is reduced from 1.9 to 1.7 %wt.

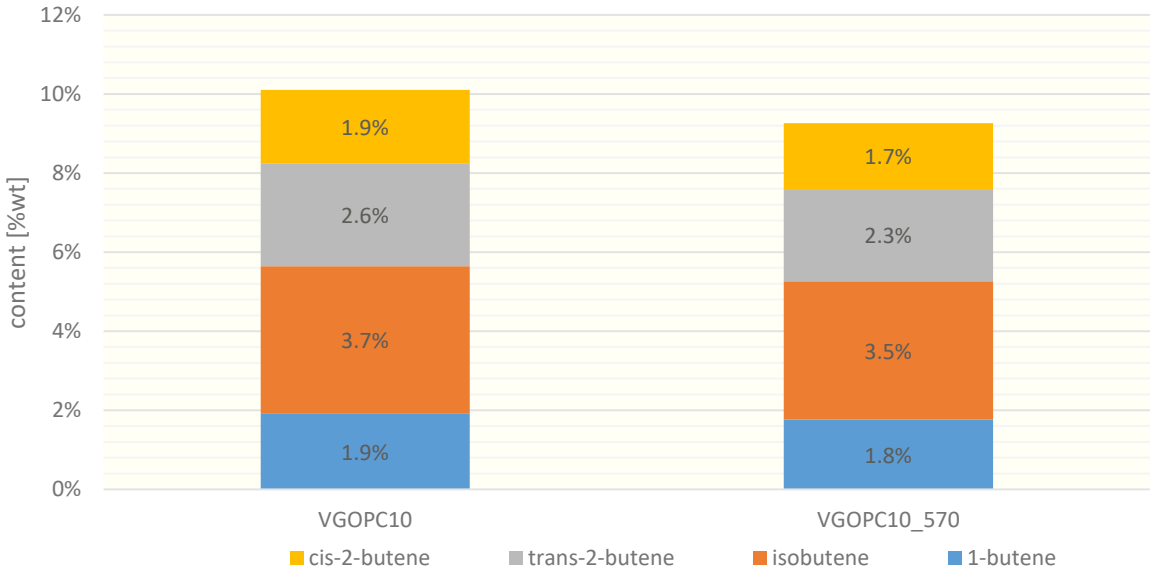

Figure 63: Butene yields of VGO/pyoil co-processing at normal versus high severity cracking

The produced alkenes drop significantly, most prominently isobutane. Isobutane reduces from 8.7 to 6.1 %wt. Methane is reduced from 1.1 to 0.9 %wt and ethane is reduced marginally from 0.6 to 0.5 %wt. The propane production drops from 2.9 to 2.2 %wt. N-butane declines from 1.5 to 1.1 %wt.
The production rate of the carbon oxides is inconsistent, whilst carbon oxide stays constant at 0.10 %wt, the production rate of carbon dioxide increases from 0.1 to 0.3 %wt.

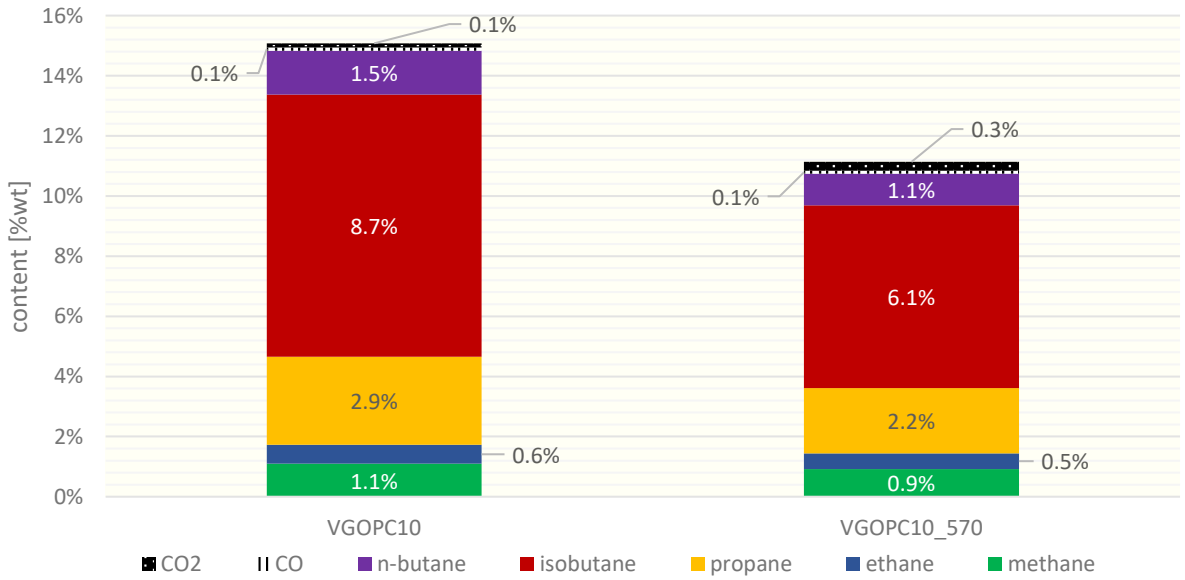

Figure 64: Alkane and COx yields of VGO/pyoil co-processing at normal versus high severity cracking

High severity cracking of UCO-based admixtures

To elaborate the influence of a higher severity on the cracking of UCO the same experimental structure as it was used for VGO and pyoil mixtures was utilized.

Pure UCO at 570 °C

The influence of an elevated cracking on pure UCO showed more anticipated outcomes than the experiments from pure VGO. Increasing the temperature increases the gas production significantly from 37.5 to 40.5 %wt and gasoline production marginally from 37.5 to 37.6 %wt. Increasing the high-value product fractions increases the conversion, rising from 74.9 to 78.1.

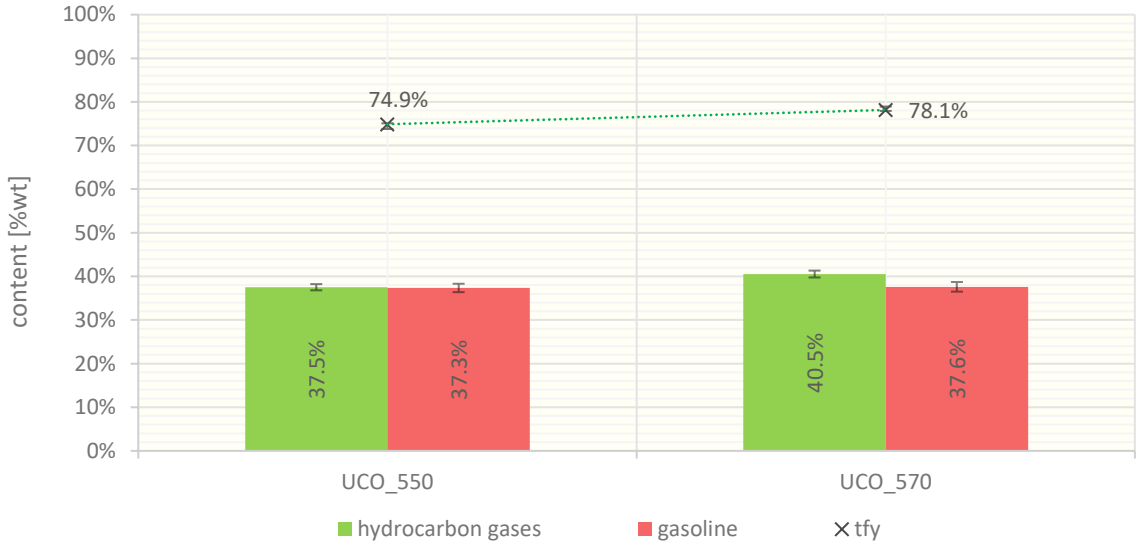

Figure 65: Hydrocarbon gases, gasoline yield and tfy of high severity cracking experiments with pure UCO

The lower-value product yields changed too. LCO reduces from 6.6 to 4.9 %wt. The heaviest liquid product, residue, reduces from 1.7 to 1.3 %wt. Coke production rises from 6.8 to 7.1 %wt. Interestingly, the production of water decreases from 7.5 to 6.1 %wt.

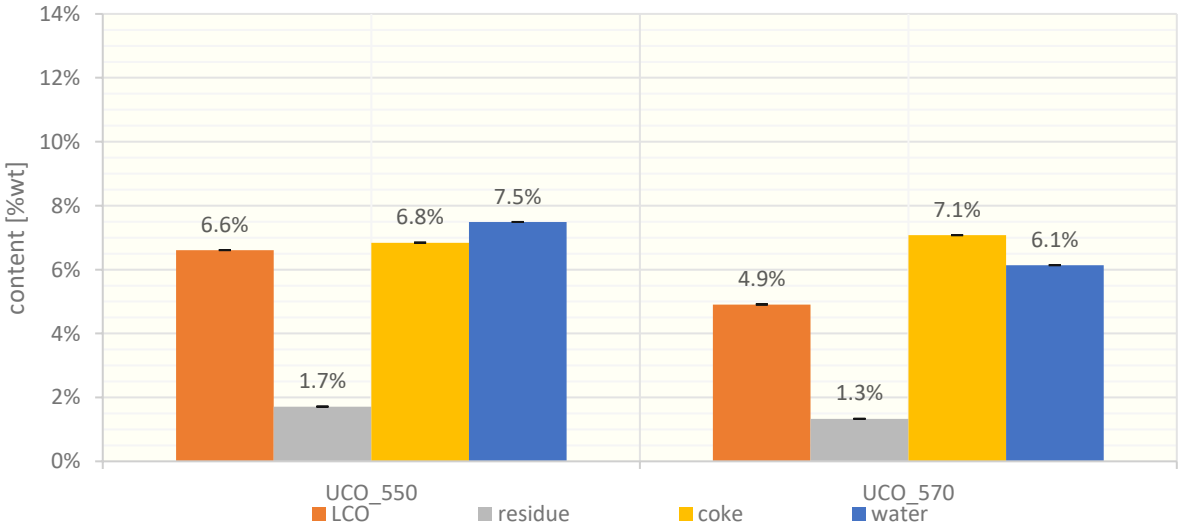

Figure 66: LCO, residue, coke and water yield of high severity cracking experiments with pure UCO

The more detailed gas composition reveals a rise for all olefins. Ethene rises from 3.6 to 4.0 %wt. Propene is increased from 14.8 to 16.4 %wt. The butenes rise from 9.1 to 10.9 %wt. The only decreasing gas fraction is the group of alkanes, decreasing from 10.0 %wt to 9.2 %wt.

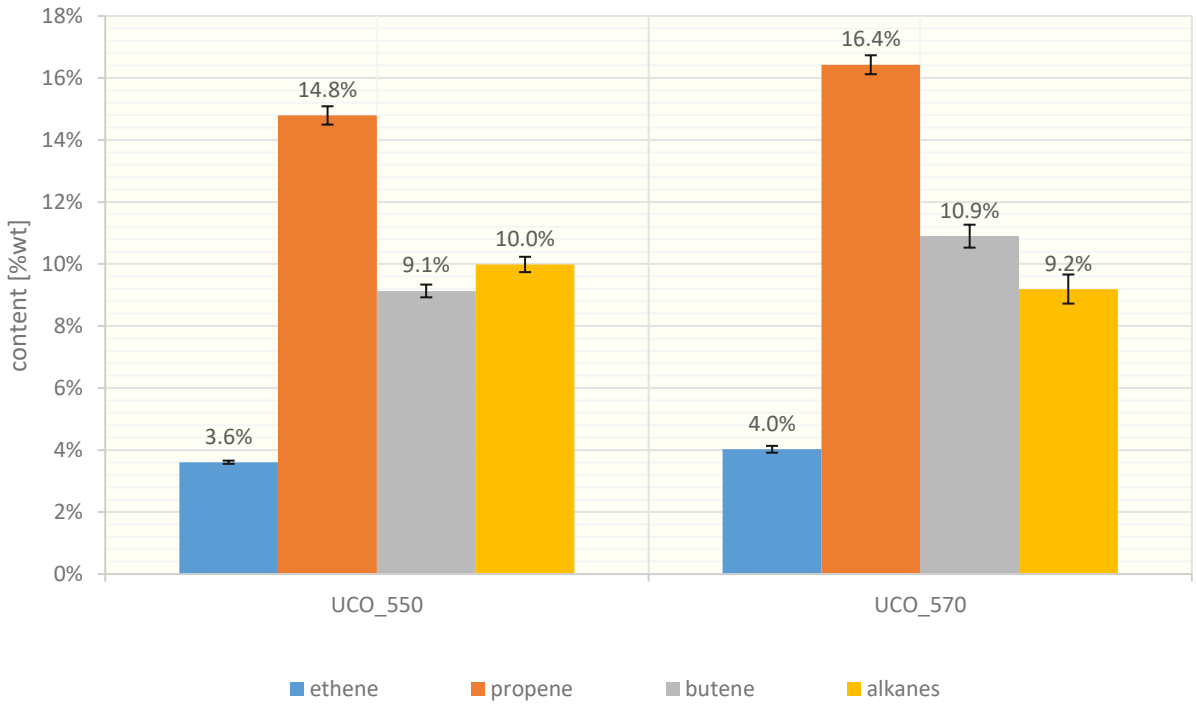

Figure 67: Ethene, propene, butene and alkane yield of high severity cracking experiments with pure UCO

The same trend as in the above figure can be seen in the following diagram 68. The gas composition changes towards higher-value olefins with elevated cracking severity. Ethene increases relatively from 9.0 to 9.4 %wt. Propene rises from 37.0 to 38.3 %wt and the butenes rise from 22.8 to 25.4 %wt. Alkanes drop from 25.0 to 21.4 %wt. Carbon oxides production decreases from 6.2 to 5.6 %wt.

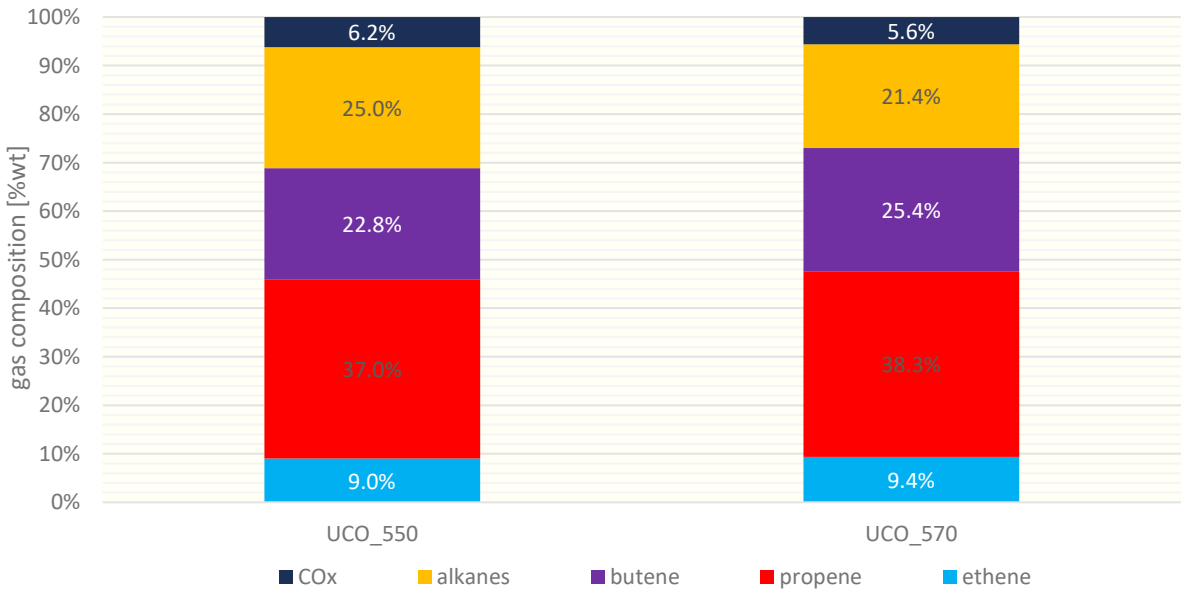

Figure 68: Gas composition of high severity cracking experiments with pure UCO

The composition of the butene fraction changes as seen in the following figure 69. 1-butene rises from 1.7 to 2.1 %wt. Isobutene is increased from 3.3 to 3.8 %wt. Trans-2-butene rises from 2.4 to 2.9 %wt and cis-2-butene increases from 1.7 to 2.1 %wt.

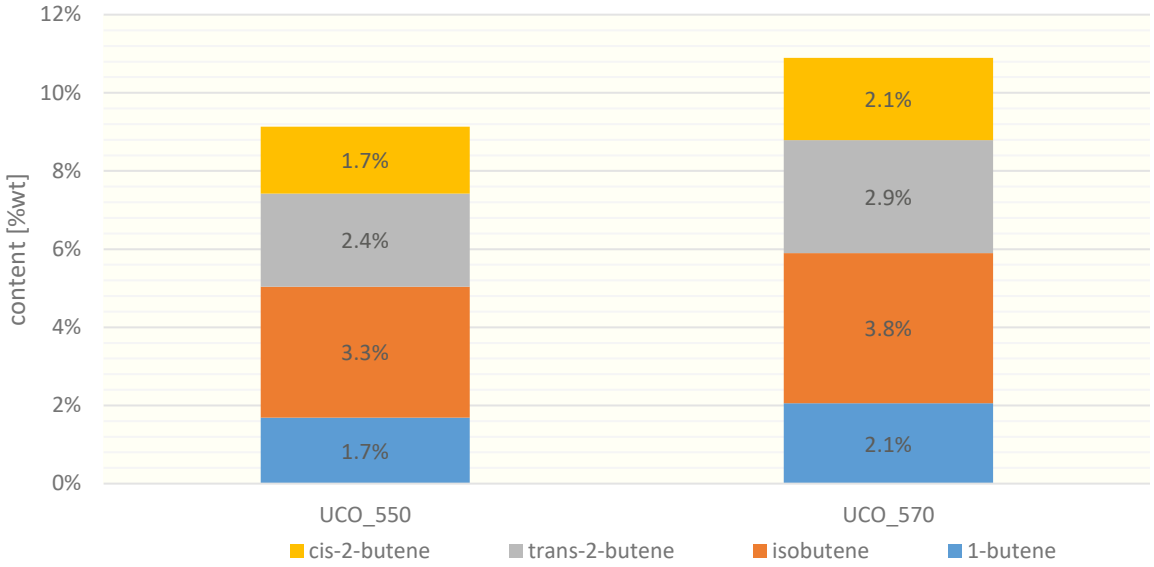

Figure 69: Butene yields of high severity cracking experiments with pure UCO

The composition of the alkanes and carbon oxides is depicted in the following figure. Methane rises from 1.0 to 1.2 %wt. Ethane stays at 0.71 %wt. Propane production drops from 2.1 to 1.8 %wt. Isobutane drops. from initial 5.3 to 4.6 %wt. N-butane stays constant at 0.9 %wt.
Another positive development can be seen when looking at the CO production. Carbon monoxide reduces from 1.9 to 1.8 %wt. Carbon dioxide stagnates at a production rate of 0.6 %wt.

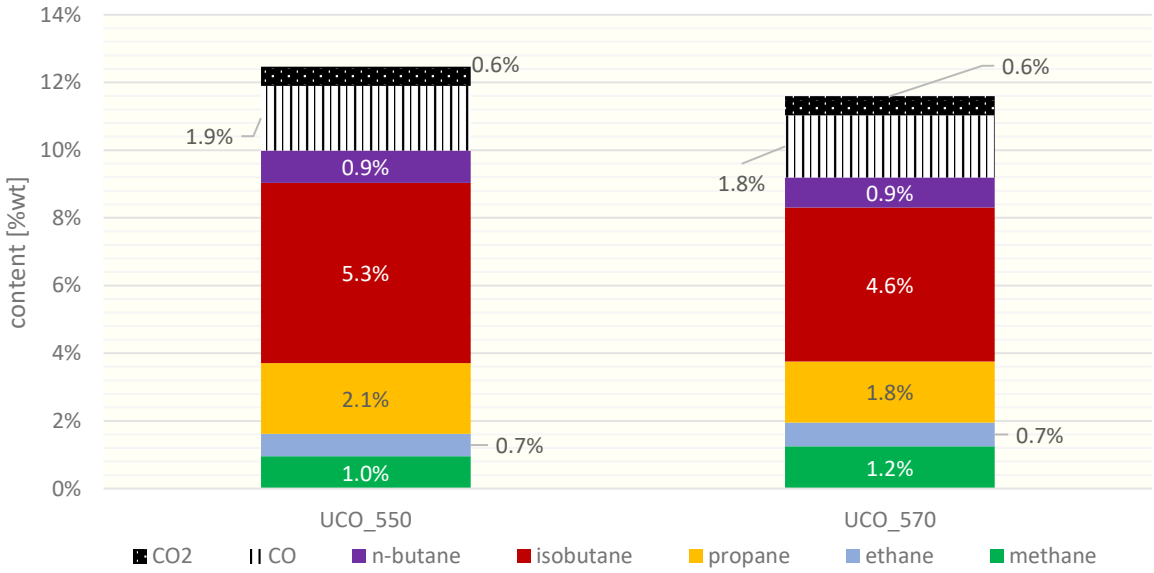

Figure 70: Alkane and COx yields of high severity cracking experiments with pure UCO

The addition of 10 %wt pyoil to UCO

Adding 10 %wt pyoil again changes the yield significantly. Hydrocarbon gas production decreases drastically from 40.5 to 31.5 %wt. Contrary to this increases the gasoline production from 37.6 to 39.7 %wt. Overall this causes the conversion to drop from 78.1 to 71.2 %wt

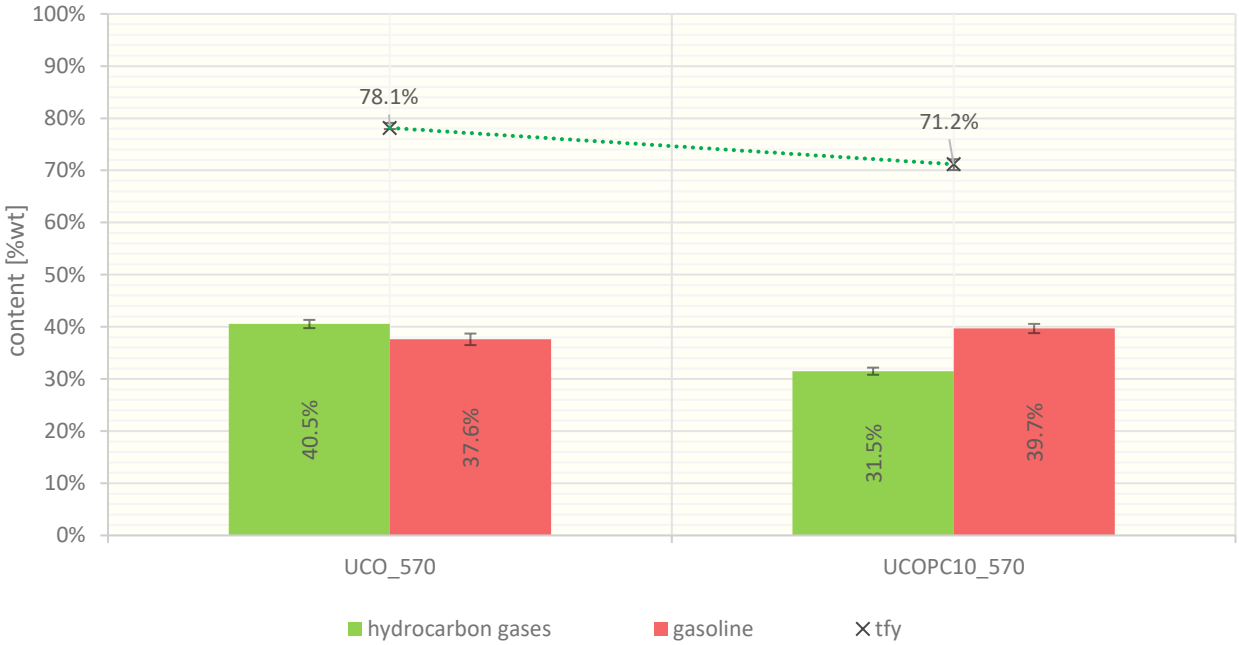

Figure 71: Hydrocarbon gases, gasoline yield and tfy of high severity cracking experiments with UCO and 10 %wt pyoil

The lower value products LCO and residue increase with the addition of pyoil at high temperatures. LCO rises from 4.9 to 7.6 %wt and residue from 1.3 to 2.3 %wt. Coke production decreases from 7.1 to 6.9 %wt. The valueless water fraction rises from 6.1 to 8.7 %wt.

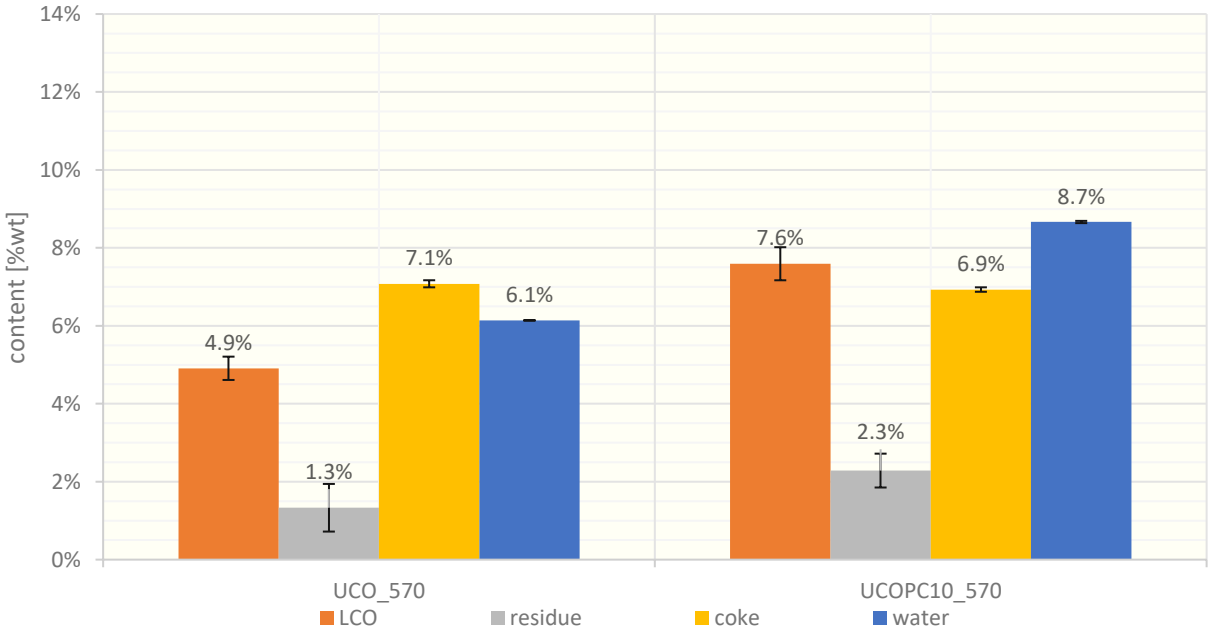

Figure 72: LCO, residue, coke and water yield of high severity cracking experiments with UCO and 10 %wt pyoil

The declining hydrocarbon gas yield is depicted in more detail in the following figure 73. Ethene decreases from 4.0 to 3.0 %wt. Propene from 16.4 to 13.3 %wt. Butenes decrease from 10.9 to 8.2 %wt. The alkanes decrease from 9.2 to 7.0 %wt.

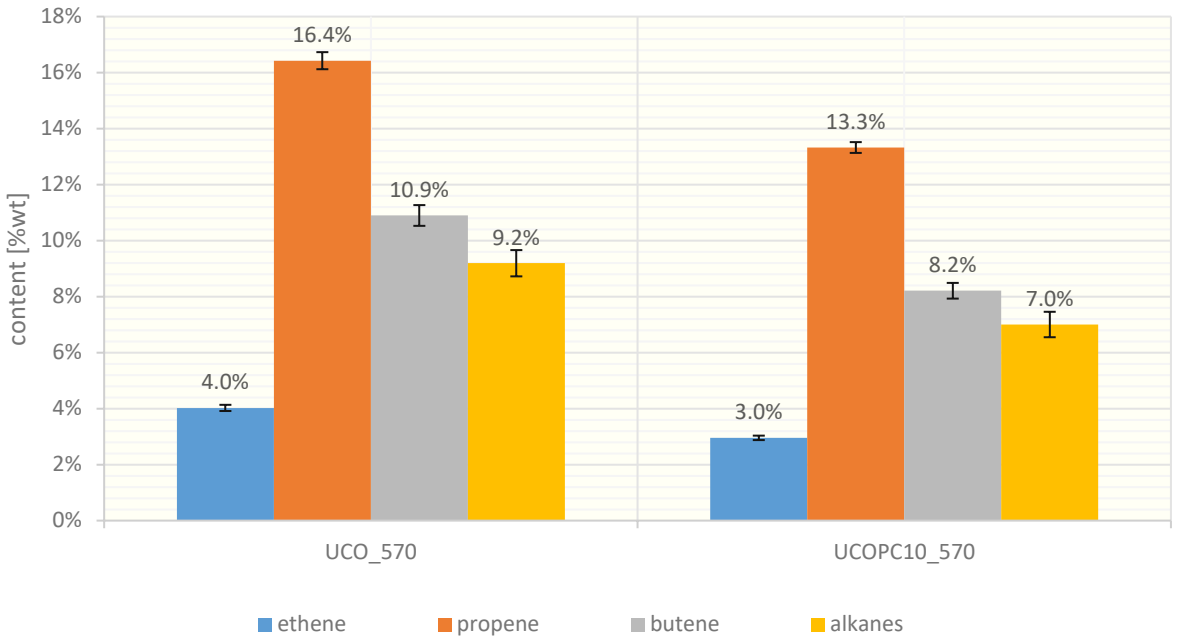

Figure 73: Ethene, propene, butene and alkane yield of high severity cracking experiments with UCO and 10 %wt pyoil

The hydrocarbon gas composition can be seen in the following figure 74. The drops in gaseous product yields are less severe in relation to the overall gas production. The ethene yield drops from 9.4 to 8.5 %wt. Propene stays constant at 38.3 %wt respectively at 38.2 %wt. Butenes reduce from 25.4 to 23.6 %wt. Alkanes drop from 21.4 to 20.1 %wt. The COx production increases from 5.6 to 9.6 %wt.

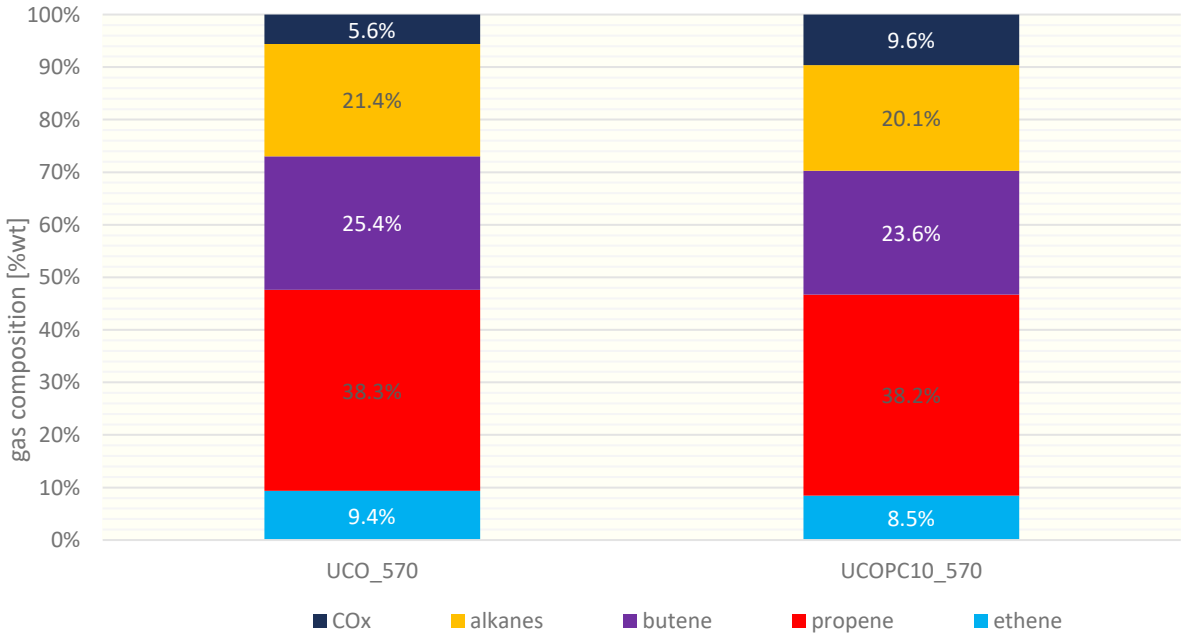

Figure 74: Gas composition of high severity cracking experiments with UCO and 10 %wt pyoil

The reducing butene yield is depicted in detail in the following figure 75. 1-butene yield reduces from 2.1 to 1.6 %wt and isobutene from 3.8 to 2.9 %wt. Trans-2-butene drops from 2.9 to 2.1 %wt. Cis-2-butene reduces from 2.1 to 1.5 %wt.

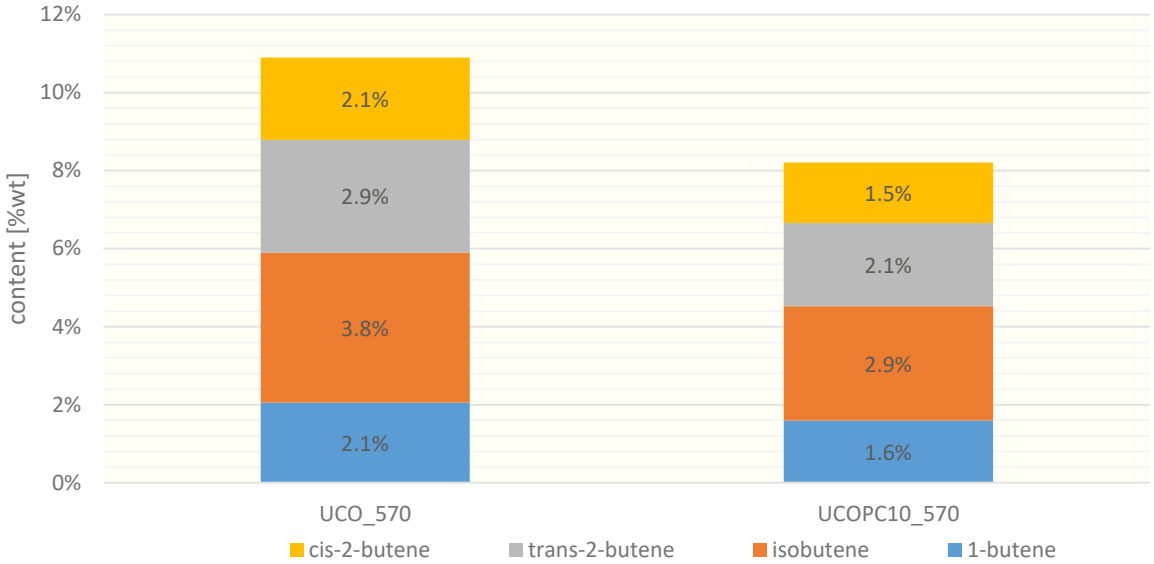

Figure 75: Butene yields of high severity cracking experiments with UCO and 10 %wt pyoil

The alkanes and carbon oxide production rates are depicted in the following figure 76. The addition of pyoil reduces the alkane yield and increases the production of carbon oxides. Methane is reduced from 1.2 to 0.8 %wt and ethane decreases from 0.7 to 0.5 %wt. Propane yield drops from 1.8 to 1.4 %wt. Isobutane and n-butane reduce from 4.6 to 3.6 %wt respectively from 0.9 to 0.7 %wt. Carbon monoxide is increased from 1.8 to 2.5 %wt and carbon dioxide rises slightly from 0.6 to 0.8 %wt.

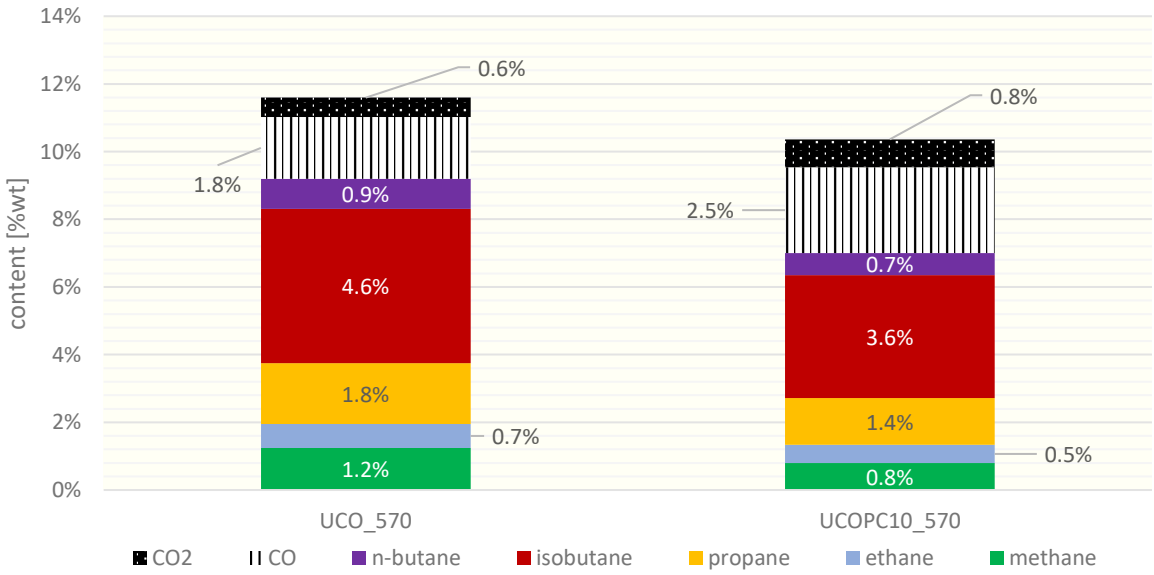

Figure 76: Alkane and COx yields of high severity cracking experiments with UCO and 10 %wt pyoil

Pyoil co-processing normal versus high severity

When pyoil is added to UCO at high temperatures, a certain shift of the product yields is obvious. The changing product yields for a 10 %wt pyoil in UCO admixture at an elevated cracking temperature is depicted in the following diagrams.
The gas production decreases from 38.5 to 31.5 %wt whilst the gasoline yield increases from 35.9 to 39.7 %wt. The conversion decreases from 74.3 to 71.2 %wt.

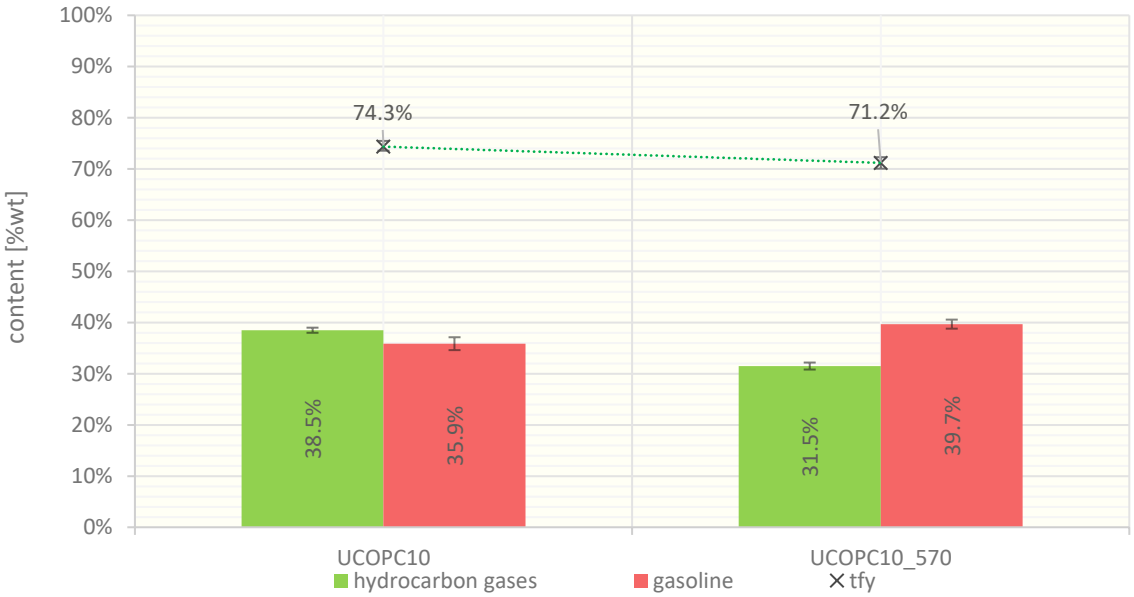

Figure 77: Hydrocarbon gases, gasoline yield and tfy of UCO/pyoil co-processing at normal versus high severity cracking

The low-value lumps of LCO and residue increase. LCO rises from 5.8 to 7.6 %wt. Residue increases from 1.7 to 2.3 %wt.
Coke production is reduced by pyoil addition at high temperatures from 7.2 to 6.9 %wt. Water shows almost no changed yield with 8.7 respectively 8.7 %wt production rate.

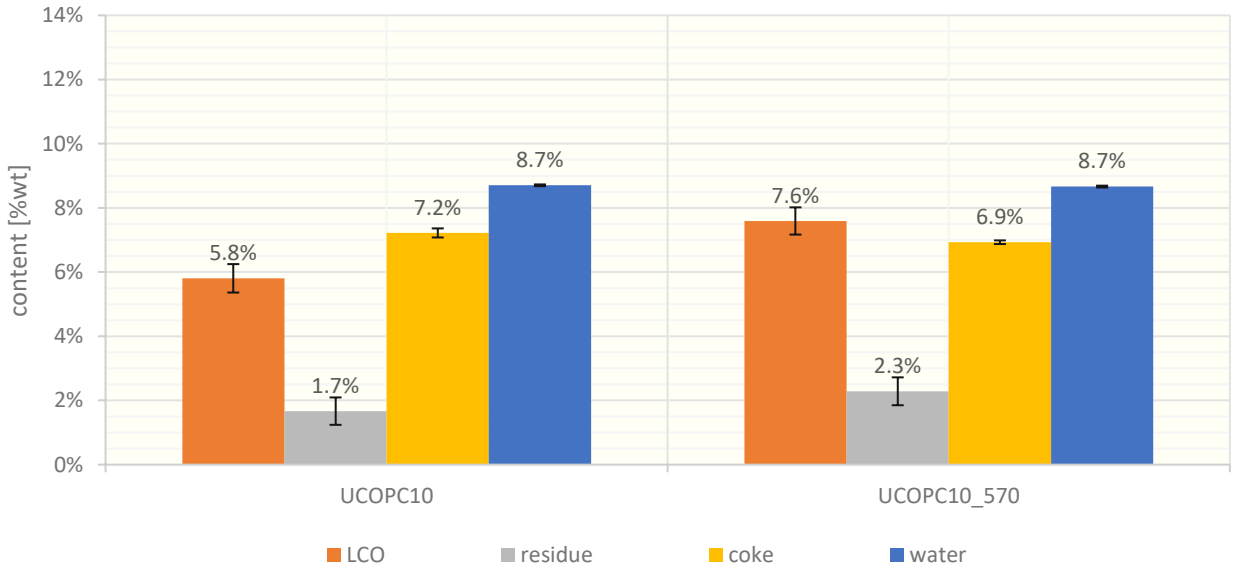

Figure 78: LCO, residue, coke and water yield of UCO/pyoil co-processing at normal versus high severity cracking

The gas yield is described in more detail in the next figure 79, showing declining trends for all olefins and the alkane yield. Ethene reduces from 3.5 to 3.0 %wt. The high-value propene reduces from 15.1 to 13.3 %wt. The same applies for the production of butenes, dropping from 10.0 to 8.2 %wt. Alkanes decrease from 9.0 to 7.0 %wt.

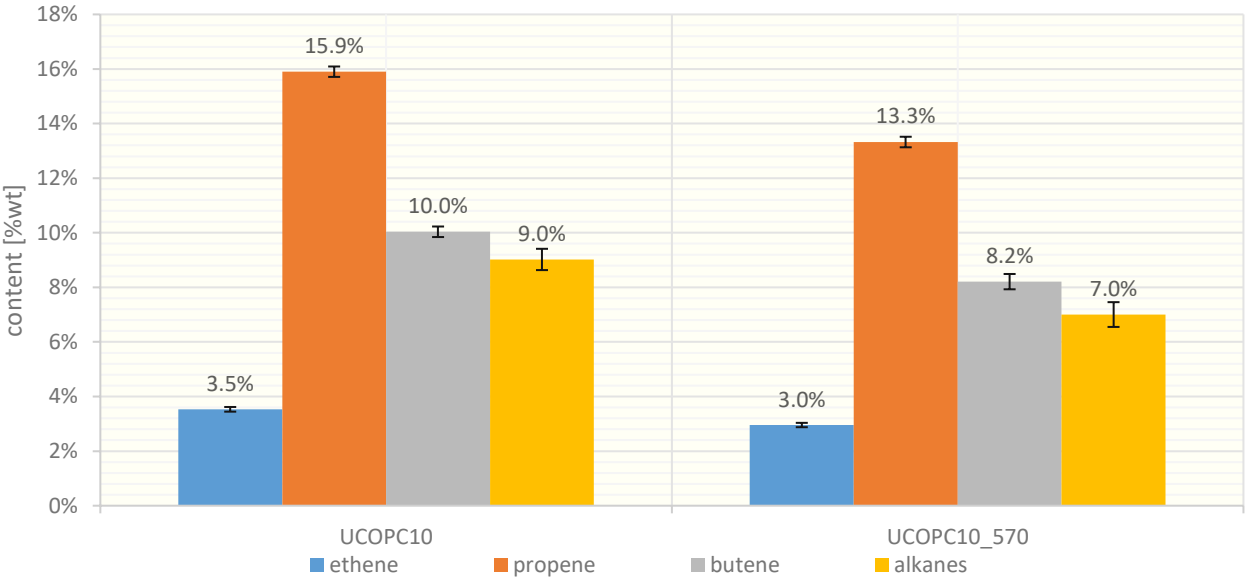

Figure 79: Ethene, propene, butene and alkane yield of UCO/pyoil co-processing at normal versus high severity cracking

The gas composition with the relative deviations in product yields is shown in the following figure 80.
Ethene decreases from 8.7 to 8.5 %wt. Propene decreases from 39.0 to 38.2 %wt. Butenes are reduced from 24.6 to 23.6 %wt. Alkanes reduce from 22.1 to 20.1 %wt. The COx production rate increases from 5.5 to 9.6 %wt.

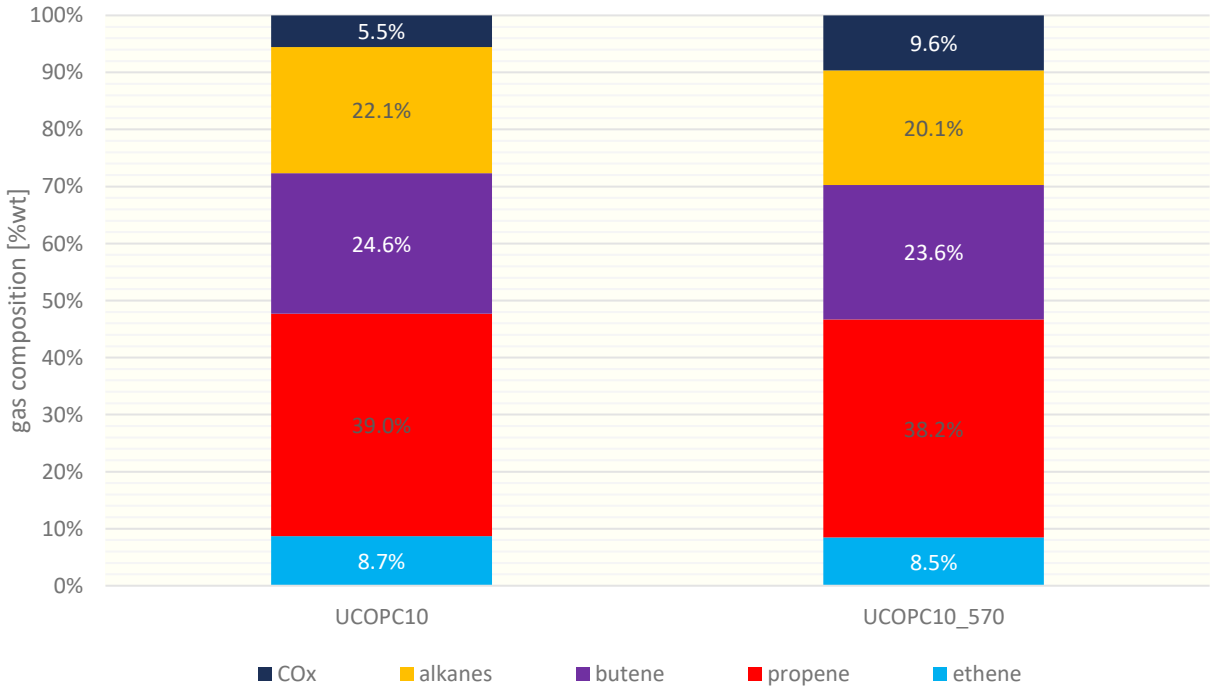

Figure 80: Gas composition of UCO/pyoil co-processing at normal versus high severity cracking

The overall declining butene yield is depicted in more detail in the following figure 81. 1- butene reduces from 1.9 to 1.6 %wt. Isobutene drops from 3.5 to 2.9 %wt. Trans-2-butene drops from 2.7 to 2.1 %wt and cis-2-butene drops from 1.9 to 1.5 %wt.

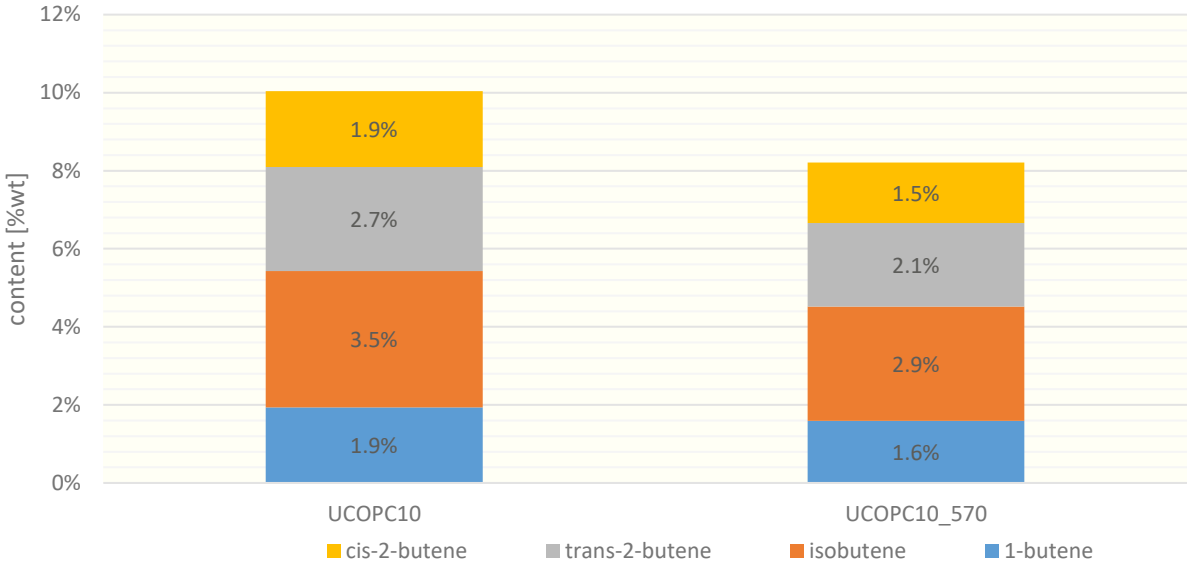

Figure 81: Butene yields of UCO/pyoil co-processing at normal versus high severity cracking

The alkenes and carbon oxides are depicted in the following figure 82. Carbon oxide production increases with increased cracking temperature. Carbon monoxide rises from 1.7 to 2.5 %wt, carbon dioxide from 0.5 to 0.8 %wt.
The hydrocarbons decrease, starting with methane from 1.0 to 0.8 %wt. Ethane decreases from 0.6 to 0.5 %wt. Propane decreases from 1.8 to 1.4 %wt. Isobutane and n-butane decrease from 4.8 to 3.6 %wt and from 0.8 to 0.7 %wt, respectively.

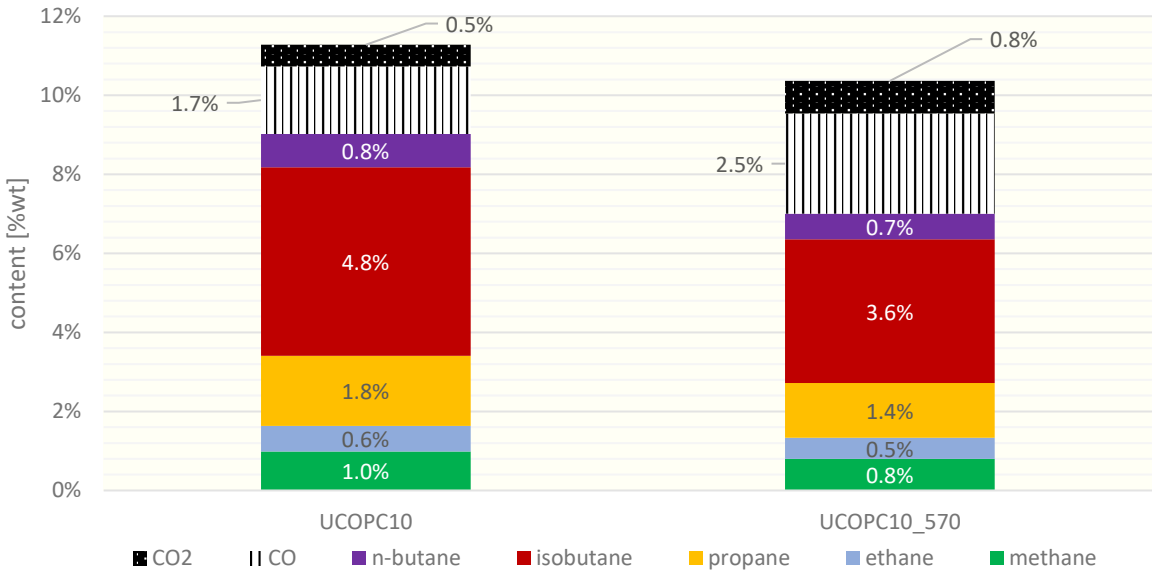

Figure 82: Alkane and COx yields of UCO/pyoil co-processing at normal versus high severity cracking

Discussion

Plant operation

Although a relative rise of 20 °C for the mean cracking temperature is feasible for industrial size plants, the final cracking temperature of 570 °C is very high compared to the common operation temperature window of FCC units.

Products

High severity cracking of VGO-based admixtures

The impact of the increased cracking temperature on pure VGO is insignificant on most product yields, except for the composition of the gas yield. Here an increased production of propene and butenes can be seen, increasing the yield of the valuable olefins significantly.
These results are unexpected, as the cracking temperature had a higher impact on product yield distribution in previous publications of the research group. [68], [85]

The picture changes when pyrolysis oil is mixed to the VGO and the temperature is raised to 570 °C. The increased temperature reverses the shown effects at 550 °C. Now, an addition of pyoil is boosting gasoline, LCO and residue production and lowers the hydrocarbon gas yield significantly. The yield reduction affects all gases, olefins as well as saturated hydrocarbon gases and carbon oxides.
This finding is significant, especially when the results are set into perspective to the VGO-pyoil experiments at 550 °C. At this “normal” cracking temperature the addition of pyoil boosts hydrocarbon gas production and lowers gasoline production. An explanation for this could be the position of the gasoline maximum on the temperature scale. The addition of pyoil could shift the maximum to higher cracking temperatures, leading to increased production rates of gasoline and heavier components when the temperature is increased.

High severity cracking of UCO-based admixtures

The experiment with pure UCO had product yields more fitting to the expectations. Raising the cracking temperature increases the hydrocarbon gas production significantly whilst the gasoline yield stays almost constant. The increased gas yield is associated to a lowered LCO production and a lower amount of saturated gases in the hydrocarbon gas yield. The overall increased gas production is therefore based on a boost of yields of the valuable olefins.

Similar behavior to the VGO-pyoil experiments can be observed when pyoil is mixed to the UCO and the temperature is raised to 570 °C. The increased temperature reverses both previously shown effects. The combination of 10 %wt PC addition and 570 °C cracking temperature lowers the hydrocarbon gas production by lowering the olefin and saturated gas yields simultaneously. This comes with a boost in gasoline, LCO and residue yield and a lowered coke production. Again, pyoil seems to shift the maximum of the gasoline yield towards higher temperatures. The shifts seem to be relatively independent from the base feedstock, as both experimental campaigns produced similar results by adding pyoil to the feedstock.

Another remarkable outcome is the gain in carbon oxides in the product gas whilst keeping the amount of produced water constant. The addition of pyoil seems to reduce the amount of oxygen contained in the liquid product in the form of oxygenates or in the coke.

10.2.7 Feeding 100 %wt Pyoil to the plant

Introduction

Going “fully circular” is one of the main goals of each recycling process. The need for circularity is born out of the natural resources available on our planet, be it the resources we extract from the earth or the amount of greenhouse gases we can safely emit into the atmosphere. Both values are subject to certain fluctuations, depending on the type of literature. However, it is common ground that we extract too much and emit way too much. Both issues need to be tackled by circular processes, in which so-called circular carbon is re-used by sufficient processes in order to reduce the amount of fresh materials needed as much as possible.
A circular carbon source could be waste plastic. Depending on the location, unsorted and deteriorated plastic waste is an abundant carbon source, potentially fulfilling tomorrows circular route paved for it by science and technology today.

Experimental Setup

A major challenge of the pyoil experiments was the scarcity of feedstock. All experiments conducted needed to be done with an amount of pyoil of less than 12 kg. After all experiments were conducted, a 100 %wt experiment was done with the remaining amount.
Due to the short time the plant was operating with the feedstock, only one sample could be taken, which of course reduces the significance of the findings.

Table 19: Composition of the feedstocks compared to the 100 %wt pyoil experiment

Experiment ID	Pyoil content	Canola oil content	VGO content	
PC100	100	0	0	%wt
RAPS 100	0	100	0	%wt
VGOBASE2	0	0	100	%wt

The shortcomings, born out of the low amount feedstock available for the PC100 experiment and the resulting short operation time of the plant, are:

- A feeding rate of 2 kg/h was chosen
- Only one sample taken
- No C/O ratio measurement possible
- No water measurement possible
- Overall error indications for PC100 experiment not accurate due to too low number of samples

Results

In order to compare the results of pure pyoil the product yields are shown next to the respective yields of the base cases of VGO and canola oil experiments.

Pure pyoil shows a product yield distribution relatively similar to pure VGO. Hydrocarbon gas production is on a similar level, ranging from 41.3 %wt for pyoil and 41.7 %wt for VGO. The same applies for the gasoline production with 42.6 %wt for pyoil and 42.8 %wt for VGO. Compared to canola oil both yields are significantly higher for pyoil, with canola oil producing only 38.0 %wt gases and 36.1 %wt gasoline.

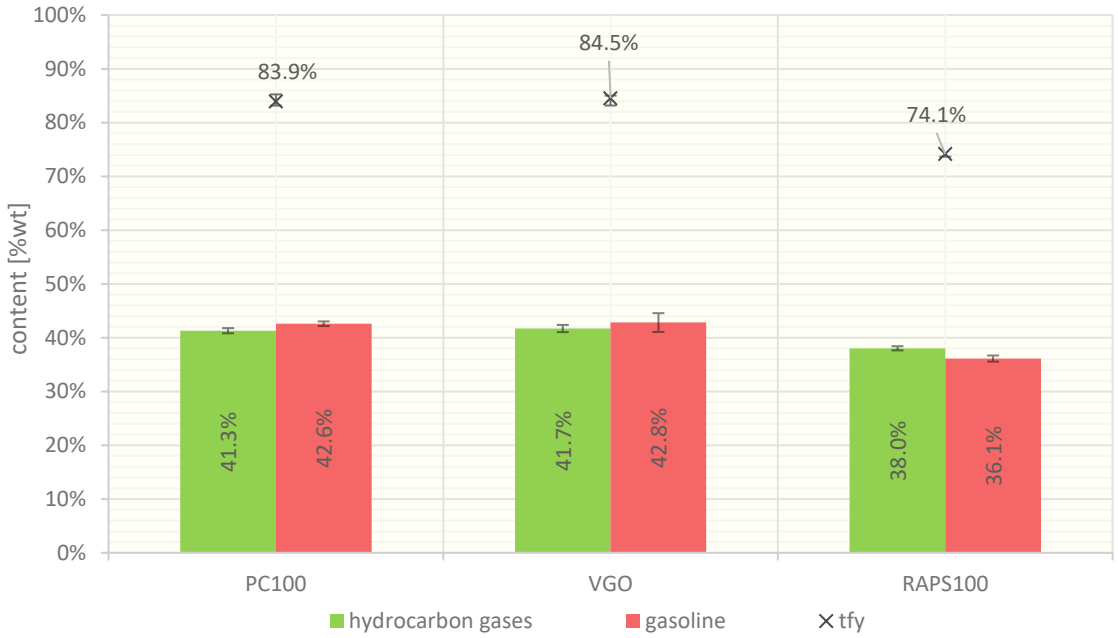

Figure 83: Hydrocarbon gases, gasoline yield and tfy of the 100 %wt pyoil experiment

Comparing the lower-value products LCO, residue and coke pyoil shows again relatively similar yield distribution to VGO. LCO with 6.1 %wt is higher than for VGO with 5.5 %wt but still far below canola oil with 8.3 %wt. The same applies to residue with 3.2 %wt for pyoil versus 3.5 %wt for VGO and 1.6 %wt for canola oil. For coke production the difference is not as significant as for the other products. Pure pyoil is producing 6.3 %wt coke, similar to VGO and significant lower than the 6.5 %wt for canola oil. Due to the low amount of feedstock no water fraction was collectable. However, due to the significant amount of oxygen in the pyoil the production of water is anticipated and indeed shown for various admixture rates.

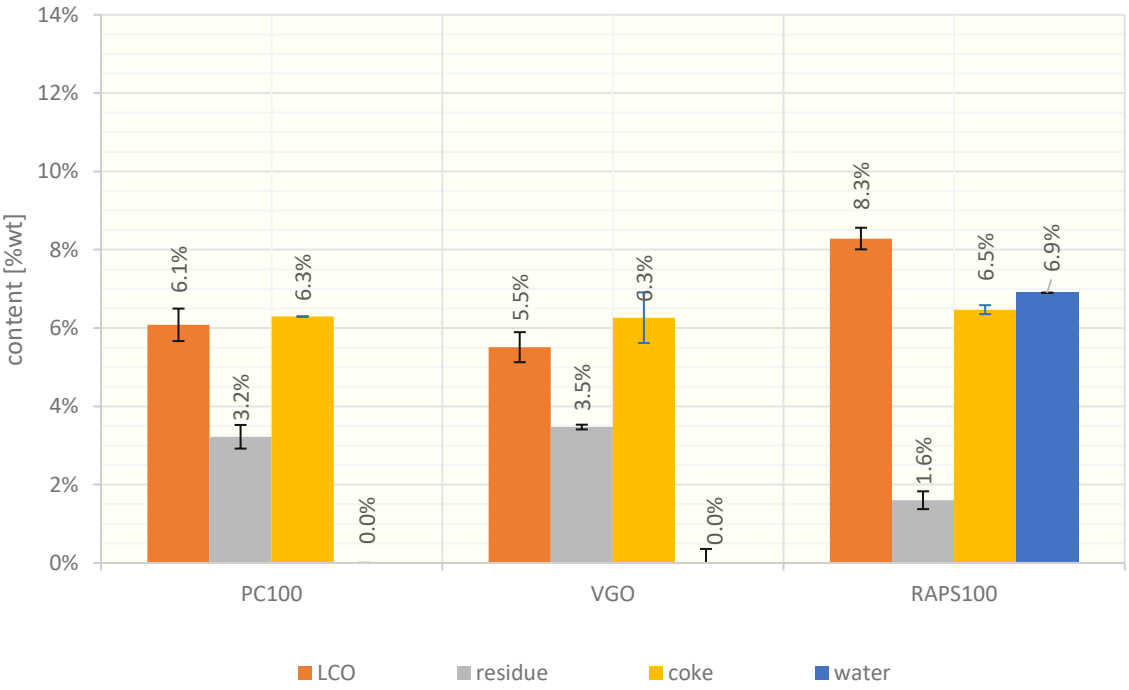

Figure 84: LCO, residue, coke and water of the 100 %wt pyoil experiment

The detailed gas composition can be seen in the following figure 85. Pyoil produces significant more propene than VGO, namely 17.4 %wt for 100 %wt pyoil versus 14.7 %wt for VGO and 14.7 %wt for canola oil. It also produces less ethene with a 2.6 %wt for pyoil compared to 3.4 %wt for VGO and 3.9 %wt for canola oil.
Butene production is increased, yielding 11.9 %wt for pyoil versus 8.8 %wt for VGO and 9.3 %wt for canola oil.
Alkanes are significant lower with 9.4 %wt for pyoil compared to 14.8 %wt from VGO canola oil with 10.2 %wt.

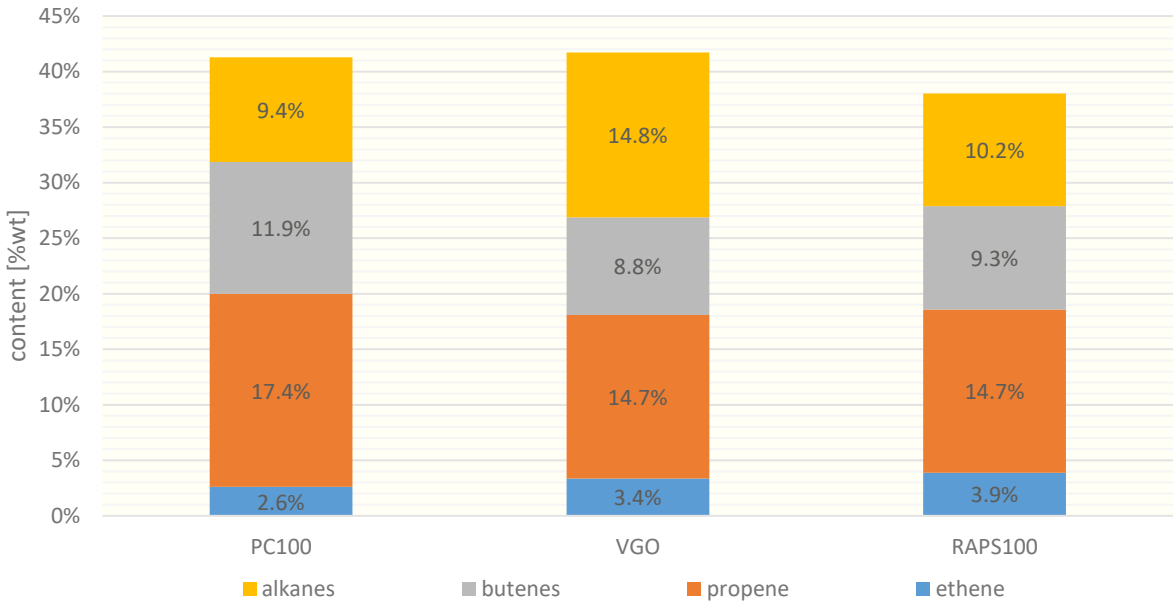

Figure 85: Ethene, propene, butene and alkane yield of the 100 %wt pyoil experiment

The detailed gas composition is shown in the following figure 86. The lower ethene yield (6.2 %wt versus 8.0 %wt for VGO and 9.6 %wt for canola oil) is compensated by the high propene yield (41.6 %wt versus 35.1 %wt for VGO and 36.1 %wt for canola oil) and the high butene yield (28.4 %wt versus 21.0 %wt for VGO and 22.9 %wt for canola oil).
Alkanes are lower, with a yield of 22.5 %wt compared to 35.4 %wt for VGO and 25.0 %wt for canola oil as a feedstock.

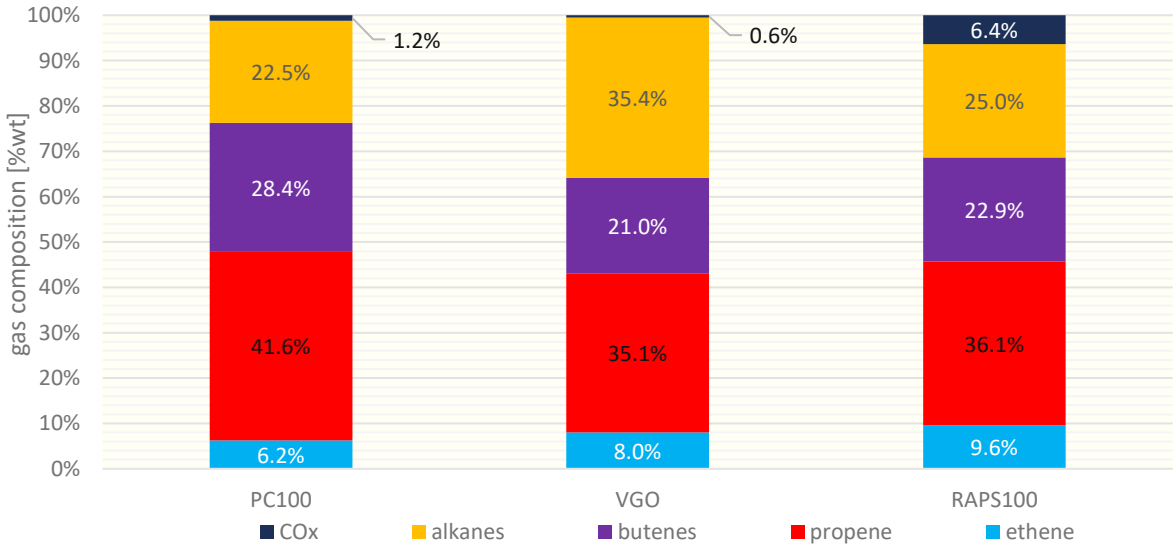

Figure 86: Gas composition of the 100 %wt pyoil experiment

The composition of the butenes is shown in the next figure 87. All butenes are significantly higher, with 2.3 %wt for 1-butene, 4.4 %wt for isobutene, 3.0 %wt for trans-2-butene and 2.2 %wt for cis-2-butene.

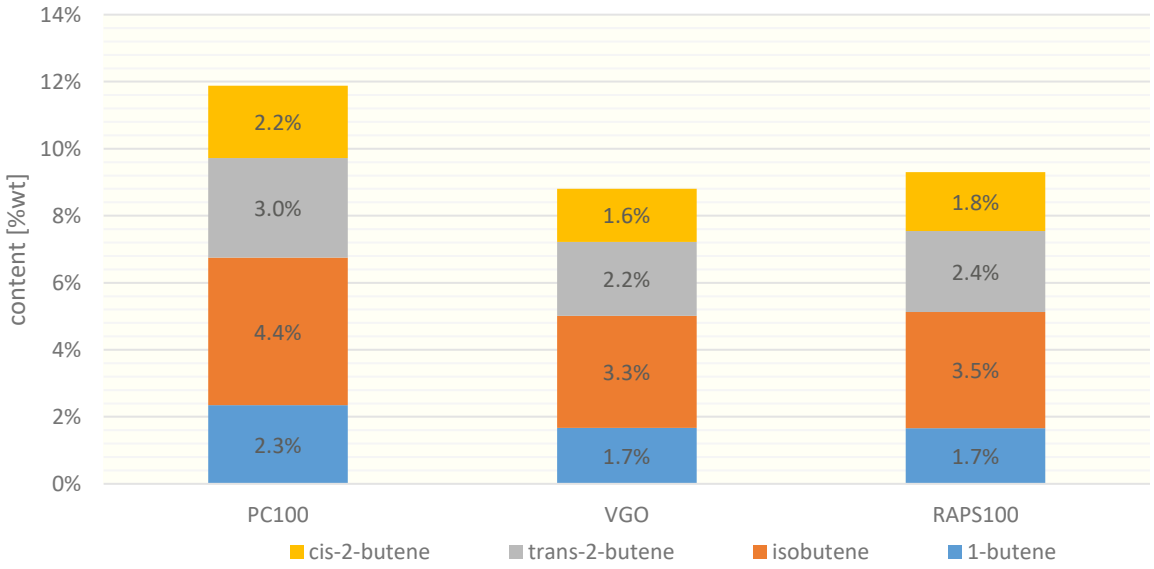

Figure 87: Butene yields of the 100 %wt pyoil experiment

The saturated hydrocarbons and the carbon oxides are depicted in the following figure. Methane production rate is at 0.9 %wt, ethane production amounts to 0.6 %wt, propane production is at 1.7 %wt, isobutane yield is at 5.4 %wt and the n-butane yield is at 0.8 %wt.
The carbon oxides are slightly lower than for pure canola oil with 0.3 %wt for CO and 0.3 %wt for CO_2. However, the carbon oxide yields are higher than those of VGO.

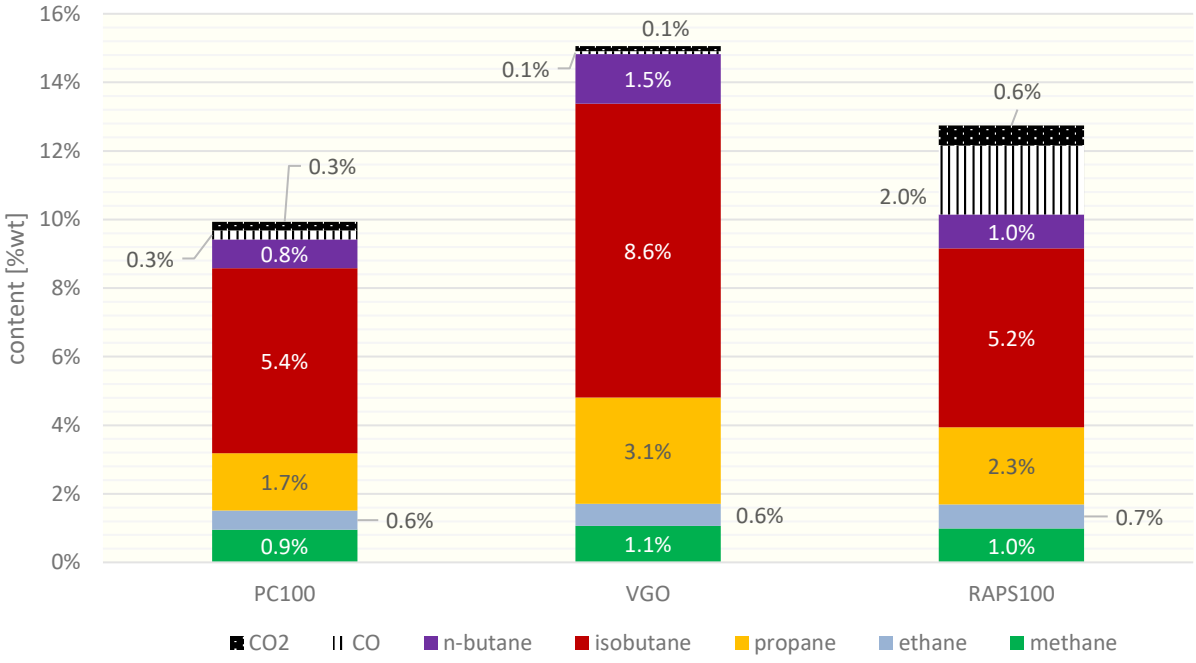

Figure 88: Alkane and COx yields of the 100 %wt pyoil experiment

Discussion

Plant operation

In a nutshell, feeding 100 %wt pyoil is a challenge for refiners. Not only is the required amount of feedstock not readily available, also the quality regarding water and oxygen content is varying depending on the supplier.
During plant operation pumping of the pyoil was challenging due to the precipitation described in chapter 10.1.2. The high-viscous mass clogged pipes and the feed pump. For industrial plants a sufficient filtration of the feedstock is obligatory (and needed!). Apart from that, the feedstock was relatively easy to handle, showing no significant polymerization tendencies in the preheating furnace.

Products

The product yields of 100%wt pyoil feeding are to some degree biased by the missing water fraction.
The shown values indicate a highly productive and economically rewarding process with a very high propene and butene yield whilst maintaining a high naphtha output for use in a steam cracker.

The high gas yield, especially the very high amount of propene in the gas yield, are no surprise as pyoil addition showed to boost propene and butene production rates. The high overall olefin yield of almost 32 %wt (including ethene, propene and the butenes) could potentially go directly into the petrochemical value chain to produce high quality polyolefins. All of this from deteriorated mixed plastic waste from a municipal waste collection system.
The fact that the olefins are produced at cost of mostly alkanes and the yields of the other products remain almost unchanged is especially interesting. This could be due to the properties of the olefin promoting catalyst, which is especially keen to the long-chained residues of polyolefins contained in the pyoil.

Due to the fact that waste-to-fuel is not counted as recycling in the European Union the produced gasoline fraction needs to be further treated in order to produce petrochemicals and avoid energetic utilization. Taking into account the yields of a steam cracker > 65 %wt of the naphtha could end up in the petrochemical value chain as either ethene, propene, butadiene, butenes, benzene or toluene. [86]

The total fuel yield indicates the high value creation of pyoil cracking. It has to be noted again that the results are biased due to the missing water yield. Future experiments with more available feedstock will most probably reveal a significant water production rate which will act as a burden on the conversion and the individual yields.

Even though the used pyoil has a relatively high oxygen content, the carbon oxide production rate is only lightly elevated. Compared to the results of VGO the carbon oxide production is marginally elevated. This is even more impressive compared to canola oil, which has approximately twice the oxygen level of pyoil but almost eight (8) times the carbon oxide content of pyoil in the product gas.

11 SYNOPSIS

Climate change is not approaching, it is already here.
To limit global warming to moderate levels, the emissions of fossil carbon to the atmosphere in form of greenhouse gases, among other measures, needs to be reduced drastically.

In addition to the known climate challenges, humanity is drowning in its own (plastic-) waste.
In order to achieve a zero-pollution economy, unavoidable plastic waste needs to be recycled.

To reduce the impact of the climate change and to mitigate the rampant pollution as much as possible legislators need to issue stricter regulations, industries need to adapt to the changing legislations and, to some degree, even anticipate them.
To meet the required recycling targets, co-processing offers an attractive alternative to incineration of plastic waste. Furthermore, the use of biogenic feedstock introduces a renewable hydrocarbon source, potentially resulting in a reduced carbon footprint of the affected process.
To do all this as quickly and economically compatible to our society as possible, existing plants need to be adapted and retrofitted to carbon reduced, or neutral feedstocks. This is especially true for the petrochemical industry.

Combining the imminent task of decarbonizing refinery processes and the challenge of integrating plastic waste into a circular economy, fluid catalytic cracking (FCC) offers substantial opportunities for the petroleum industry. The utilization of versatile FCC units, which many refineries already have in operation, to co-process vacuum gas oil (the standard feedstock for FCC units), syncrude (obtained by pyrolization of various plastic wastes) and biogenic oil (e.g. used cooking oils) can contribute to reach future defined defossilization and circular economy targets.

For the experimental work, variable admixtures of pyrolysis oil derived from municipal plastic waste, vacuum gas oil, canola oil and used cooking oil were fed into an FCC pilot plant. Despite this admixture, the FCC process offers relatively stable product yields of gasoline, olefins and other petrochemicals while coping with very heavy and complex feedstocks. The continuously operating fluid catalytic cracking pilot plant is located at TU Wien and is able to resemble the product spectrum of gasoline- and olefin-optimized industrial-scale FCC units. The pilot plant enables the identification of the associated challenges and potential synergies of co-processing in FCC units.

During the pre-tests of feedstock admixtures a tendency of the pyoil to polymerize in contact with the base feedstocks at elevated temperature was found. By stirring the cooled admixtures the gel-like liquid reduced its viscosity and was pumpable again.

Additionally, certain components of the pyoil formed a heavy, highly viscous precipitation with a high inorganic ash content. The removal of the precipitation was relatively easy, but pumps, filters and other equipment keen to blocking needs to be designed sufficiently to cope with this.

By including the unconventional feedstock pyoil into FCC feedstocks a partial circularity of the process could be achieved. The changing product yields are to a certain degree manageable. Taking into account future catalysts especially modified for pyoil cracking the potential of industrial sized co-processing is very high. Optimization of the desired product yields will be key to bring these co-feeding FCC units to the same level of conversion as they are today running on conventional feedstocks, maybe even higher.
In more detail, admixing pyrolysis oil derived from municipal plastic waste to VGO resulted in an increased cooling demand in the cooling section of the plant. This probably arose from the lighter boiling curve of the pyoil, which results in a higher C/O ratio due to the increased gain of volume at the feeding nozzle. Another result is a significant water production, which is due to the oxygen

content of the feedstock. The water production poses challenges for pyoil co-processing in industrial-scale FCC units, requiring re-evaluation of downstream equipment to handle the higher steam and water flow rates.
On the product side, the reduced gasoline production is offset by increased gas production, particularly by the higher yields of olefins. This is probably due to a high ratio of polyolefins in the pyoil feedstock, which readily reacts with the catalyst to produce olefins. Conversely, the production of C3 and C4 alkanes is reduced. This phenomenon may be attributed to the catalyst, which is specifically designed to enhance the production of C3 and C4 olefins, indicating its selectivity.

The second objective, apart from increasing the circularity of the FCC process by adding pyoil, was to decarbonize by means of adding biogenic oil to the feedstock.
One significant challenge for the profitability of fluid catalytic cracking (FCC) units is the decrease in gasoline lump size. A drop of more than 5% by weight results in a substantial loss in process profitability. This is primarily due to the increased yield of hydrocarbon gases, light cycle oil (LCO), residue, water, and carbon oxides, which have lower value compared to high-octane FCC gasoline. While LCO and residue have some value and can be recycled or used as blending components, they do not offer the same level of value creation as high-octane gasoline.
However, there is a positive aspect in terms of the hydrocarbon gas yield, as its quality improves. Notably, the yield of olefins increases significantly, both in relative terms and absolute numbers. Given the diminishing prospects of traditional fossil fuels, the growing petrochemical industry sees the production of direct-to-use olefins as a promising opportunity for FCC units.
The increasing amount of carbon oxides and water in the product yields is a characteristic feature when using biogenic oils like canola oil in FCC units. Handling elevated water content in the product gas poses challenges, but the challenges are even greater when it comes to removing substantial amounts of carbon oxides. Industrial-scale FCC units are designed to handle high levels of steam as they are fluidized with steam, whereas efficiently removing carbon oxides necessitates extensive gas scrubbing and treatment.
Since the future of traditional fossil fuels is seen predominantly in decline, a gain in direct-to-use olefins for the constantly and massively growing petrochemical industry can be a main source of revenue for FCC units in the future.

Pushing the limits of defossilization further meant increasing the co-fed amount of bio oil to the maximum. A full substitution of VGO by biogenic oil changed the product spectrum significantly. Biogenic oils produce different yields, although the products themselves are chemically similar or identical to VGO-derived FCC products. A comparison of the base cases with the feedstocks VGO, canola oil and UCO was conducted in order to show these differences. Bio oils generally produced lower gaseous, gasoline and residue yields and boosted LCO production. A notable outcome is that, even though the amount of hydrocarbon gases in the product is reduced, the amount of produced olefins is on the same level as for VGO as feedstock. As aforementioned, the high oxygen content of bio oils increases water and carbon oxide production and presumably increases the formation of oxygenates in the organic liquids, although due to a lack of sufficient analytic capabilities the assumption regarding oxygenate concentration couldn't be verified.

Incorporating canola oil as a base feedstock in the FCC process presents its own set of challenges as mentioned before. The introduction of pyoil slightly alters these challenges, shifting the focus from high water and CO_X (carbon monoxide and carbon dioxide) production to an even higher water but a lowered CO_X production.
A slightly increasing gasoline production and a slightly decreasing hydrocarbon gas production causes the overall conversion to decrease. Although the gas production decreases, the addition of pyoil increases the gas quality by increasing the amount of olefins, especially propene. This development can be described in the case of the changing gasoline and hydrocarbon gas yields by the increased amount of aromatics in the feedstock and in the case of an increased gas quality by the polyolefin chains present in the pyoil, boosting olefin production. Less valuable heavy products decrease, probably due to the lighter boiling curve of the pyoil.

The results of co-processing UCO and pyoil showed relatively positive outcomes. The addition of pyoil enhances the yield of hydrocarbon gas while causing only a slight reduction in gasoline production. When a 5 %wt admixture rate is applied, the inclusion of pyoil actually improves gasoline production compared to the benchmark, with a negligible impact on hydrocarbon gas yields. This indicates a certain level of synergy between the two feedstocks.
Similar to the previous experiments with the base feed canola oil, the addition of pyoil significantly boosts propene production. This can be attributed to the change in feedstock composition. The same trend applies to the yield of butene, which increases substantially, particularly when compared to the results from the canola oil experiments.

As previously stated the olefin yield of the FCC unit is key to its profitability, especially in its growing role as a source of petrochemicals such as olefins and BTX aromatics. Increasing the cracking severity of base feeds and pyoil admixtures in order to investigate the potential maximization was the goal of these experiments. Although an increased cracking temperature increased the olefin yields for the base feeds, the picture changed fundamentally when pyoil was co-fed. The addition of pyoil to high temperature cracking experiments shifted the product spectrum of both, VGO and UCO admixtures, towards increasing the gasoline and heavier product yields. Instead of a controlled overcracking of the gasoline fraction in order to produce more gases the pyoil seemingly shifts the gasoline maximum to higher cracking temperatures. This could have a positive twist if refineries seek to increase the naphtha fraction due to a local steam cracker. However, in order to maximize the olefin fraction by means of an increased cracking temperature a more detailed investigation is needed.

Pyoil can hardly be compared to easy-to handle feeds like VGO or lipids. Cracking pure pyoil derived from municipal plastic waste showed high yields of gasoline and hydrocarbon gases, especially of the olefins. The good overall conversion indicates a highly productive process, although the results are biased to some degree due to the missing water fraction. Operating an FCC unit solely on pyoil from municipal plastic waste is currently not realistic, first because there is a lack of readily available feedstock (pyoil) and secondly because this requires years of research and development into this specialized direction.
However, as previously discussed a possible approach can be to co-feed plastic pyrolysis oils to an FCC unit in order to raise the level of circularity of a refinery. Increasing the amount gradually could lead to repurposing single, presumably old, FCC units to this kind of feedstock. Similar to resid FCC units (so-called RFCC) dedicated FCC units for plastic recycling could be possible in the future. The high amount of produced olefins (especially propene) and the relatively constant yield of naphtha (gasoline fraction) can be seen as an indication of a feasible business case of these “re-FCC” units dedicated for recycling of mixed plastic waste in the future.

12 OUTLOOK

The co-processing of renewable feedstocks can contribute to defossilization of FCC and, thus, the defossilization of fuels and petrochemicals. However, in order to quantify the effects of co-processing on the fossil carbon footprint, a detailed Life Cycle Assessment (LCA) of the overall process including the feedstocks, the products and their usage is advisable.

In order to optimize the product yields of the FCC process, the catalysts need to be closer investigated. The optimization of the catalyst to renewable feedstocks and to pyoil from plastic waste could open up economical opportunities for FCC in the future. Adapting the catalyst towards higher conversion and the maximization of the olefin yield could be a chance for chemical recycling of highly deteriorated plastics.

As previously mentioned, the amount of available feedstock was a challenge for these experiments. Obtaining a bigger amount of pyoil for extensive tests in order to obtain more reliable data could show synergies between different feedstocks in co-processing not recognizable in the current research due to the relatively high error margins. This is especially true for the experiment with 100 %wt pyoil.

An investigation of the exact temperature of the gasoline maximum of VGO/UCO and pyoil admixtures should be conducted, in order to find the maximum olefin yield and the corresponding cracking conditions.

A more detailed look into the liquid fraction by means of a PIONA analysis to investigate the detailed composition should be conducted. Associated with this an analysis of the suspected amount of oxygenates contained in the liquid fraction is required, in order to clarify in detail the fate of the oxygen in the feedstock.

Finally, test runs with hydrotreated pyoil could be conducted to investigate the impact of the reduced oxygen content in the feedstock. Additionally, the hydrotreatment will remove a large amount of the contaminants inherent to the used pyoil due to the used contaminated plastic waste feedstock (containing PVC, heavy metals and sulfur among others).

Closing statement

During this thesis, active and passive participation on conferences in Europe and the Middle East was conducted, giving insight into the petrochemical and petroleum industry.
The perceived optimism regarding large scale co-processing and inclusion of renewable feedstocks instead of fossil-based petroleum products was a constant among all conferences and its speakers, delegates and organizers.

The wind of change in this industry needs to be fueled by academia, research and development and legislation to not let it decay to a mild breeze.

13 LITERATURE

[1] The European Commission, *A new Circular Economy Action Plan*. Brussels, 2020. Accessed: Jun. 21, 2023. [Online]. Available: https://eur-lex.europa.eu/legal-content/EN/TXT/?uri=COM:2020:98:FIN

[2] The Senate and House of Representatives of the United States of America, *Inflation reduction act, COMMITTEE ON FINANCE: Deficit Reduction*.

[3] The Eurean Parliament and Council, "RED II: Directive (EU) 2018/2001 of the European Parliament and of the Council of 11 December 2018 on the promotion of the use of energy from renewable sources," 2018. Accessed: Jun. 21, 2023. [Online]. Available: https://eur-lex.europa.eu/legal-content/EN/TXT/?uri=uriserv:OJ.L_.2018.328.01.0082.01.ENG

[4] ASIAN DEVELOPMENT BANK, "The 14th Five-Year Plan of the People's Republic of China —Fostering High-Quality Development," 2021. doi: http://dx.doi.org/10.22617/BRF210192-2.

[5] S. Kaza, L. Yao, P. Bhada-Tata, and F. Van Woerden, *What a Whaste 2.0*. Washington: The World Bank, 2018. doi: 10.1596/978-1-4648-1329-0.

[6] OECD, *Global Material Resources Outlook to 2060: Economic Drivers and Environmental Consequences*. Paris: OECD Publishing, 2019. doi: 10.1787/9789264307452-en.

[7] Bundesministerium der Justiz und für Verbraucherschutz, *Gesetz für den Ausbau erneuerbarer Energien (Erneuerbare- Energien-Gesetz - EEG 2021)*. 2020, p. 154.

[8] Österreichischer Nationalrat, *Bundesgesetz über den Ausbau von Energie aus erneuerbaren Quellen (Erneuerbaren- Ausbau-Gesetz – EAG)*. 2020, pp. 1–89.

[9] European Comission, "The European Green Deal".

[10] Cambridge Econometrics, Trinomics, and ICF, "Impacts of circular economy policies on the labour market - Publications Office of the EU ANNEX," 2018. [Online]. Available: https://op.europa.eu/en/publication-detail/-/publication/fc373862-704d-11e8-9483-01aa75ed71a1/language-en

[11] United Nations Framework Convention on Climate Change, "The Paris Agreement," 2015.

[12] W. M. Burton, "Medal Address. Chemistry in the Petroleum Industry," *J. Ind. Eng. Chem*, vol. 10, no. 6, pp. 484–486, 1918, doi: 10.1021/ie50102a030.

[13] A. M. McAfee, "The manufacture of gasoline as a by-product from high boiling petroleum oil, and the Manufacture of Gasoline as a By-product There from, by the Action of Aluminum Chloride.," *Ind. Eng. Chem.*, vol. 7, no. 10, pp. 737–741, 1915, doi: 10.1021/ie50082a046.

[14] Sun Company, "A NATIONAL HISTORIC CHEMICAL LANDMARK: THE HOUDRY PROCESS FOR THE CATALYTIC CONVERSION OF CRUDE PETROLEUM TO HIGH-OCTANE GASOLINE," Marcus Hook, Pennsylvania, 1996.

[15] E. Houdry, W. F. Burt, A. E. Pew, and W. A. Peters, "The Houdry process," *The Oil and Gas Journal*, vol. 37, pp. 40–45, 1938.

[16] A. A. Avidan, *Fluid Catalytic Cracking: Science and Technology*, vol. 76. Elsevier Science Publishers B.V., 1993.

[17] A. M. Squires, "STORY OF FLUID CATALYTIC CRACKING: THE FIRST 'CIRCULATING FLUID BED'.," Pergamon Press, 1986, pp. 1–19. doi: 10.1016/b978-0-08-031869-1.50007-7.

[18] Z. Zhang, Z. Liu, R. Feng, P. Liu, and Z. Yan, "The development of FCC catalysts for producing FCC gasoline with high octane numbers," *Appl Petrochem Res*, vol. 4, no. 4, pp. 379–383, Oct. 2014, doi: 10.1007/s13203-014-0075-9.

[19] J. H. Gary, J. H. Handwerk, M. J. Kaiser, and D. Geddes, "Fluid Catalytic Cracking," in *Petroleum Refining: Technology and Economics*, 2007, pp. 121–160.

[20] W. Letzsch, "Fluid catalytic cracking," in *Handbook of Petroleum Processing*, D. S. J. S. Jones and P. R. Pujadó, Eds., 1st ed.Dordrecht: Springer Netherlands, 2006, pp. 237–287. doi: 10.1007/1-4020-2820-2.

[21] S. Hafeez, E. Pallari, G. Manos, and A. Constantinou, “Catalytic Conversion and Chemical Recovery,” in *Plastics to Energy*, Elsevier, 2019, pp. 147–172. doi: 10.1016/B978-0-12-813140-4.00006-6.
[22] M. R. S. Manton and J. C. Davidtz, “Controlled pore sizes and active site spacings determining selectivity in amorphous silica-alumina catalysts,” *J Catal*, vol. 60, no. 1, pp. 156–166, Oct. 1979, doi: 10.1016/0021-9517(79)90078-2.
[23] R. Sadeghbeigi, “FCC catalysts,” in *Fluid Catalytic Cracking Handbook*, 4th ed.Elsevier, 2020, pp. 83–110. doi: 10.1016/B978-0-12-812663-9.00005-9.
[24] J. G. Speight, “Catalytic Cracking Processes,” in *Heavy Oil Recovery and Upgrading*, Ed. Gulf Professional Publishing, 2019, pp. 357–421.
[25] P. Seidel, *Schweres Erdöl - ein alternativer Rohstoff zur Erzeugung von Treibstoffen*. Renningen - Malmsheim: Expert Verlag, 1994.
[26] H. Lutz, “Alternative Feedstocks from Waste and Renewable Resources in the FCC Process for a Sustainable Production of Light Olefins and High-Octane Gasoline,” Dissertation, Technische Universität Wien, 2022.
[27] M. Büchele, “Heavy residues and pyrolysis oils as feedstocks in the FCC process for a more sustainable production of olefins and high-octane gasoline,” 2022. doi: 10.34726/hss.2022.104221.
[28] P. Bielansky, A. Weinert, C. Schönberger, and A. Reichhold, “Catalytic conversion of vegetable oils in a continuous FCC pilot plant,” *Fuel Processing Technology*, vol. 92, no. 12, pp. 2305–2311, Dec. 2011, doi: 10.1016/J.FUPROC.2011.07.021.
[29] M. Büchele, M. Swoboda, A. Reichhold, and W. Hofer, “Canola oil/glycerol mixtures in a continously operated FCC pilot plant and comparison with vacuum gas oil/glycerol mixtures,” *Chemical Engineering and Processing - Process Intensification*, vol. 142, p. 107553, Aug. 2019, doi: 10.1016/J.CEP.2019.107553.
[30] C. Ramakrishnan, *Umfassende Untersuchungen zur katalytischen Konversion von Bioölen in einer vollkontinuierlichen FCC-Technikumsanlage*. 2004.
[31] J. Tan, C. McKenzie, M. Potamitis, A. N. Thorburn, C. R. Mackay, and L. Macia, “The Role of Short-Chain Fatty Acids in Health and Disease,” *Adv Immunol*, vol. 121, pp. 91–119, Jan. 2014, doi: 10.1016/B978-0-12-800100-4.00003-9.
[32] A. S. Salsinha, M. Machado, L. M. Rodríguez-Alcalá, A. M. Gomes, and M. Pintado, “Bioactive lipids: Chemistry, biochemistry, and biological properties,” in *Bioactive Lipids*, Elsevier, 2023, pp. 1–35. doi: 10.1016/b978-0-12-824043-4.00014-2.
[33] R. Aluko, “Bioactive Lipids,” in *Functional Foods and Nutraceuticals* , 2012, pp. 23–36. doi: 10.1007/978-1-4614-3480-1_2.
[34] B. Marten, M. Pfeuffer, and J. Schrezenmeir, “Medium-chain triglycerides,” *Int Dairy J*, vol. 16, no. 11, pp. 1374–1382, Nov. 2006, doi: 10.1016/J.IDAIRYJ.2006.06.015.
[35] P. T. Bozza and J. P. B. Viola, “Lipid droplets in inflammation and cancer,” *Prostaglandins Leukot Essent Fatty Acids*, vol. 82, no. 4–6, pp. 243–250, Apr. 2010, doi: 10.1016/j.plefa.2010.02.005.
[36] G. Feiner, “Meat and Fat,” in *Salami*, Elsevier, 2016, pp. 3–30. doi: 10.1016/b978-0-12-809598-0.00001-9.
[37] B. J. F. Hudson, “FATTY ACIDS | Properties,” in *Encyclopedia of Food Sciences and Nutrition*, B. Caballero, Ed., 2nd ed.Academic Press, 2003, pp. 2297–2300. doi: 10.1016/B0-12-227055-X/00446-6.
[38] H. C. Deeth, “Milk Lipids | Lipolysis and Hydrolytic Rancidity,” in *Encyclopedia of Dairy Sciences*, Elsevier, 2011, pp. 721–726. doi: 10.1016/B978-0-12-374407-4.00343-5.
[39] J. H. J. Huis in’t Veld, “Microbial and biochemical spoilage of foods: an overview,” *Int J Food Microbiol*, vol. 33, no. 1, pp. 1–18, Nov. 1996, doi: 10.1016/0168-1605(96)01139-7.
[40] N. George and T. Kurian, “Recent developments in the chemical recycling of postconsumer poly(ethylene terephthalate) Waste,” *Ind Eng Chem Res*, vol. 53, no. 37, pp. 14185–14198, Aug. 2014, doi: 10.1021/ie501995m.
[41] M. Goto, “Chemical recycling of plastics using sub- and supercritical fluids,” *J Supercrit Fluids*, vol. 47, no. 3, pp. 500–507, Jan. 2009, doi: 10.1016/J.SUPFLU.2008.10.011.

[42] J. Kaushal, M. Khatri, and S. K. Arya, “Recent insight into enzymatic degradation of plastics prevalent in the environment: A mini - review,” *Clean Eng Technol*, vol. 2, p. 100083, Jun. 2021, doi: 10.1016/J.CLET.2021.100083.
[43] V. Tournier *et al.*, “An engineered PET depolymerase to break down and recycle plastic bottles,” *Nature*, vol. 580, no. 7802, pp. 216–219, Apr. 2020, doi: 10.1038/s41586-020-2149-4.
[44] A. Gonzalez-Quiroga, M. R. Djokic, K. M. Van Geem, and G. B. Marin, “Conversion of Solid Waste to Diesel via Catalytic Pressureless Depolymerization: Pilot Scale Production and Detailed Compositional Characterization,” *Energy and Fuels*, vol. 30, no. 10, pp. 8292–8303, Oct. 2016, doi: 10.1021/acs.energyfuels.6b01639.
[45] N. Aryal, M. Odde, C. Bøgeholdt Petersen, L. Ditlev Mørck Ottosen, and M. Vedel Wegener Kofoed, “Methane production from syngas using a trickle-bed reactor setup,” *Bioresour Technol*, vol. 333, Aug. 2021, doi: 10.1016/j.biortech.2021.125183.
[46] H. Gruber, *Synthesis and refining of biomass-derived Fischer-Tropsch paraffin waxes*. Wien, 2020.
[47] V. Wilk and H. Hofbauer, “Conversion of mixed plastic wastes in a dual fluidized bed steam gasifier,” *Fuel*, vol. 107, pp. 787–799, May 2013, doi: 10.1016/j.fuel.2013.01.068.
[48] S. H. Chang, “Plastic waste as pyrolysis feedstock for plastic oil production: A review,” *Science of The Total Environment*, p. 162719, Jun. 2023, doi: 10.1016/j.scitotenv.2023.162719.
[49] Y. Zhang, Z. Fu, W. Wang, G. Ji, M. Zhao, and A. Li, “Kinetics, Product Evolution, and Mechanism for the Pyrolysis of Typical Plastic Waste,” *ACS Sustain Chem Eng*, vol. 10, no. 1, pp. 91–103, Jan. 2022, doi: 10.1021/acssuschemeng.1c04915.
[50] R. Prurapark, K. Owjaraen, B. Saengphrom, I. Limthongtip, and N. Tongam, “Effect of Temperature on Pyrolysis Oil Using High-Density Polyethylene and Polyethylene Terephthalate Sources From Mobile Pyrolysis Plant,” *Front Energy Res*, vol. 8, Nov. 2020, doi: 10.3389/fenrg.2020.541535.
[51] R. Thahir, M. Irwan, A. Alwathan, and R. Ramli, “Effect of temperature on the pyrolysis of plastic waste using zeolite ZSM-5 using a refinery distillation bubble cap plate column,” *Results in Engineering*, vol. 11, Sep. 2021, doi: 10.1016/j.rineng.2021.100231.
[52] P. Basu, *Biomass gasification and pyrolysis : practical design and theory*. Academic Press, 2010.
[53] A. V Bridgwater, “Principles and practice of biomass fast pyrolysis processes for liquids,” 1999.
[54] G. Lopez, M. Amutio, G. Elordi, M. Artetxe, H. Altzibar, and M. Olazar, “A CONICAL SPOUTED BED REACTOR FOR THE VALORISATION OF WASTE TIRES,” in *The 13th International Conference on Fluidization - New Paradigm in Fluidization Engineering*, 2010. [Online]. Available: http://dc.engconfintl.org/fluidizationxiii/87
[55] K. Murata, K. Sato, and Y. Sakata, “Effect of pressure on thermal degradation of polyethylene,” *J Anal Appl Pyrolysis*, vol. 71, no. 2, pp. 569–589, 2004, doi: 10.1016/j.jaap.2003.08.010.
[56] L. Cheng, J. Gu, Y. Wang, J. Zhang, H. Yuan, and Y. Chen, “Polyethylene high-pressure pyrolysis: Better product distribution and process mechanism analysis,” *Chemical Engineering Journal*, vol. 385, Apr. 2020, doi: 10.1016/j.cej.2019.123866.
[57] R. Miranda, H. Pakdel, C. Roy, and C. Vasile, “Vacuum pyrolysis of commingled plastics containing PVC II. Product analysis,” *Polym Degrad Stab*, vol. 73, no. 1, pp. 47–67, Jan. 2001, doi: 10.1016/S0141-3910(01)00066-0.
[58] G. K. Parku, F. X. Collard, and J. F. Görgens, “Pyrolysis of waste polypropylene plastics for energy recovery: Influence of heating rate and vacuum conditions on composition of fuel product,” *Fuel Processing Technology*, vol. 209, Dec. 2020, doi: 10.1016/j.fuproc.2020.106522.
[59] M. Arabiourrutia, G. Elordi, G. Lopez, E. Borsella, J. Bilbao, and M. Olazar, “Characterization of the waxes obtained by the pyrolysis of polyolefin plastics in a conical spouted bed reactor,” *J Anal Appl Pyrolysis*, vol. 94, pp. 230–237, 2012, doi: 10.1016/j.jaap.2011.12.012.

[60] S. D. Anuar Sharuddin, F. Abnisa, W. M. A. Wan Daud, and M. K. Aroua, “A review on pyrolysis of plastic wastes,” *Energy Conversion and Management*, vol. 115. Elsevier Ltd, pp. 308–326, May 01, 2016. doi: 10.1016/j.enconman.2016.02.037.
[61] Y. Peng *et al.*, “A review on catalytic pyrolysis of plastic wastes to high-value products,” *Energy Conversion and Management*, vol. 254. Elsevier Ltd, Feb. 15, 2022. doi: 10.1016/j.enconman.2022.115243.
[62] J. Wang *et al.*, “Enhanced BTEX formation via catalytic fast pyrolysis of styrene-butadiene rubber: Comparison of different catalysts,” *Fuel*, vol. 278, Oct. 2020, doi: 10.1016/j.fuel.2020.118322.
[63] Y. Xue, Y. Zhou, J. Liu, Y. Xiao, and T. Wang, “Comparative analysis for pyrolysis of sewage sludge in tube reactor heated by electromagnetic induction and electrical resistance furnace,” *Waste Management*, vol. 120, pp. 513–521, Feb. 2021, doi: 10.1016/j.wasman.2020.10.015.
[64] W. Posch, *Applied Plastics Engineering Handbook*, 2nd ed., vol. 1. Elsevier, 2011. doi: 10.1016/C2010-0-67336-6.
[65] R. Le Van Mao, H. Yan, A. Muntasar, and N. Al-Yassir, *New and Future Developments in Catalysis*. Elsevier, 2013. doi: 10.1016/C2010-0-68688-3.
[66] R. Sadeghbeigi, “Chemistry of FCC reactions,” in *Fluid Catalytic Cracking Handbook*, 4th ed.Elsevier, 2020, pp. 119–128. doi: 10.1016/B978-0-12-812663-9.00007-2.
[67] A. Reichhold, “ Entwicklung von Reaktions/Regenerationssystemen für Adsorptions/Desorptionsprozesse und für katalytisches Cracken auf der Basis von intern zirkulierenden Wirbelschichten,” Technische Universität Wien, Vienna, 1997.
[68] P. Bielansky, “Alternative Feedstocks in Fluid Catalytic Cracking,” Technische Universität Wien, Vienna, 2012.
[69] A. Weinert, “Durchführung von Crackversuchen an einer Technikumsanlage im Rahmen der Entwicklung eines FCC-Konzepts mit Aspekten der Nachhaltigkeit,” Technische Universität Wien, Vienna, 2013.
[70] M. A. Fahim, T. A. Alsahhaf, and A. Elkilani, “Fluidized catalytic cracking,” in *Fundamentals of Petroleum Refining*, Elsevier, 2010, pp. 199–235. doi: 10.1016/C2009-0-16348-1.
[71] IFA, *GESTIS data base entry for gasoline (Ottokraftstoff)*. Physikalisch-Technische Bundesanstalt (PTB), 2023.
[72] American Society for Testing and Materials, “Standard Test Method for Conradson Carbon Residue of Petroleum Products; ASTM D189-06(2019),” *Book of Standards*, vol. 05.01. p. 7, 2019.
[73] D. S. J. Jones, “An introduction to crude oil and its processing,” in *Handbook of Petroleum Processing*, D. S. J. S. Jones and P. R. Pujadó, Eds., 1st ed.Dordrecht: Springer Netherlands, 2006, pp. 1–45. doi: 10.1007/1-4020-2820-2.
[74] DerGrünePunkt, “Produktspezifikation 03/2018 Fraktions-Nr. 350 Mischkunststoffe.” DerGrünePunkt.
[75] DerGrünePunkt, “Produktspezifikation 05/2012 Fraktions-Nr. 352 Mischkunststoffe neu.” DerGrünePunkt.
[76] M. Tomasi Morgano, H. Leibold, F. Richter, D. Stapf, and H. Seifert, “Screw pyrolysis technology for sewage sludge treatment,” *Waste Management*, vol. 73, pp. 487–495, Mar. 2018, doi: 10.1016/j.wasman.2017.05.049.
[77] M. Tomasi Morgano, H. Leibold, F. Richter, and H. Seifert, “Screw pyrolysis with integrated sequential hot gas filtration,” *J Anal Appl Pyrolysis*, vol. 113, pp. 216–224, May 2015, doi: 10.1016/j.jaap.2014.12.019.
[78] Office of the Provincial Government of Lower Austria - Department of Provincial Office Management, “Nöli - Altspeisefettsammlung,” *https://www.noe.gv.at/noe/Abfall/NOELI_-_Altspeisefett.html*, 2023.
[79] Deutsches Institut für Normung, “DIN EN ISO 27107:2010-08: Tierische und pflanzliche Fette und Öle – Bestimmung der Peroxidzahl – Potentiometrische Endpunktbestimmung.” 2010.

[80] C. Gertz, “Analytische Verfahren zur Qualitätsbeurteilung von Fetten und Öelen,” *DGF Workshop “Fast Alles über Rapsöl.”* Chemisches Untersuchungsamt Hagen, Hagen, 2005.
[81] Deutsches Institut für Normung, “DIN EN ISO 660:2020-12 Tierische und pflanzliche Fette und Öle - Bestimmung der Säurezahl und der Azidität.” 2020.
[82] F. Knaus, H. Lutz, M. Büchele, A. Reichhold, A. Pazso Costa, and W. Tesch, “Chemical Recycling – Beyond Thermal Use of Plastic and other Waste,” in *Plastic to Petrochemicals – Recycling of Pyrolyzed Municipal Plastic Waste by FCC Co-Processing* , Hamburg: DGMK, 2021, pp. 68–79.
[83] H. Ritchie, M. Roser, and P. Rosado, “CO_2 and Greenhouse Gas Emissions,” *https://ourworldindata.org/co2-and-greenhouse-gas-emissions*, 2020.
[84] F. Knaus, H. Lutz, M. Büchele, A. Reichhold, and A. Pazos-Costa, “Municipal plastic waste recycling in fluid catalytic cracking units: Production of petrochemicals and fuel in an fluid catalytic cracking pilot plant from biogenic and recycled feedstocks,” *Chemical Engineering and Processing - Process Intensification*, vol. 182, Dec. 2022, doi: 10.1016/j.cep.2022.109204.
[85] C. Schönberger, “Fischer-Tropsch und Fluid Catalytic Cracking: Zwei alternative Technologien zur Herstellung von flüssigen Treibstoffen aus Biomasse,” Technische Universität Wien, Vienna, 2010.
[86] A. Akah and M. Al-Ghrami, “Maximizing propylene production via FCC technology,” *Appl Petrochem Res*, vol. 5, no. 4, pp. 377–392, Dec. 2015, doi: 10.1007/s13203-015-0104-3.

14 PUBLICATIONS AS CORRESPONDING AUTHOR

- F. Knaus, H. Lutz, M. Büchele, A. Reichhold, A. Pazso Costa, and W. Tesch, “Chemical Recycling – Beyond Thermal Use of Plastic and other Waste,” in *Plastic to Petrochemicals – Recycling of Pyrolyzed Municipal Plastic Waste by FCC Co-Processing* , Hamburg: DGMK, 2021, pp. 68–79. ISBN 978-3-947716-30 2, ISSN 1433-9013

- F. Knaus, H. Lutz, M. Büchele, A. Reichhold, and A. Pazos-Costa, “Municipal plastic waste recycling in fluid catalytic cracking units: Production of petrochemicals and fuel in an fluid catalytic cracking pilot plant from biogenic and recycled feedstocks,” *Chemical Engineering and Processing - Process Intensification*, vol. 182, Dec. 2022, https://doi.org/10.1016/j.cep.2022.109204

15 PUBLICATIONS AS CO-AUTHOR

- M. Büchele, H. Lutz, F. Knaus, A. Reichhold, Catalyst Testing in a Continuously Operated Fluid Catalytic Cracking Pilot Plant, Conference: 16th Minisymposium Verfahrenstechnik and 7th Partikelforum, September 2020, https://doi.org/10.34726/561

- M. Büchele, H. Lutz, F. Knaus. A. Reichhold, R. Venderbosch, W. Vollnhofer, Co-feeding of vacuum gas oil and pinewood-derived hydrogenated pyrolysis oils in a fluid catalytic cracking pilot plant to generate olefins and gasoline [version 1; peer review: 2 approved]. Open Research Europe 2021, 1:143 https://doi.org/10.12688/openreseurope.14198.1

- H. Lutz, M. Büchele, A. Reichhold, F. Knaus, Evaluation of co-feeding lipstick mass in a Fluid Catalytic Cracking-process as possible way of chemical recycling, currently under preparation

- H. Lutz, M. Büchele, F. Knaus, A. Reichhold, W. Vollnhofer, and R. Venderbosch, Wood Derived Fast Pyrolysis Bio-liquids as Co-feed in a Fluid Catalytic Cracking Pilot Plant: Effect of Hydrotreatment on Process Performance and Gasoline Quality, Energy & Fuels 2022 36 (17), 10243-10250 https://doi.org/10.1021/acs.energyfuels.2c01736

16 ANNEX

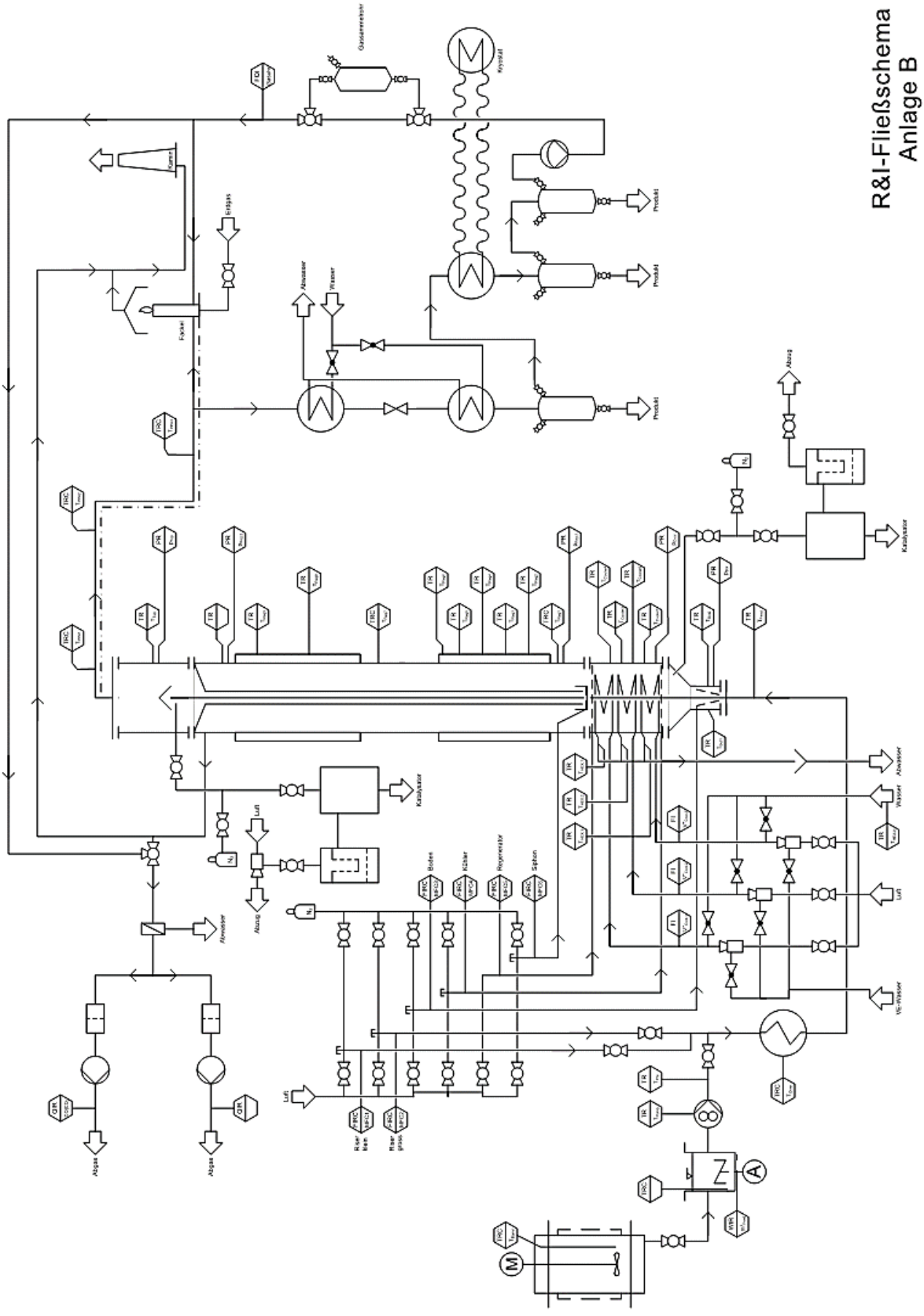

Figure 89: Process flow diagram of the FCC pilot plant B at TU Wien